Palaeoceanography of the interglacial eastern Mediterranean Sea

Gianluca Marino

LPP Foundation 2008

Gianluca Marino
Palaeoecology
Institute of Environmental Biology
Department of Biology
Faculty of Science
Utrecht University
Laboratory of Palaeobotany and Palynology
Budapestlaan 4
3584 CD Utrecht, the Netherlands
G.Marino@uu.nl

Dipartimento di Science della Terra
Università di Napoli "Federico II"
L.go San Marcellino, 10
80138 Napoli, Italy
gianluca.marino@iamc.cnr.it

ISBN 978-90-393-4762-1
NSG publication No. 2008 02 21
LPP Contributions Series No. 24

Cover design by Leonard P.M. Bik
Printed by Gildeprint Drukkerijen, Enschede

Palaeoceanography of the interglacial eastern Mediterranean Sea

Palaeoceanografie van de interglaciale oostelijke Middellandse Zee

(met samenvattingen in het Nederlands en in het Italiaans)

Proefschrift
ter verkrijging van de graad van doctor aan de Universiteit Utrecht,
op gezag van de rector magnificus, prof. dr. J.C. Stoof,
ingevolge het besluit van het college voor promoties
in het openbaar te verdedigen
op donderdag 21 februari 2008 des middags om 16.15 uur

door

Gianluca Marino

geboren op 13 april 1976 te Napoli (Italië)

Promotoren:
Prof. dr. H. Brinkhuis
Prof. B. D'Argenio

Co-Promotoren:
Prof. dr. E. J. Rohling
dr. F. Sangiorgi

The research was financially supported by the Department of Biology, Faculty of Science, Utrecht University, The Netherlands, by the LPP Foundation, Utrecht, The Netherlands, by the Institute for Coastal Marine Environment, National Research Council (IAMC-CNR), Napoli, Italy, by the Department of Earth Sciences, University Federico II, Napoli, Italy, by the Stazione Zoologica A. Dohrn, Napoli, Italy, and by the department of Palaeontology, Frankfurt University

Members of the assessment committee:

Prof. dr. G. J. de Lange
Utrecht University

Prof. dr. K.-C. Emeis
University of Hamburg

Prof. dr. D. Kroon
University of Edimburg

Prof. dr. Ir. J. S. Sinninghe Damsté
Royal Netherlands Institute for Sea Research (NIOZ) and Utrecht University

Contents

11 **General introduction and synopsis**

25 **Chapter 1** The Aegean Sea as driver of hydrographic and ecological changes in the eastern Mediterranean
with Eelco J. Rohling, W. Irene C. Rijpstra, Francesca Sangiorgi, Stefan Schouten, and Jaap S. Sinninghe Damsté
Published in Geology, 35, 675-678 (2007)

39 **Chapter 2** Hydrogen isotopic compositions of long-chain alkenones record freshwater flooding of the eastern Mediterranean at the onset of sapropel deposition
with Marcel T.J. van der Meer, Marianne Baas, W. Irene C. Rijpstra, Eelco J. Rohling, Jaap S. Sinninghe Damsté, and Stefan Schouten
Published in Earth and Planetary Science Letters, 262, 594-600 (2007)

49 **Chapter 3** Early and middle Holocene in the Aegean Sea: interplay between high- and low-latitude climate variability
with Francesca Sangiorgi, Eelco J. Rohling, Angela Hayes, James L. Casford, André F. Lotter, Michal Kucera, and Henk Brinkhuis

73 **Chapter 4** Reconstructing changes in marine productivity at the time of S1 deposition in the eastern Mediterranean; a marine palynological approach
with Francesca Sangiorgi and Henk Brinkhuis

91 **Chapter 5** Amplified response of the eastern Mediterranean to insolation changes; insights from the last two interglacial periods
with Eelco J. Rohling, Francesca Sangiorgi, Jaap S. Sinninghe Damsté, and Henk Brinkhuis

105 **Samenvatting** (summary in Dutch)

111 **Riassunto** (summary in Italian)

117 **References**

141 **Acknowledgments**

145 **Curriculum Vitae**

alla mia famiglia.....

General introduction and synopsis

The sensitivity of the present interglacial climate to the ongoing anthropogenic atmospheric greenhouse gas increase poses a fundamental concern to modern society. For example, for the Mediterranean region reconstructions based on historical instrumental records reveal a distinct trend towards drier and warmer conditions, while model climate experiments signal that these changes are likely to continue in the near future, and to be even larger than the global average (IPCC, 2007). Moreover, in the Mediterranean area the effects of the current climate change, likely supplemented by human activities (Rohling and Bryden, 1992), are rapidly (within decades) transferred to the deep sea via an effective thermohaline circulation (Béthoux et al., 1990, 1998; Roether et al., 1996; Skliris et al., 2007), pointing to the exceptional sensitivity of the coupled ocean and atmosphere dynamics to combined anthropogenic and natural climate forcing in the region.

This thesis rises from the need to advance our understanding of the sensitivity of the Mediterranean region to perturbations in the atmosphere/ocean system during interglacials. There exists ample evidence of dramatic changes in the hydrological forcing of the Mediterranean during both the current (Holocene) and the last interglacial periods. This promoted major hydrographic and ecosystem changes, which in the sediment record are witnessed by the deposition of organic-rich layers (sapropels) (see, e.g., Cita and Grignani, 1982; Mangini and Schlosser, 1986; Rohling, 1994; Cramp and O'Sullivan, 1999; Emeis et al., 2003). These layers are associated with deep water anoxia and therefore represent near ideal, not bioturbated or otherwise disturbed, archives of Mediterranean environmental and climate change during relatively warm episodes. Sapropel S1, deposited during the Holocene, and sapropel S5, deposited during the last interglacial, are the main archives chosen for the purpose of this study. Paleoceanographic reconstructions are developed for sapropels S1 and S5 based on a broad range of proxy records, including marine palynological (organic-walled dinoflagellate cysts), stable isotope, and organic geochemical proxies. These analyses are performed on the aforementioned sapropels in sediment cores from key locations of the eastern Mediterranean Basin (Aegean Sea, Adriatic Sea, Strait of Sicily).

The modern Mediterranean Sea

Geographic location and climate

The Mediterranean Sea is a land-locked marginal sea of the Atlantic Ocean and it is divided by the Strait of Sicily into two main sub-basins; the western and eastern Mediterranean. It is bordered by Europe to the north, Asia to the east, and Africa to the south.

Climatologically, the Mediterranean resides at the transition between the high- to mid-latitude and the subtropical atmospheric systems, which interact and, in a way, may be regarded to compete with one another (Figure 1) (Lionello et al., 2006). As a consequence, the Mediterranean climate depends on the latitudinal shift of these climate systems with the seasons, and typically varies between mild, wet winters and hot, dry summers (Eshel, 2002; Rohling et al., 2008a).

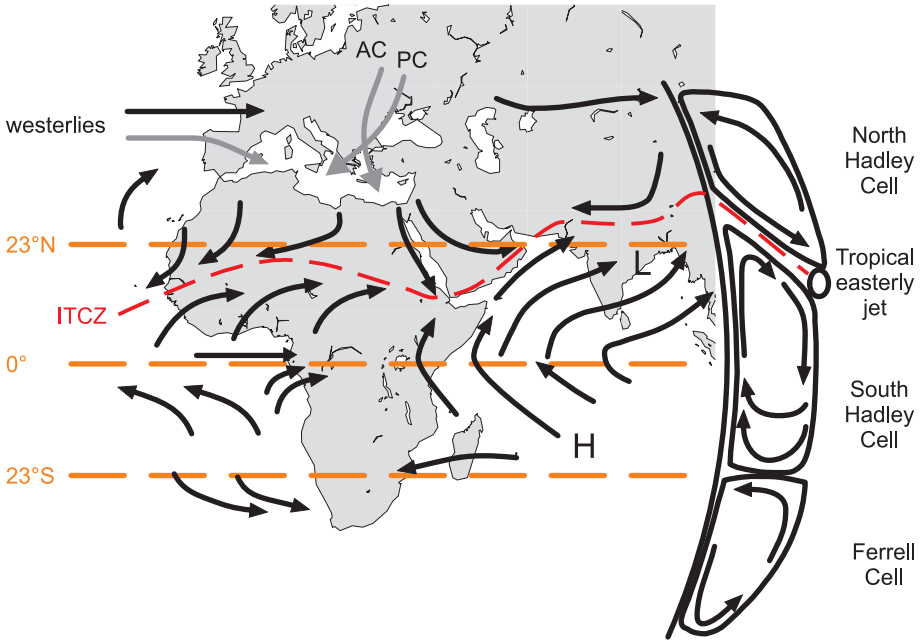

Figure 1: Northern Hemisphere summer atmospheric circulation. Main winds are indicated as black arrows. ITCZ = intertropical convergence zone; H and L = areas of high and low sea-level pressure, respectively. Main air masses reaching the eastern Mediterranean in winter as grey arrows. AC and PC = Arctic continental and Polar air masses, respectively (slightly modified after Reichart, 1997 and Rohling et al., 2008a).

Specifically, the winter regime is dominated by mild and wet conditions related to the southward spreading of the temperate westerlies from central and northern Europe (Lolis et al., 2002), with occasional outbreaks of cold polar/continental air masses funnelled through the valleys of the northern Mediterranean margin (Maheras et al., 1999). In summer, warm and dry conditions prevail due to

a northward shift of subtropical high-pressure belt over the basin (Rodwell and Hoskins, 1996; Saaroni et al., 2003; Ziv et al., 2004). It is worth noting that before the anthropogenic curtailment of the freshwater discharge of the Nile River, another climate system, namely the northern African monsoon, used to have an impact on the Mediterranean system and specifically on the basin's hydrography. The influence of the African monsoon on the Mediterranean hydrography is however indirect as there is no actual latitudinal displacement of this climate system onto this region but rather a modulation of the basin's freshwater inputs via the Nile River and other North African drainage systems (Rohling and Bryden, 1992; Rohling et al., 2002b, 2004; Scrivner et al., 2004; Skliris and Lascaratos, 2004).

Oceanography

The Mediterranean Sea is a concentration basin; evaporative losses (E) exceed the freshwater inputs resulting from precipitation (P) and river runoff (R) (Béthoux, 1979; Garrett, 1996; Gilman and Garrett, 1994). This feature is apparent over the Mediterranean as a whole as well as over the two sub-basins in particular, as exemplified by the two-layer exchange systems at Gibraltar (Bryden and Kinder, 1991) and at the Strait of Sicily (Garzoli and Maillard, 1979), in which the eastward surface flow of warmer, fresher surface waters overlies the westward flow of colder, saline (i.e., denser) subsurface waters (Figure 2) (Astraldi et al., 1999).

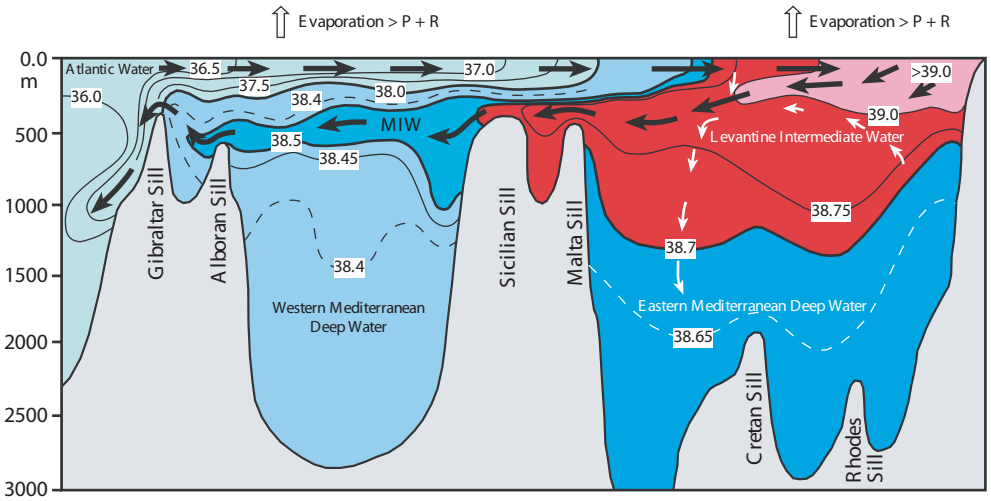

Figure 2: West - East cross-section showing water mass circulation in the Mediterranean Sea during winter (after Wüst, 1961). Isolines indicate salinity values and arrows indicate the direction of water circulation in the Mediterranean Sea (Rohling et al., 2008a).

The Mediterranean circulation is driven by water exchange through the various straits, wind stress, and thermohaline fluxes, with the latter depending on the basin's freshwater and heat budgets (Robinson et al., 2001). The vertical distribution of the Mediterranean water masses includes the surface (0-200 m), the intermediate (200-600 m), and the deep waters (> 600 m) (Pinardi and Masetti, 2000; Tsimplis et al., 2005), which circulation is shown in Figure 3.

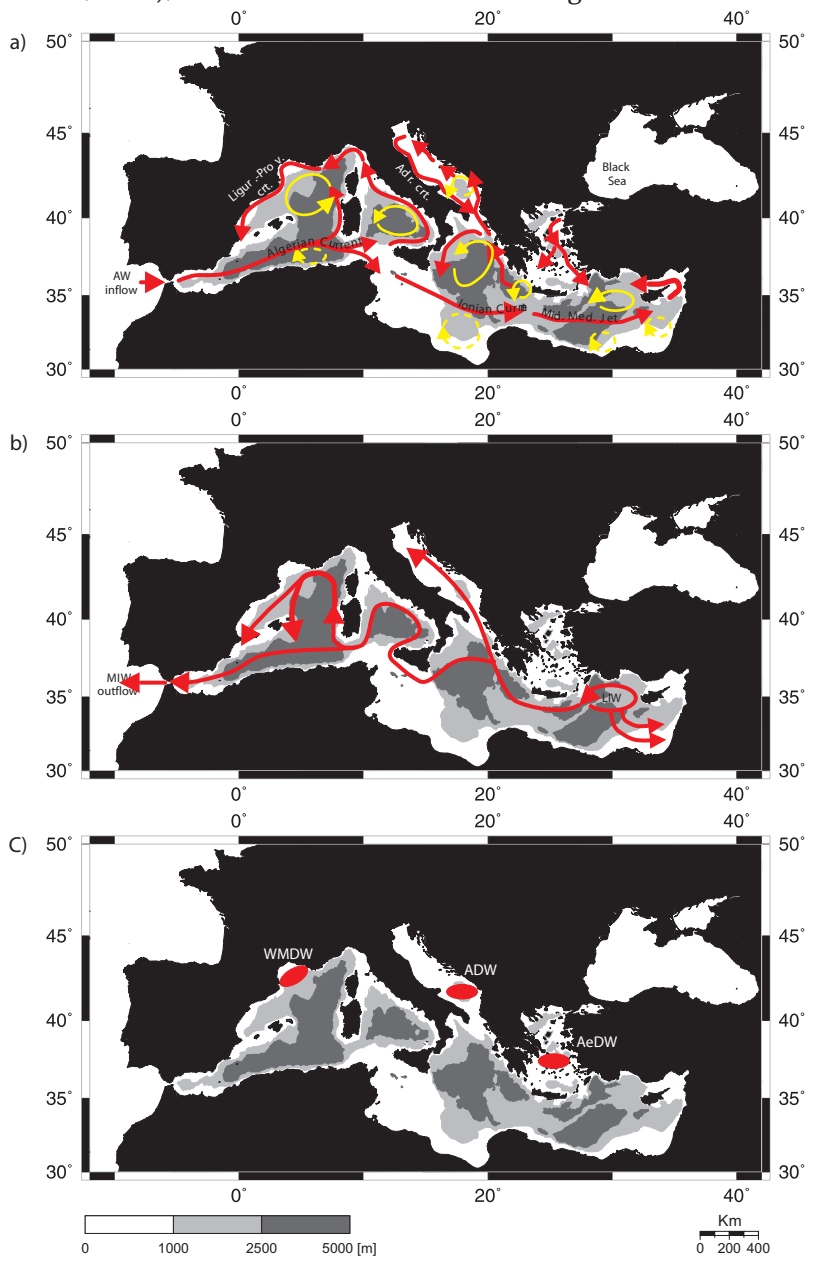

In the northern sectors of the basin the surface patters are dominated by cyclonic gyres. In the southern sectors surface waters derived from the Atlantic Ocean flow eastwards through currents, jets (western basin) and anticyclonic gyres (eastern basin) (Pinardi and Masetti, 2000) (Figure 3a), while undergoing temperature gain and net evaporative loss, with the latter leading to strong west-east salinity gradients (Wüst, 1961). In the northern Levantine basin the advection of winter (cool) northerly air masses neutralizes the temperature gain, thereby causing the formation of Levantine intermediate water (LIW) in the Rhodes Gyre (Malanotte-Rizzoli and Hecht, 1988; Georgopoulos et al., 1989; Buongiorno Nardelli and Salusti, 2000). This water mass subsequently settles between 200 and 600 m and spreads out in the entire Mediterranean basin to eventually enter the Atlantic Ocean at Gibraltar (Figure 3b).

The interaction of the LIW with cold surface waters in the northern basins of the Mediterranean governs the deep-water formation processes, which is responsible for the deep-sea ventilation of the entire basin (Pinardi and Masetti, 2000). Sites of deep water overturning are the Gulf of Lions for the western basin (western Mediterranean Deep Waters, WMDW), and the Adriatic (Adriatic Deep Waters, ADW), and Aegean (Aegean Deep Waters, AeDW) Seas for the eastern basin (Figure 3c). Overall, the Mediterranean thermohaline circulation has proven to be primarily tied to the basin's negative freshwater budget (Myers and Haines, 2002), whose variations are dominated by processes acting in the eastern Mediterranean (Rohling and Bryden, 1992).

Perturbations of the Mediterranean freshwater budget and sapropel formation

The (eastern) Mediterranean sedimentary record, spanning the past 13.5 million of years (Hilgen et al., 2003), reveals (quasi)periodic intervals of oxygen depleted bottom waters, witnessed by the widespread deposition of organic-rich sediments, so-called sapropels (Cita and Grignani, 1982; Mangini and Schlosser, 1986; Rohling, 1994; Cramp and O'Sullivan, 1999; Emeis et al., 2003).

Figure 3 (left): Water mass circulation in the Mediterranean Sea. **(a)** Schematic representation of the major features of the surface water circulation. **(b)** Circulation pattern of the Levantine Intermediate Waters (LIWs). **(c)** sites of deep water overturning (modified after Pinardi and Masetti, 2000). Ligur. - Prov. crt. = Ligurian-Provencal current; Adr. crt. = Adriatic current; Mid Med. Jet = Mid Mediterranean Jet.

Sapropels form during orbitally modulated intervals of Northern Hemisphere insolation maxima and consequent intensification of the African monsoon-fuelled river discharge into the southern margin of the basin (Figure 4) (Rossignol-Strick et al., 1982; Rossignol-Strick, 1983, 1985; Hilgen, 1991). Increased freshwater supply (i.e., a positive shift of the basin's freshwater budget) leads to buoyancy gain at the sea surface, thereby preventing the surface aerated waters from sinking to the seafloor. This curtailment of oxygen delivery to the deep sea, likely complemented by enhanced primary productivity (e.g., Rohling and Gieskes, 1989; Howell and Thunnell, 1992; Strohle and Krom, 1997), is widely acknowledged as the main trigger for the sapropel deposition (Rohling, 1994).

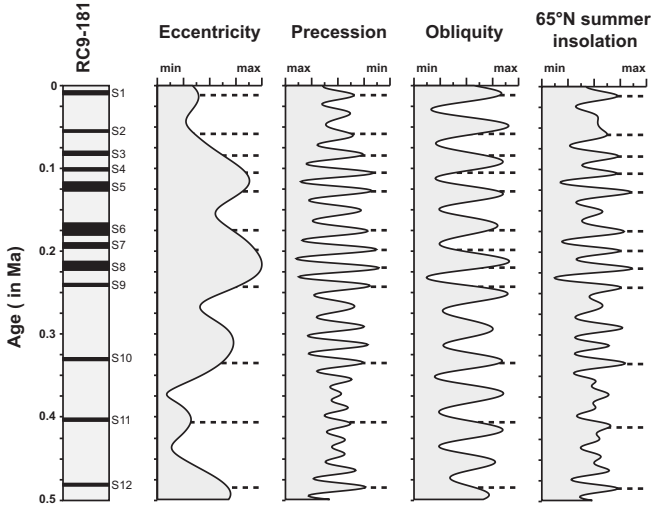

Figure 4: Phase relationships between Quaternary sapropels and the astronomical curves of eccentricity, obliquity, precession and summer insolation at 65°N (from Hilgen, 1991).

Since their first discovery at the end of the 1940's (Kullenberg, 1952) a wealth of information has become available on the mechanisms of sapropel formation. Sapropel studies mostly fall along two central themes: (1) the phase relationships between the deposition of the organic-rich layers and the changes in the Earth's orbital parameters (e.g., Hilgen, 1991; Lourens et al., 1996); (2) the detailed assessment of the complex sequence of hydrographic (e.g., Rohling, 1991,1994; Myers et al., 1998; Rohling et al., 2002b, 2004, 2006) and biogeochemical and ecological (e.g., Sarmiento et al., 1988; Sachs and Repeta, 1999, Kemp et al., 1999; Struck et al., 2001; Rohling et al., 2004) changes associated to their deposition.

In the past decades numerous highly resolved (centennial- to millennial-scale) reconstructions have become available. The vast majority of these investigations targeted either the Pliocene (Rohling et al., 1993; Passier et al., 1999; Nijenhuis

and de Lange, 2000; Rinna et al., 2002; Menzel et al., 2002, 2003, 2004, 2005, 2006; Arnaboldi and Meyers, 2006) or the late Quaternary sapropel layers (Rohling and Gieskes, 1989; Robertson et al., 1998; Emeis et al., 2000), with emphasis on the Holocene sapropel S1 (De Rijk et al., 1999; Thomson et al., 1999; Mercone et al., 2000, 2001; Casford et al., 2002, 2003; Scrivner et al., 2004; Bianchi et al., 2006; Principato et al., 2006; Reitz and de Lange, 2006; Reitz et al., 2006) and to a lesser extent on last interglacial sapropel S5 (Struck et al., 2001; Cane et al., 2002; Corselli et al., 2002; Rohling et al., 2002b, 2004, 2006; Scrivner et al., 2004; Capotondi et al., 2006; Giunta et al., 2006; Sangiorgi et al., 2006).

Scope of this study

Due to the climatological and oceanographic sensitivity of the region, the eastern Mediterranean sedimentary record may be expected to contain much essential information about past interactions between the high/mid-latitude and tropical/subtropical climate systems. In addition, the anoxic/dysoxic sedimentation during periods of sapropel deposition prevents bioturbation, thereby allowing highly resolved reconstructions in the time domain. The present thesis focuses on decadal- to centennial-scale assessment of the response of the eastern Mediterranean climate and circulation to both high/mid-latitude and tropical/subtropical climate systems during the monsoon maxima of the current (sapropel S1) and last (sapropel S5) interglacial periods. Both intervals allow sound insight into the duration of processes and rates of change, due to the excellent chronological constraints provided by radiocarbon-based chronologies for the Holocene (Casford et al., 2007) and the robust correlation found between the period of S5 deposition and the last interglacial humid period in U/Th-dated speleothems in Israel (Bar-Matthews et al., 2000).

Several equally important reasons have driven the choice to predominantly focus this work on Aegean Sea sediment cores. First, along with the Adriatic, the Aegean is a region of deep convective overturning where deep waters form and then spread out to the open eastern Mediterranean (Roether et al., 1996), consequently supplying oxygen to the deep-sea. Accordingly, changes in Aegean sea surface properties (e.g., temperature, salinity) during periods of enhanced monsoon-fuelled freshwater supply may potentially affect the hydrography of the entire eastern Mediterranean. In addition, the high sedimentation rates reported for the Aegean Sea (Casford et al., 2007) and the remoteness of this basin from the foci of monsoon-sourced freshwater injections during intervals of sapropel deposition (Rohling et al., 2002b; Scrivner et al., 2004) make this basin ideal for high resolution studies and assessment of basin-integrated responses to freshwater dis-

turbances, respectively.

Finally, the location in the northern sector of the eastern Mediterranean and the orographic configuration of the southern European margin bring the Aegean (in winter) under the direct influence of cold polar/continental air masses derived from high latitudes. Accordingly, Aegean paleorecords are expected to improve the current understanding of the role of the high latitude climate forcing on the lower latitudes and consequently the interplay of the two climatic systems during interglacial periods.

By bringing together diverse but complementary tools of paleoceanographic investigation, such as marine palynology, stable isotope and organic geochemistry, performed at high temporal resolution (decadal to centennial), the present thesis aims to provide detailed and integrated reconstructions of sea surface temperatures, salinities, productivity patterns and water mass/atmosphere dynamics during the current and the last interglacial period in the eastern Mediterranean.

Synopsis

A profound change has occurred in the eastern Mediterranean deep sea over the past decades, comprising a shift of the dominant locus of Eastern Mediterranean deep water formation from the Adriatic to the Aegean Sea. This phenomenon, known as the Eastern Mediterranean Transient (EMT), was likely preconditioned by increases in the basin's net evaporation (freshwater budget). This apparent sensitivity of the eastern Mediterranean thermohaline circulation to perturbations of the basin's freshwater budget is treated in **Chapter 1**. Species specific planktonic foraminiferal stable isotopes ($\delta^{18}O$ and $\delta^{13}C$) and organic geochemical data (alkenones, isorenieratene, and total organic carbon) from south-eastern Aegean core LC21 are integrated to provide a detailed reconstruction of the Aegean deep-water overturning system during the last interglacial period, and compared to similar proxies from contemporaneous sediments in open eastern Mediterranean ODP Site 971A. Following a large freshwater injection into the open eastern Mediterranean, the Aegean subsurface ventilation is found to have collapsed within 40±20 yr, promoting euxinic conditions - hostile to aerobic life - which expanded toward the photic layer within 650±250 yr. Another 300±120 yr later, similar conditions extended throughout the eastern Mediterranean. This study highlights the exceptional sensitivity of the Aegean to changes in wider eastern Mediterranean climatic forcing of any sign, with responses that lead to profound hydrographic adjustments that subsequently propagate throughout the basin.

Sapropels are organic-rich sediment layers that were intermittently deposited in the Mediterranean Sea, especially in its eastern basin, during the last 13.5

million of years. The associated anoxic events that gave rise to sapropel formation resulted indirectly from the impact of African monsoon maxima on the basin's hydrography. Sharp shifts in oxygen isotopes ($\delta^{18}O$) to values more depleted in the heavy isotope (^{18}O) in carbonates from surface-dwelling planktonic foraminifera, slightly preceding sapropel deposition, suggest that the Mediterranean was flooded by large amounts of freshwater leading to the development of a low salinity of the surface water and a strong density stratification of the water column. However, the degree of freshwater flooding and concomitant drop in sea surface salinity (SSS) remain elusive. A novel approach to assess SSS changes exploits the hydrogen isotope (δD) composition of long-chain alkenones produced by haptophyte algae, which has been found to depend mostly on the δD of the water and on salinity, and may therefore offer a new tool for salinity reconstructions. In **Chapter 2**, the results of the analysis of the δD of alkenones from last interglacial sapropel S5 from the south-eastern Aegean Sea core LC21 are discussed. Results show a large decrease in δD of 25‰ at the onset of sapropel formation, suggesting a drop in SSS of 6, from 39 to 33. Although the absolute SSS estimates should be interpreted with care as they are subject to relatively large uncertainties, the estimated SSS values appear quite reasonable as they, for example, yield SSS before sapropel deposition similar to that of the present day Aegean Sea. To reduce uncertainties in SSS estimates, the δD-salinity relationship has to be better constrained with cultures and also tested in field studies. However, our results do illustrate the promise of a combined use of δD of alkenones, $U^{k'}_{37}$ of alkenones, and $\delta^{18}O$ of surface dwelling planktonic foraminifera, for SSS reconstructions.

The Aegean region resides at the boundary between the high- to mid-latitude and the tropical/subtropical climate systems. The seasonal latitudinal shift of this boundary controls the region's climate and hydrography. Obtaining multiproxy season-specific reconstructions from the same sample series of Aegean sea surface temperature (SST) and hydrography may therefore be critical to advance our understanding of the large-scale climate interactions during past episodes of climate change. Such information is instrumental in **Chapter 3**, which centres on the early to mid Holocene interval of Northern Hemisphere insolation/monsoon maximum. We reconstruct the south-eastern Aegean $\delta^{18}O_{seawater}$ and note a distinct negative shift (1.5‰) between 10.6 and 9.6 ka BP. This decrease in surface-water $\delta^{18}O$ represents the regional expression of the intensification of the African monsoon and its related freshwater flooding, which affected the entire eastern Mediterranean during the early to mid Holocene. A contemporaneous shift of similar magnitude has been noted in $\delta^{18}O_{speleothem}$ at Soreq Cave (northern Israel). Consequently, we suggest that the $\delta^{18}O_{speleothem}$ changes may not be due to changes in the amount of precipitation over the cave's catchment area, but instead may reflect our reconstructed changes in the isotopic composition of the moisture source

region (Aegean-Levantine basin). Superimposed upon these long-term hydrographic changes are Aegean multi-centennial episodes of winter cooling by up to 1.8°C. These episodes display a positive correlation with non-seasalt [K^+] series from the Greenland GISP2 ice core, suggesting that they were intimately linked to meridional displacements of the atmospheric polar vortex. The three main episodes of Aegean winter cooling at about 10.5 ka BP, 9.8-9.1 ka BP, and 8.6-8.0 ka BP coincide closely with previously described centennial-scale deteriorations of the Indian summer monsoon. We propose a linking mechanism by which Eurasian winters of increased severity led to more pronounced snow cover in the Asian highlands, causing delayed/weakened summer monsoons, and contemporaneous yet independent intensification of the Siberian High, a component of the atmospheric polar vortex. Finally, we report the first indications of a particularly sharp Aegean cooling event between 8.3 and 8.15 ka BP, embedded within an underlying cooling episode of 8.6-8.0 ka BP. In both timing and duration, this sharp event agrees with the so-called 8.2 ka BP event reported from several records from the wider North Atlantic region, which has been related to a brief weakening of the Atlantic Meridional Overturning Circulation.

Reconstructions of the primary productivity patterns during sapropel deposition remain problematic mostly due to the limitations of the paleoproductivity proxies commonly used in palaeoceanography. An approach based on quantitative dinoflagellate analysis is discussed in **Chapter 4**. Fluctuations in the heterotrophic dinoflagellate cysts (dinocysts) due to the dietary preference of their motile counterparts have been used to reconstruct past changes in the eukaryotic primary productivity patterns at the sea surface. Recently, some studies have warned that aerobic degradation under oxic conditions may affect abundances of heterotrophic dinocysts in the sediments and high abundances of these dinocysts in anoxic sediments may thus reflect enhanced preservation at the sea floor rather than increased sea surface productivity. To further investigate this issue, dinocyst data from early to mid Holocene sedimentary records (including time of sapropel S1) of the Strait of Sicily, Adriatic and Aegean Seas are here discussed in the context of recently published contemporaneous oxyphillic benthic foraminifer records as indicators of bottom water ventilation. We note a 4 kyr maximum in the absolute abundance of heterotrophic dinocysts in the Aegean Sea starting at about 10 ka BP. Similar changes in the concentration of heterotrophic dinocysts in the Adriatic Sea occurred much later (at about 8.5 ka BP) and terminated earlier, at about 7.1 ka BP. An increase in the concentration of heterotrophic dinocysts between 10 and 6.5 ka BP is also reported for the Strait of Sicily, albeit absolute values are much too low to allow conclusive speculations. Given the presence of oxyphillic benthic foraminifera in Adriatic and Aegean Seas during sapropel S1

deposition and the lack of significant correlations between changes in the deep sea ventilation of the two basins and fluctuations in the concentrations of heterotrophic dinocysts, we contend that the latter most likely reflect changes in the sea surface productivity. Interestingly, the onset and the spatial trends of the productivity increase at times of sapropel S1 deposition, imply that the presence of a reservoir of nutrients at intermediate depths, likely tied to weakening of the basin's thermohaline circulation, boosted productivity.

The overarching discussions in the final **Chapter 5** pertain to the sensitivity of the Mediterranean region to climate forcing. Notably it tackles the long-term sensitivity of the eastern Mediterranean circulation to insolation forcing over the last two intervals of peak interglacial conditions, i.e., at times of sapropels S1 and S5 formation. We compare a set of highly resolved paleoceanographic proxy records from one sediment core (south-eastern Aegean core LC21) that includes both the last and the current (Holocene) interglacial peak periods of sapropel S1 and S5 deposition. Specifically, we discuss combined oxygen ($\delta^{18}O$) and carbon ($\delta^{13}C$) isotopes for surface water (*Globigerinoides ruber*) and sub-thermocline dwelling (*Neogloboquadrina pachyderma*) planktonic foraminifera, and total organic carbon (C_{org} wt%) data in order to reconstruct the water mass dynamics and the magnitude of C_{org} burial. We find overall more pronounced environmental changes in the last interglacial records than during the Holocene. During deposition of the last interglacial sapropel S5, C_{org} mass accumulation rates (MAR) reached about 3 g C m^{-2} yr^{-1}, an order of magnitude higher than the highest C_{org} MARs for the Holocene sapropel S1. In addition, the negative shift in the $\delta^{18}O$ record of the summer mixed layer planktonic foraminifer *Globigerinoides ruber* at the onset of S5 deposition is twice as large as the shift occurred at the S1 onset. $\delta^{13}C$ gradients in surface to intermediate waters during deposition of S5 are larger than during deposition of S1, and similar to the intermediate to deep waters $\delta^{13}C$ gradients for S1. This suggests that intermediate waters during S5 were as poorly ventilated (thus strongly isolated) as the deep waters during S1. Taken together, the datasets suggest a stronger water mass stratification during sapropel S5, with a significantly shallower depth of the chemocline, relative to S1.

This conclusive chapter summarizes the leitmotif of this thesis, i.e., the exceptional sensibility of the eastern Mediterranean Sea interglacial climate to climate forcing, as it rapidly responds to atmospheric/sea surface forcing, transferring the signal through the water column to the deep sea and, in turn, to the ecosystems.

N.B. The chapters of this thesis are or will be published as separate papers in peer reviewed scientific journals. Hence, some repetition of statements cannot be avoided. The datasets presented in this thesis are available upon request to the corresponding author.

Chapter 1

The Aegean Sea as driver of hydrographic and ecological changes in the eastern Mediterranean

Based on:
Gianluca Marino, Eelco J. Rohling, W. Irene C. Rijpstra, Francesca Sangiorgi, Stefan Schouten, and Jaap S. Sinninghe Damsté

Published in *Geology*, vol. 35, no. 8, p. 675-678

Abstract

The eastern Mediterranean Sea is undergoing a long-term increase in net evaporation, which may have preconditioned the profound changes that occurred in its deep-sea ventilation over the past two decades. Here we test the sensitivity of Aegean convective deep-water formation system to hydrological forcing in the opposite sense, based on a last interglacial episode of enhanced freshwater injection into the eastern Mediterranean. The Aegean subsurface ventilation is found to have abruptly collapsed within 40±20 years, promoting euxinic conditions, hostile to aerobic life, which rapidly expanded towards the photic layer within 650±250 years. Another 300±120 years later, similar conditions extended throughout the eastern Mediterranean. These findings emphasize the exceptional sensitivity of Aegean deep-water formation to climatic forcing, driving large-scale hydrographic adjustments throughout the eastern Mediterranean, and beyond.

1.1. Introduction

On a global scale, new deep-water formation delivers oxygen to the deep-sea (Ganachaud and Wunsch, 2002). In the eastern Mediterranean, this process has long been dominated by the sinking and spreading of cool and salty (dense) water masses formed in the Adriatic Sea (Malanotte-Rizzoli and Hecht, 1988). During the late 1980s and early 1990s, an abrupt shift to dominance of Aegean Deep-Waters in the eastern Mediterranean deep-sea ventilation occurred. This change usually referred to as Eastern Mediterranean Transient (EMT) (Roether et al., 1996; Klein et al., 1999; Malanotte-Rizzoli et al., 1999), eventually influenced even the density of the Mediterranean outflow into the North Atlantic (Millot et al., 2006). According to several studies this profound reorganization in the eastern Mediterranean hydrography has been preconditioned by a long-term increase in net evaporation from the eastern Mediterranean (Béthoux et al., 1998; Boscolo and Bryden, 2001; Skliris and Lascaratos, 2004; Skliris et al. 2007). Other studies, however, have emphasised the role of synoptic changes in the wind stress field affecting the upper thermocline circulation and, in turn, the salt supply to the Aegean Sea (Malanotte-Rizzoli et al., 1999; Samuel et al., 1999; Stratford and Haines, 2002).

The present study seeks to establish the sensitivity of the Aegean thermohaline circulation to hydrological changes in the opposite sense, namely to a reduction of eastern Mediterranean net evaporation caused by freshwater flooding. The (quasi)periodical occurrence of organic-rich layers (sapropels) in the eastern Mediterranean sedimentary archive offers a unique opportunity for answering this question. Sapropels reflect periods of sluggish bottom-water ventilation in response to

enhanced monsoon-fuelled river discharge along the North-African margin (Rossignol-Strick et al., 1982; Rohling et al., 2002b, 2004; Emeis et al., 2003). The last interglacial sapropel S5 is intensively developed and holds excellent potential for highly resolved studies (Cane et al., 2002; Rohling et al., 2002b, 2004, 2006). However, a lack of Aegean S5 records has to date limited our understanding of the hydrographic responses of this critical region to a sharp reduction in eastern Mediterranean net evaporation.

Here we present the first systematic high-resolution multi-proxy study of an Aegean sapropel S5, which was retrieved from south-eastern Aegean Sea core LC21 (Figure 1.1). Results are discussed within the context of previously described contemporaneous records from the open eastern Mediterranean, especially ODP site 971A (Cane et al., 2002; Rohling et al., 2002b, 2004, 2006).

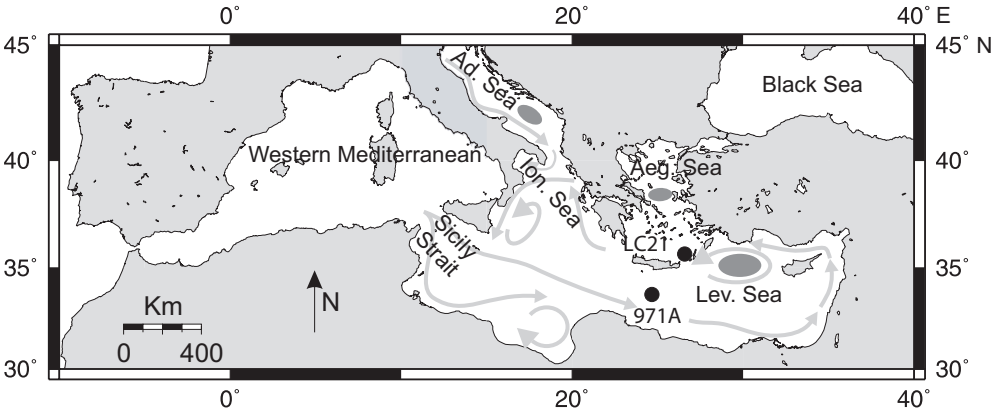

Figure 1.1: Map of the Mediterranean basin. The main patterns of surface circulation (grey arrows) and sites of dense water formation (shaded areas) in the eastern Mediterranean (Pinardi and Masetti, 2000) are shown. Black dots indicate the locations of core LC21 (35°40'N; 26°35'E; 1522 m water depth) and ODP Site 971A (33°43'N; 24°41'E; 2026 m water depth). Aeg. Sea = Aegean Sea; Lev. Sea = Levantine Sea; Ad. Sea = Adriatic Sea; Ion. Sea = Ionian Sea.

1.2. Materials and methods

Core LC21 was recovered in 1995 by RV *Marion Dufresne* for the EC-MAST2 (Marine, Science, and Technology Programme) PALEOFLUX (Biogeochemical Fluxes in the Mediterranean Water-Sediment System) program. We have analysed core sections 5 and 6 through S5 at 1 cm (decadal) resolution for $\delta^{18}O$ and $\delta^{13}C$ in *Globigerinoides ruber* (white) and *Neogloboquadrina pachyderma* (dextral), and at 5 cm (centennial) resolution for alkenone-based sea surface temperatures (SSTs), total organic carbon (C_{org}), and isorenieratene concentrations (see Figure 1.2, panel I).

1.2.1. Foraminiferal oxygen and carbon stable isotopes ($\delta^{13}C$ and $\delta^{18}O$)

All stable isotope analyses were performed at the National Oceanography Centre (Southampton, United Kingdom) with a Europa Geo2020 dual inlet mass spectrometer following individual acid-bath reaction of 15-20 handpicked and cleaned adult specimens in the size ranges 300-350 µm for *Globigerinoides ruber* (white) and 250-300 µm for *Neogloboquadrina pachyderma* (right coiling). Isotope ratios are expressed as $\delta^{13}C$ and $\delta^{18}O$, in per mil (‰) values relative to Vienna PeeDee Belemnite (VPDB). External precision was better than 0.06 ‰ for both $\delta^{13}C$ and $\delta^{18}O$.

1.2.2. Organic geochemistry

Organic geochemistry analyses were performed at the NIOZ Royal Netherlands Institute for Sea Research (Den Burg, Texel, The Netherlands). The total organic carbon (C_{org} wt%) contents were determined by elemental analysis (EA)/ isotope-ratio-monitoring mass spectrometry (EA/irmMS). EA/irmMS analyses were performed on decalcified (by reaction with 1 N HCl for 18 h) sediments using a Carlo Erba Flash elemental analyzer coupled to a Thermofinnigan DeltaPLUS irmMS system. The C_{org} was determined using external standards with known carbon content.

For alkenone analysis sediment samples were freeze-dried and homogenized by mortar and pestle and then extracted using Dionex™ accelerated solvent extraction (ASE) technique using dichloromethane (DCM)/methanol (2:1, v/v) at high temperature (100°C) and pressure ($7.6x10^6$ Pa). The extracts were separated by Al_2O_3 column chromatography using first hexane/DCM (9:1, v/v) and then hexane/DCM (1:1, v/v) to elute the alkenone fraction. The alkenone fraction was analysed by gas chromatrography (GC) and GC/mass spectrometry and C_{37} alkenones were quantified by integrating their peak areas in gas chromatogram. The alkenone-derived SST data are based on the alkenone unsaturation index $U^{k'}_{37} = C_{37:2} / (C_{37:2} + C_{37:3})$, which is translated into temperatures using: SST (°C) = $(U^{k'}_{37} - 0.044)/0.033$ (Müller et al., 1998). Today, the alkenone producers bloom in winter/spring in the eastern Mediterranean (Ziveri et al., 2000).

Isorenieratene concentrations were determined as described in Hopmans et al., 2005. Carotenoids were extracted using acetone and a carotenoid fraction was prepared using a silica column and DCM as eluent. The carotenoid fractions were analysed on using high performance liquid chromatography/UV-Vis/atmospheric pressure positive ion chemical ionization mass spectrometry. Isorenieratene was quantified based on UV-vis response by comparing the peak area at 454 nm to peak areas at 454 nm of known amounts of an authentic β-carotene standard.

1.3. Stratigraphic framework

The approach used here to build a stratigraphic framework for core LC21 statistically seeks the best correlation with ODP core 971A, which was previously proposed as "master record" for S5 in the eastern Mediterranean (Cane et al., 2002). In this correlation none of the correlation markers were a priori assumed to be syn-/dia-chronous. Distinct and unambiguously defined stratigraphic markers based on five independent proxy records have been recognized on a basin scale during the S5 deposition (Figure 1.2, panel II).

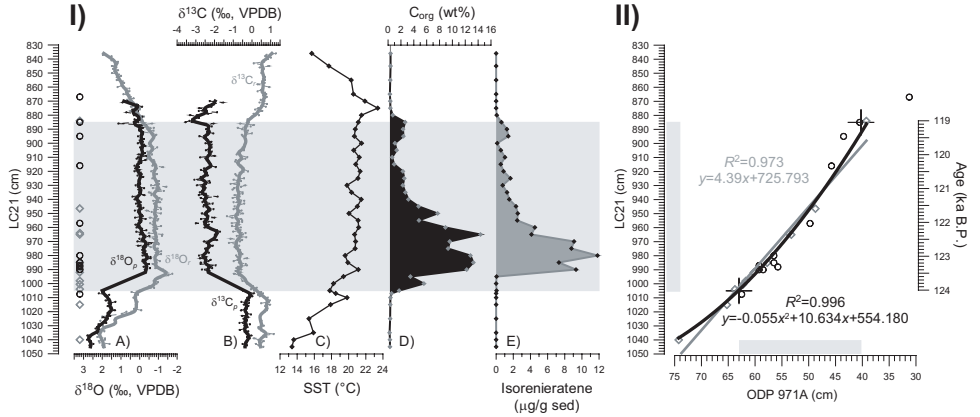

Figure 1.2: Left I) Down-core records of different geochemical proxies through S5 for core LC21. Shaded area represents the visual extent of the dark-coloured sapropel S5 sediments. It corresponds to a partly laminated, benthic azoic interval indicating persistent seafloor anoxia. **(A)**: $\delta^{18}O$ records for the summer mixed layer dwelling *Globigerinoides ruber* (white) (grey dashed line) and top intermediate water dwelling *Neogloboquadrina pachyderma* (dextral) (black dashed line) planktonic foraminifera. **(B)**: $\delta^{13}C$ records for *G. ruber* (white) and *N. pachyderma*. The isotopic records ($\delta^{18}O$ and $\delta^{13}C$) of *G. ruber* (grey solid line) and *N. pachyderma* (black solid line) were lowess smoothed (tension 0.04 and 0.05, respectively) in order to highlight main trends. **(C)**: SST reconstructions based on the long-chain alkenone unsaturation index (black solid line). **(D)**: Organic carbon content (C_{org}, wt. %) (black filled area). **(E)**: Isorenieratene abundance calculated with respect to the total amount of sediment (grey filled area). **Right II)** Linear (grey line) and polynomial (black line) fits through the primary correlation markers (grey open diamonds), using ODP 971A as the independent variable ("bench mark") and LC21 as dependent variable. Black open circles represent secondary correlation markers. Big + and grey blocks indicate the visual extent of the dark-coloured sapropel sediments. The time scale on the right is based on the correlation between major shifts in the $\delta^{18}O_{ruber}$ at sapropel onset and termination and the onset and termination of the humid period in Soreq Cave (Rohling et al., 2002b).

Remarkable O and C isotope shifts, clear faunal presence/absence and sharp peaks in the C_{org} and isorenieratene abundance have been recognized in Aegean LC21 and western Levantine 971A (Figure 1.2, panel II, Table 1.1). Markers, such as faunal zero abundance levels of the most abundant foraminiferal species, and sharp peaks in the isotopic profiles have been assigned a primary role, and

these were used to establish the correlation between the two sites. Markers deriving from less well-defined events, and shifts in organic carbon content and isorenieratene abundance have been assigned a secondary role and were used for validation of the regression only. In order to avoid possible bias caused by post-depositional oxidation, the visual extent of the dark-coloured sapropel sediments was not used to identify the calibration (Cane et al., 2002).

In Figure 1.2 (panel II), 11 primary (grey open diamonds) and the 12 secondary (black solid circles) correlation marker pairs for LC21 and 971A are plotted against one-another. Linear regression between primary correlation markers is highly significant (R^2=0.97). Moreover, the regression is corroborated by the proximity of the secondary markers to the linear fit. Nevertheless, a second-order polynomial regression between primary correlation markers (R^2=0.996), albeit statistically indistinct from the linear regression, yields a visual "point to point" improvement. Therefore, the latter regression has been employed to calibrate the LC21 depth scale to 971A-equivalent depths. The 1σ uncertainty that applies to the correlation based on the second-order polynomial fit through the primary correlation markers equals ±0.83 cm.

Table 1.1: List of the primary and secondary correlation markers.

Correlation point	Species/stable isotope/org. geochem.	Definition	Confidence	971A Depth	LC-21 Depth
i1	*N. pachyderma* $\delta^{13}C$	prominent isotopic depletion peak at sapropel cessation	primary	39.25	884.00
f2	*G. sacculifer* faunal	sample before species reappears	primary	48.75	946.50
f4	*G. scitula* faunal	species no longer present (zero abundance)	primary	53.25	965.00
i5	*N. pachyderma* $\delta^{13}C$	first prominent isotopic enrichment peak	primary	53.75	964.00
f5	*G. sacculifer* faunal	species no longer present (zero abundance)	primary	57.75	985.00
f6	*N. pachyderma* faunal	sample before species reappears after short absence	primary	60.25	992.00
f8	*G. inflata* faunal	species no longer present (zero abundance)	primary	61.75	998.00
i7	*G. ruber* $\delta^{18}O$	mid-point of isotopic depletion at sapropel onset	primary	62.25	1000.5
f9	pink *G. ruber* faunal	sample before the species appears	primary	63.75	1004.0
f10	*N. pachyderma* faunal	prominent peak below sapropel preceding sharp drop in abundance	primary	62.25	1015.0
i13	*N. pachyderma* $\delta^{18}O$	shoulder before depletion trend	primary	74.25	1040.0
i9	*G. ruber* $\delta^{13}C$	prominent peak in isotopic enrichment after sapropel	secondary	31.25	867.00
i2	*N. pachyderma* $\delta^{13}C$	second prominent isotopic enrichment peak	secondary	45.75	916.00
i3	*N. pachyderma* $\delta^{13}C$	prominent isotopic depletion between i1 and i11	secondary	49.75	957.00
i12	*N. pachyderma* $\delta^{18}O$	first major depletion	secondary	55.75	988.00
i10	*G. ruber* $\delta^{13}C$	shoulder during isotopic depletion in basal third of the sapropel	secondary	59.25	987.00
i11	*N. pachyderma* $\delta^{13}C$	prominent isotopic depletion peak after sapropel onset	secondary	59.25	990.00
isor1	isorenieratene org. geochem.	last peak in isorenieratene abundance	secondary	43.50	895.00
isor2	isorenieratene org. geochem.	Highest value in isorenieratene abundance after the sapropel onset	secondary	56.50	980.0
isor3	isorenieratene org. geochem.	sample before preceding isorenieratene occurrence	secondary	58.50	990.0
C_{org} 1	C_{org} org. geochem.	last sample at the sapropel termination where C_{org}<2%	secondary	40.50	885.00
C_{org}2	C_{org} org. geochem.	peak in C_{org} after sapropel onset	secondary	62.50	1007.0
C_{org}3	C_{org} org. geochem.	last sample before C_{org}>1% at the sapropel onset	secondary	56.50	985.00
top black				40.25	885.00
base black				63.00	1005.0

1.3.1. Chronology

The onset of the monsoon-fuelled freshwater dilution of the eastern Mediterranean surface waters is expected to be virtually synchronous throughout the basin, preceding the organic-rich sedimentation (Rohling et al., 2002b). Since the

eastern Mediterranean sea surface is the principal source of moisture for precipitation over Soreq Cave (Northern Israel) (Matthews et al., 2000), any appreciable change in the oxygen isotopic composition of eastern Mediterranean sea surface waters (as reflected in $\delta^{18}O_{ruber}$) will be recorded directly by a comparable shift in the $\delta^{18}O_{calcite}$ of Soreq Cave speleothems (Bar-Matthews et al., 2000). Therefore, in agreement with Rohling et al. (2002a), we contend that the onset of the humid phase in the eastern Mediterranean region during the Marine Isotopic Stage 5e (MIS 5e) is synchronous at a basin-scale and can be assigned an approximate age of 124 thousand years (ka) Before Present (BP) (Bar-Matthews et al., 2000). Similarly, the major return of $\delta^{18}O_{ruber}$ to pre-sapropel values near the end of S5 deposition is synchronous between LC21 and 971A and throughout the eastern Mediterranean (Rohling et al., 2002b), and matches the termination of the humid phase in Soreq Cave dated at around 119 ka B.P. (Bar-Matthews et al., 2000).

The chronology for S5 provided in the present study relies on a simple linear interpolation (i.e. assuming a constant sedimentation rate throughout the S5) between the estimated ages of the onset (124 ka BP) and the termination (119 ka BP.) of the depletion and enrichment trends in $\delta^{18}O_{ruber}$, respectively. On the basis of this very simple calculation, and taking into account a 2 kyr uncertainty in the duration of the humid period in Soreq Cave (Bar-Matthews et al., 2000), 1 cm corresponds to 39.7±20 years in core LC21, and 199.4±80 years in core 971A. An analogous coincidence between major shifts in $\delta^{18}O_{calcite}$ of the Soreq Cave speleothems and in $\delta^{18}O_{ruber}$ in LC21 (Rohling et al., 2002a) is associated with a widespread humid event at the time of deposition of early- to mid-Holocene sapropel S1 (see Chapter 3). The timing relationship between LC21 and Soreq Cave during the early- to mid-Holocene is supported by independent datings performed on both archives (Bar-Matthews et al., 2000; Mercone et al., 2000), and the close agreement between those results corroborates our approach of using the datings from Soreq Cave to provide a chronology for sapropel S5.

1.4. Results and discussion

Sapropel S5 in LC21 is the most intensely developed sapropel known from the Pleistocene, with C_{org} concentrations up to 14% and a thickness of about 120 cm (Figure 1.2, panel I), deposited over a period of about 5 kyr (Cane et al., 2002; Rohling et al., 2002b, 2006). We observed a complete absence of benthic fossils, occurrence of preserved sedimentary lamination in several intervals, and an abundance of specific biomarkers (see below), which together indicate intense anoxic (euxinic) conditions in the Aegean water column during the deposition of S5. In the absence of bioturbation, the great thickness of S5 in LC21 allows sampling at an

exceptionally high resolution. It therefore presents a unique opportunity to develop a decadal-scale assessment of changes in the physical properties of the surface/intermediate waters that (pre)condition eastern Mediterranean deep-water formation (e.g., Pinardi and Masetti, 2000).

The statistical correlation method between LC21 and ODP 971 indicates an exact coincidence of the two cores' large shift to light $\delta^{18}O_{ruber}$ near the onset of S5 (Figure 1.3B). Given the prevalent wind-driven surface circulation in the basin and the small distance between the two core sites (<300 km), such a large and abrupt signal is indeed expected to be synchronous within the 40±20 year temporal resolution of our record. We are therefore confident that our statistical method constrains the correlations well within the 1σ bounds for this crucial segment of the records.

The sediment mass accumulation rate (SMAR) in LC21 exceeds that in 971A by 5 times. Given this SMAR difference and that C_{org} concentrations reach 14% in LC21 compared to 7% in 971A, it appears that the C_{org} burial flux during S5 deposition was a full order of magnitude higher in the Aegean Sea than in the open eastern Mediterranean.

Figure 1.3 shows the signals through S5 in core LC21 along with their counterparts in ODP Site 971A (all data are now presented on the common 971A depth scale). At sites LC21 and 971A the absolute $\delta^{18}O_{pachyderma}$ values are virtually identical (Figure 1.3C). This supports the previous notion that the isotopic composition of *N. pachyderma* (d) reflects basin-integrated property changes, which suggests a habitat in (top) intermediate waters deriving from a single source region (Rohling et al., 2004).

Figure 1.3 (right): Different geochemical proxies through S5 in LC21 (black lines and symbols) along with their counterparts in ODP Site 971A (grey lines and symbols). **(A)**: alkenone-based SST reconstructions. Alkenones are today produced by coccolithophores that bloom in winter/spring in the eastern Mediterranean (Ziveri et al., 2000). SST axis is calibrated relative to the $d^{18}O$ axis so that every 1°C change in temperature corresponds to 0.23‰ in $\delta^{18}O$ (Kim and O'Neil, 1997). **(B)**: $\delta^{18}O$ record for *Globigerinoides ruber* (white). **(C)**: $\delta^{18}O$ record for *Neogloboquadrina pachyderma* (dextral). **(D)**: $\delta^{13}C$ records for *G. ruber* (w). **(E)**: $d^{13}C$ records for *N. pachyderma* (d). Isotopic records (B, C, D and E) were lowess smoothed (solid lines) (tension 0.04 and 0.05, respectively) in order to highlight main trends. **(F)** Organic carbon contents. **(G)** Isorenieratene abundances. All profiles are plotted versus the 971A-equivalent depth scale. Grey shaded area and dashed lines represent the visual extent of the dark-coloured sapropel S5 sediments in 971A and in LC21, respectively.Dotted inset identifies the $\delta^{18}O_{ruber}$ (heavy) anomaly in core 971A (Rohling et al., 2002b). The onset of the freshwater flooding discussed in the paper is also indicated. The age scale (right) is based on linear interpolation between the estimated ages of 124 and 119 ka BP for the depletion and enrichment trends in $\delta^{18}O_{ruber}$ preceding and following the S5 onset and end, respectively.

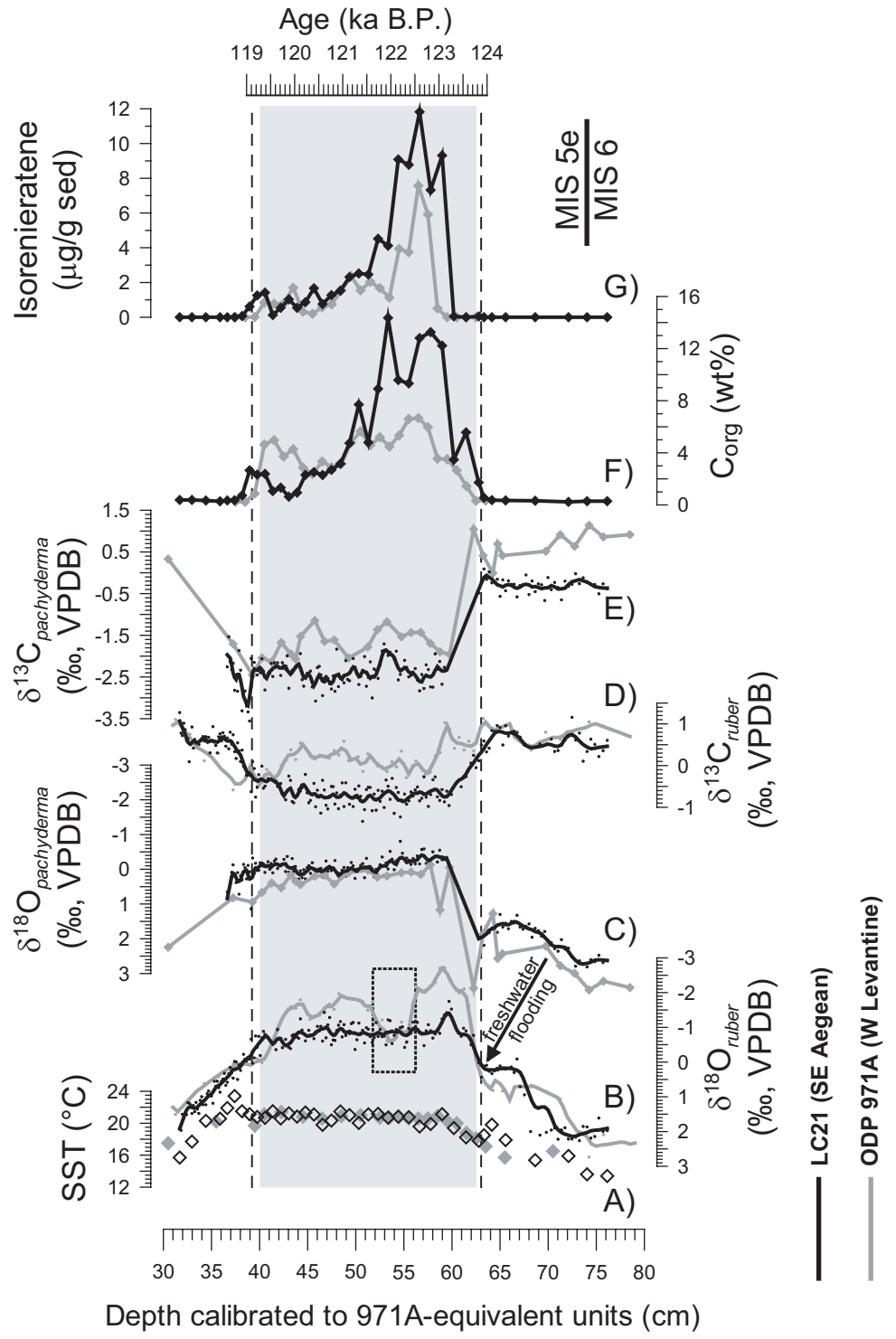
Age (ka B.P.)
119 120 121 122 123 124
Isorenieratene (µg/g sed)
MIS 5e
MIS 6
G)
F)
C_{org} (wt%)
$\delta^{13}C_{pachyderma}$ (‰, VPDB)
E)
D)
$\delta^{13}C_{ruber}$ (‰, VPDB)
$\delta^{18}O_{pachyderma}$ (‰, VPDB)
C)
freshwater flooding
$\delta^{18}O_{ruber}$ (‰, VPDB)
SST (°C)
B)
A)
LC21 (SE Aegean)
ODP 971A (W Levantine)
30 35 40 45 50 55 60 65 70 75 80
Depth calibrated to 971A-equivalent units (cm)

In Aegean core LC21, changes in $\delta^{18}O_{ruber}$ appear to closely track $\delta^{18}O_{pachyderma}$ within S5 (Figure 1.4B), which contrasts with strong variable offsets between $\delta^{18}O_{ruber}$ and $\delta^{18}O_{pachyderma}$ in 971A (Figure 1.4A). As the isotopic signals in *G. ruber* (w) were reconstructed to represent near-surface conditions in the summer mixed layer (Rohling et al., 2004), the similarity between $\delta^{18}O_{ruber}$ and $\delta^{18}O_{pachyderma}$ in LC21 suggests that both species inhabited water masses with rather similar properties. This agrees with modern observations that the south-eastern Aegean site of LC21 is directly in the path of northward inflow of Levantine surface water (Theocharis et al., 2002), which derives from the area where Levantine intermediate water is formed, and that the intermediate water itself reaches depths as shallow as 70 m in the Aegean due to prevailing northerly winds and the basin's general cyclonic circulation (Poulos et al., 1997; Pinardi and Masetti, 2000; Zervakis et al., 2004). These conditions were found to also prevail during times of decreased eastern Mediterranean net evaporation, as reconstructed for the Holocene period of S1 deposition (Casford et al., 2002). Modelling studies also suggest that these are robust long-term features of the eastern Mediterranean circulation (Myers et al., 1998).

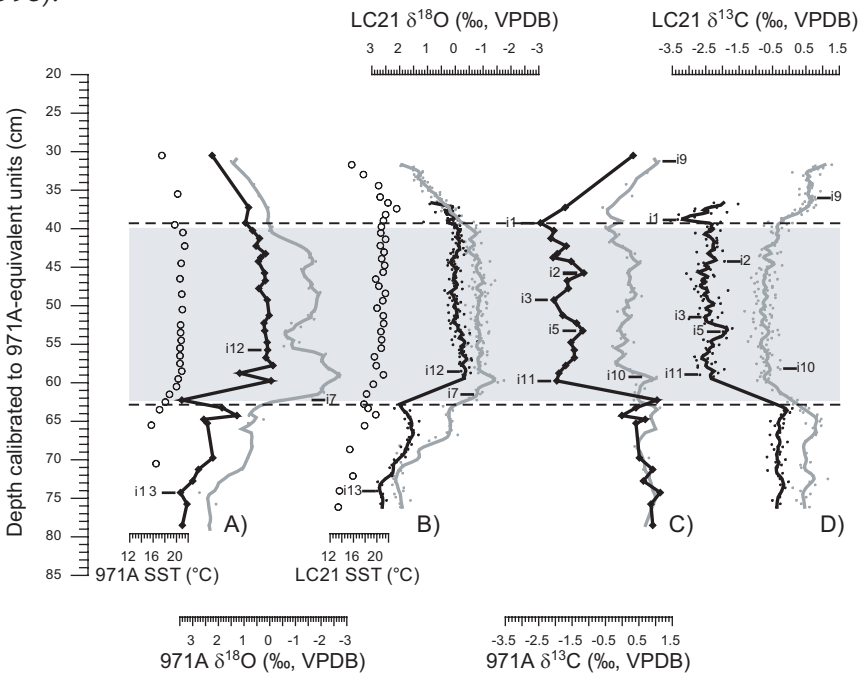

Figure 1.4: (A): alkenone-based SST (open circles), $\delta^{18}O_{pachyderma}$ (black line), and $\delta^{18}O_{ruber}$ (grey line) records in 971A. **(B)**: alkenone-based SST (open circles), $\delta^{18}O_{pachyderma}$ (black line), and $\delta^{18}O_{ruber}$ (grey line) records in LC21. **(C)**: $\delta 13C_{pachyderma}$ (black line), and $\delta^{13}C_{ruber}$ (grey line) records in 971A. **(D)**: $\delta^{13}C_{pachyderma}$ (black line), and $\delta^{13}C_{ruber}$ (grey line) records in LC21. Labels identify correlation markers (Table 1.1).

Given the observation that the $\delta^{18}O_{pachyderma}$ values are very similar through S5 at both sites LC21 and 971A, the strong contrast between $\delta^{18}O_{ruber}$ and $\delta^{18}O_{pachyderma}$ in 971A can be entirely attributed to variability in $\delta^{18}O_{ruber}$. The $\delta^{18}O_{ruber}$ signal in 971A displays much lighter values (the offset from $\delta^{18}O_{pachyderma}$ reaches more than 1.5‰; see Figure 1.4A) and also is much more variable than in LC21 (Figure 1.3B). Since both sites show very similar SST developments (Figure 1.3A), this difference in $\delta^{18}O_{ruber}$ is unlikely to have resulted from SST changes. The $\delta^{18}O_{ruber}$ differences within S5 contrast with the distinct similarity of $\delta^{18}O_{ruber}$ at the two sites before and after S5. The observed differences between the $\delta^{18}O_{ruber}$ signals within S5, along with high similarity of $\delta^{18}O_{pachyderma}$ and SST signals in LC21 and 971A as well as other sites throughout the eastern Mediterranean (Rohling et al., 2002b), may only be explained by very limited interaction between surface and intermediate waters at the location of Site 971A, which is remote from the intermediate-water source region.

Spatially, site 971A shows the lightest $\delta^{18}O_{ruber}$ values throughout the open eastern Mediterranean (Rohling et al., 2002b), similar to patterns found for other sapropels (Rohling and De Rijk, 1999; Emeis et al., 2003). This has been ascribed to extensive (monsoon-fuelled) freshwater drainage along the wider Northern African margin, through currently dry river (wadi) systems, supplementing - but more variable than - Nile river discharge (Rohling et al., 2002b, 2004; Scrivner et al., 2004).

Remarkably, $\delta^{18}O_{ruber}$ values in the brief interval of reduced discharge (Rohling et al., 2002b) from the wider N African margin (56-52 cm in 971A) fall back to the typical $\delta^{18}O_{ruber}$ values found throughout S5 in LC21 (Figure 1.3B). This suggests that the Aegean record reflects an underlying $\delta^{18}O_{ruber}$ controlled by a less intense freshwater dilution that is most likely due to propagation throughout the basin of the sea surface freshening caused by North African river input into the open eastern Mediterranean (Rohling et al., 2002b; Scrivner et al., 2004). Superimposed on this widespread 'average' mixed signal, large regional $\delta^{18}O_{ruber}$ anomalies are found in the open eastern Mediterranean which reflect the more direct impacts of the river-borne monsoon flooding (with a focus on the area of Site 971A).

LC21 and 971A simultaneously reach the lightest $\delta^{18}O_{ruber}$ values, some 650±250 years after the sharp $\delta^{18}O_{ruber}$ shift that marks the onset of freshwater flooding into the basin (Figure 1.3B). This peak in eastern Mediterranean sea surface freshening coincides with the appearance of very light $\delta^{13}C_{pachyderma}$ values (lighter by about 2‰ than $\delta^{13}C_{ruber}$, see Figure 1.4) at both sites, following about 400 years of near absence of this species throughout the eastern Mediterranean (Rohling et al., 2006). The shift to light $\delta^{13}C_{pachyderma}$ values, observed in both

records, has been suggested to reflect the close proximity of a subsurface reservoir of isotopically light metabolised carbon to the subsurface habitat of *N. pachyderma* (Rohling et al., 2006). At the same level in LC21, high concentrations appear of isorenieratene (>9 μg/g sed.), a specific aromatic carotenoid of anaerobic, photolithotrophic green sulphur bacteria (Chlorobiaceae) (Figure 1.3G). These bacteria require both sulphide and light (Repeta et al., 1989; Koopmans et al., 1996; Passier et al., 1999). Similar to the reconstruction for the open eastern Mediterranean (Rohling et al., 2006), the sudden appearance of high isorenieratene concentrations in the Aegean Sea, combined with the occurrence of sub-thermocline foraminiferal species (e.g. *N. pachyderma*), reflects the development of euxinic conditions throughout the Aegean water-column up to about 200 m. Comparison of LC21 with 971A (Figure 1.3G) illustrates that such conditions had developed in the Aegean Sea about 100±40 to 300±120 years before they became established in the open eastern Mediterranean.

A clear sequence of causes and effects can now be summarised for the last interglacial episode of freshwater flooding into the eastern Mediterranean. Given that benthic azoic conditions and a sharp C_{org} increase developed immediately following the onset of surface freshening (from one sample to the next in LC21), we infer that Aegean ventilation experienced a complete collapse within 40±20 years in response to the change in hydrological forcing, despite the fact that most of the hydrological change was predominantly driven by monsoon flooding into the open eastern Mediterranean rather than being centred directly on the Aegean Sea. Increased preservation of C_{org} due to oxygen starvation (Moodley et al., 2005), first at the sea floor and then rapidly throughout the water column (Bianchi et al., 2006), would (partly) explain the large jump in the C_{org} record (Figure 1.3F). Within ~650 years, euxinic conditions had expanded through the Aegean water column to depths of 200 m or less, fuelling populations of Chlorobiaceae, with concomitant shoaling of the reservoir of isotopically light metabolised carbon into the habitat of *N. pachyderma* (d). Some 100 to 300 years later, euxinic conditions reached similar depths in the open eastern Mediterranean (Figure 1.3G).

1.5. Conclusions

Our results highlight an intriguing similarity in the timescale of Aegean response to climatic forcing between the recent and the last interglacial events. In the mid-1960s, construction of major dams, such as the Aswan High Dam, initiated a relatively long-term (estimated 80 year) adjustment in the basin to the effects of enhanced net evaporation (Rohling and Bryden, 1992). This has been proposed as an important multi-decadal preconditioning for the modern eastern

Mediterranean hydrographic changes (Boscolo and Bryden, 2001; Skliris, and Lascaratos, 2004; Skliris et al. 2007). Here we find that another dramatic Aegean-focussed response occurred during the last interglacial within a remarkably similar period of time (less than 40±20 years), even though that response was to a perturbation in the eastern Mediterranean freshwater budget of the opposite sign.

Combined with the instrumental record of the EMT, our findings for the S5 period highlight an exceptional sensitivity of the Aegean to changes in wider eastern Mediterranean climatic forcing of any sign, with responses that lead to profound hydrographic adjustments that subsequently propagate throughout the open eastern Mediterranean, and which potentially affect even the North Atlantic (Millot et al., 2006). Both increases (preconditioning modern changes) and decreases (this study) in eastern Mediterranean net evaporation are found to drive basin-scale reorganisations in subsurface water-mass dynamics with extensive ecological impacts.

Chapter 2

Hydrogen isotopic compositions of long-chain alkenones record freshwater flooding of the Eastern Mediterranean at the onset of sapropel deposition

Based on:
Marcel T.J. van der Meer, Marianne Baas, W. Irene C. Rijpstra, Gianluca Marino, Eelco J. Rohling, Jaap S. Sinninghe Damsté, and Stefan Schouten

Published in *Earth and Planetary Science Letters*, vol. 262, no. 3-4, p. 594-600

Abstract

Sapropels are organic-rich sediment layers that were intermittently deposited in the Mediterranean Sea, especially in its eastern basin, during the last 13.5 million of years. The associated anoxic events that gave rise to sapropel formation resulted indirectly from the impact of African monsoon maxima on the basin's hydrography. Sharp shifts in oxygen isotopes ($\delta^{18}O$) to values more depleted in the heavy isotope (^{18}O) in carbonates from surface-dwelling planktonic forminifera, slightly preceding sapropel deposition, suggest that the Mediterranean was flooded by large amounts of freshwater leading to the development of a low salinity of the surface water and a strong density stratification of the water column. However, the degree of freshwater flooding and concomitant drop in sea surface salinity (SSS) remain elusive. Recent work has shown that the hydrogen isotope (δD) values of long-chain alkenones produced by haptophyte algae depend mainly on the δD of the water and on salinity, and may therefore offer a new tool for salinity reconstructions. Our analysis of the δD of alkenones from last interglacial sapropel S5 from the Aegean Sea shows a large decrease in δD of 25‰ at the onset of sapropel formation, suggesting a drop in SSS of 6, from 39 to 33. Although the absolute SSS estimates should be interpreted with care as they are subject to relatively large uncertainties, the estimated SSS values appear quite reasonable as they, for example, yield SSS before sapropel deposition similar to that of the present day Aegean Sea. To reduce uncertainties in SSS estimates, the δD-salinity relationship has to be better constrained with cultures and also tested in field studies. However, our results do illustrate the promise of a combined use of δD of alkenones, $U^{k'}_{37}$ of alkenones, and $\delta^{18}O$ of surface dwelling planktonic foraminifera, for SSS reconstructions.

2.1. Introduction

Sapropels are organic-rich sediment layers that were deposited in the Mediterranean (especially in the eastern Mediterranean; i.e., east of the Strait of Sicily) at times of orbitally induced insolation maxima (Rossignol-Strick et al., 1982; Rossignol-Strick, 1983, 1985). These sapropels are often readily visually recognizable by their distinctly dark color and are associated with times of anoxia in the water column, even extending towards the photic zone (Passier et al., 1999; Menzel et al., 2002; Rohling et al., 2006; Chapter 1). The anoxic events that gave rise to sapropel formation reflect an indirect impact of African monsoon maxima on the basin's hydrography. This impact concerns the routing of African monsoon precipitation into the Mediterranean via the Nile River (Rossignol-Strick et al., 1982; Rossignol-Strick, 1983, 1985) and other, currently dry, systems along the wider

North African margin (Rohling et al., 2002b). It has also been suggested, based on metal signatures, that significant amounts of freshwater arrived in the eastern Mediterranean Sea from the Southern European continent (Rinna et al., 2002). At the onset of sapropel deposition the Mediterranean was flooded by large amounts of freshwater leading to the development of low salinity surface water and inducing a strong density stratification of the water column.

Sapropel S5 formed during one of the insolation/monsoon maxima of the last interglacial period (124-119 thousand years Before Present; ka BP). This monsoon maximum was interrupted by a dry interlude of several centuries, with concomitant cooling over the north of the basin (Rohling et al., 2002b; Rohling et al., 2004). The S5 sapropel is intensely developed, characterized by high organic carbon accumulation rates (e.g., Fontugne and Calvert, 1992), a lack of benthic fossils that suggests persistent anoxia below 300 m water depth (Rohling and Gieskes, 1989; Rohling et al., 1993), and the presence of the carotenoid isorenieratene which indicates euxinia at the base of the photic layer (Rohling et al., 2006, Chapter 1). Previous studies have attempted to quantify the freshwater flooding that promoted the development of stratification and collapse of deep-sea ventilation that caused sapropel formation (Rohling, 1999; Rohling et al., 2004), particularly with respect to the strong $\delta^{18}O$-depletion in surface dwelling planktonic foraminifera (up to 3.5‰) at the onset of sapropel formation. However, the degree of freshwater flooding and concomitant drop in sea surface salinity (SSS) is uncertain due to several factors which affect the isotopic composition of water/foraminifera (e.g., evaporation, isotopic composition of precipitation and runoff, sea-water temperature, etc.). Previous studies have, therefore, used modeling (Rohling et al., 2004) and simplified $S:\delta^{18}O$ relationships to arrive at estimates of past salinity changes during sapropel formation.

Krishnamurthy et al. (2000) used an alternative approach to estimate the amount of freshwater flooding, by analyzing the δD of bulk organic matter in sapropels. They found a substantially depleted δD signal within sapropels compared to the adjacent marls in the Tyrrhenian Sea, also suggesting a substantially enhanced flux of freshwater and drop in SSS during sapropel deposition. However, bulk organic matter represents different types of organic matter from all kind of different sources, including organic compounds that may have exchanged hydrogen atoms with their environment (e.g., Schimmelmann et al., 2004).

A potentially new tool for salinity reconstructions considers δD values of long-chain alkenones produced by haptophyte algae, since they only possess covalently bound hydrogen atoms, which are not likely to be exchanged during diagenesis (Sessions et al., 2004). Paul (2002) found that the fractionation between δD of the culture medium water and the C_{37} alkenones produced by *Emiliania*

huxleyi was relatively constant at about 232‰ when varying the δD value of the culture medium. Englebrecht and Sachs (2005) reported a similar fractionation of about 225‰. However, recent work on *E. huxleyi* and another common oceanic haptophyte algae, *Gephyrocapsa oceanica*, cultured at different salinities and temperatures, suggests that hydrogen isotope fractionation by these algae depends both on the δD of the water and on salinity, and to some degree growth rate (Schouten et al., 2006). Thus, the δD of C_{37} alkenones of *E. huxleyi* largely depends on salinity and the δD of water, which itself is again strongly correlated with salinity (Mook, 2001). Salinity changes, therefore, form a key aspect of changes in the δD of C_{37} alkenones, suggesting it could be useful as a paleosalinity proxy.

In this study we analyzed the δD of alkenones in the S5 sapropel from the Aegean Sea (cf. Chapter 1) and compared that with the $\delta^{18}O$ of carbonates from surface dwelling foraminifera. In addition, we estimated SSS based on our δD record and the $\delta^{18}O$ of carbonates from surface dwelling foraminifera in combination with $U^{k'}_{37}$ based sea surface temperature reconstructions.

2.2. Materials and Methods

Samples analyzed are from the S5 sapropel retrieved from south-eastern Aegean Sea core LC21, recovered in 1995 during the EC-MAST2 (Marine, Science, and Technology Programme) PALEOFLUX (Biogeochemical Fluxes in the Mediterranean Water-Sediment System) program (35°40'N; 26°35'E; 1522 m water depth; see Figure 1.1 in Chapter 1). For this core, stable oxygen and carbon isotope records of the carbonate tests of shallow (*Globigerinoides ruber*) and subthermocline (*Neogloboquadrina pachyderma*) dwelling planktonic foraminifera, total organic carbon (C_{org}), $U^{k'}_{37}$ sea surface temperatures, and isorenieratene concentrations have been previously reported in Chapter 1.

For determination of δD of alkenones sediment core slices were extracted ultrasonically using methanol, methanol:dichloromethane (1:1, v:v) and dichloromethane. The total lipid extract was separated using column chromatography with aluminium oxide as stationary phase and a mixture of hexane and dichloromethane (9:1, v:v) to elute the apolar fraction and a mixture of hexane and dichloromethane (1:1, v:v) to elute the alkenone fraction.

Alkenone fractions were analyzed by gas chromatography (GC) using a Agilent 6890 gas chromatograph with a flame ionization detector using a fused silica capillary column (25m x 0.32 mm) coated with CP Sil-5 (film thickness = 0.12 μm) with helium as carrier gas. The fractions (in ethyl acetate) were injected on-column at 70 °C. The oven was programmed to subsequently increase the temperature to 130 °C with 20 °C min^{-1}, and then with 4 °C min^{-1} to 320 °C at

which it was held isothermal for 10 min.

Compound-specific hydrogen isotopic compositions of the alkenones were determined by GC/thermal conversion/isotope ratio monitoring mass spectrometer using a Thermo Electron DELTA^{Plus} XL mass spectrometer. GC conditions were similar to conditions for GC analysis except that the film thickness of the CPSil 5 column was 0.4 mm and that a constant flow of He was used at 1.5 ml min^{-1}. Compounds were pyrolyzed at 1450 °C in an empty ceramic tube, which was pre-activated by a methane flow of 0.5 ml min^{-1} for 5 min. H_3^+-factors were determined daily on the isotope mass spectrometer and varied between 2 and 3. H_2 gas with known isotopic composition was used as reference and a mixture of C_{16}-C_{32} *n*-alkanes of known isotopic composition (ranging from -42‰ to -256‰ vs. VSMOW) was used to monitor the performance of the system. The average offsets between the measured hydrogen isotopic composition of the C_{16}-C_{32} *n*-alkanes and their values determined off-line were generally 5‰ or less. Analyses were done at least in duplicate and the reproducibility was always better than 7‰. A squalane standard was co-injected with every sample and its average value was -171±5‰ which compared favorably with its offline determined value of -170‰.

2.3. Results and Discussion

2.3.1. Stable hydrogen isotopic composition of C_{37} alkenones

The onset of S5 sapropel deposition occurs at about 1005 cm sediment depth as indicated by C_{org} values rising from about 0.3% below the sapropel to an initial maximum of about 13% within the sapropel at about 985 cm depth. After a decrease to about 9% at 970 cm depth a maximum C_{org} content of about 14% is reached at about 965 cm depth. Above 965 cm sediment depth C_{org} values slowly drop to about 0.3% at 875 cm depth (Chapter 1) indicating that sapropel deposition has ended (see Figure 1.2 in Chapter 1).

The hydrogen isotope composition of the C_{37} alkenones is about -185‰ below the S5 sapropel. It then rapidly decreases to about -210‰ at the base of the S5 sapropel before it slowly returns to about -190‰, close to the pre-sapropel value, before sapropel deposition ended and then remained more or less constant (Figure 2.1D). Based on the culture studies by Schouten et al. (2006) for alkenone-producing algae, the large shift in δD can be explained by three factors: salinity; growth rate; and δD of water. Growth rate is likely to have had a minor effect as extremely large increases in growth rate would be needed to cause a 25‰ depletion in δD (Schouten et al., 2006). Furthermore, analysis of Pliocene (5.3 to 1.8 Ma) eastern Mediterranean sapropels showed that C_{37} alkenones within sapropels

are slightly depleted in ^{13}C relative to values below the sapropel (Menzel et al., 2003). As $\delta^{13}C$ of alkenones strongly depends on growth rate (Laws et al., 1995; Popp et al., 1998) this depletion suggests a slight decrease in haptophyte growth rates. Likely, the increase in bulk primary production during deposition of the S5 sapropel is mainly due to enhanced diatom production, rather than increased haptophyte production (Kemp et al., 1999; Giunta et al., 2006). Thus, the large depletion in δD of C_{37} alkenones during the onset of sapropel deposition was caused by either a large depletion in δD of the water, a substantial lowering in SSS,

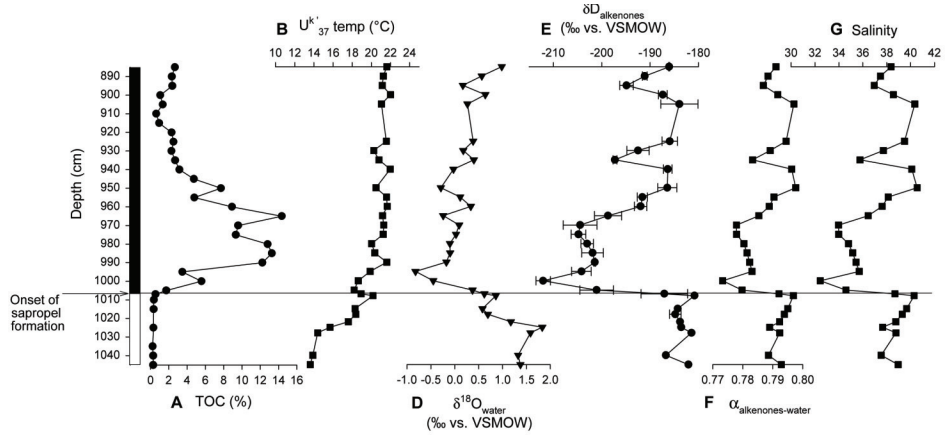

Figure 2.1: Stratigraphic record of south eastern Aegean Sea core LC21 from the Mediterranean Sea. **(A)**: Total organic carbon (C_{org}) in weight percent (wt%) (from Chapter 1). **(B)**: $U^{k'}_{37}$ sea surface temperatures in degree Celsius (°C) (from Chapter 1). **(C)**: $\delta^{18}O_{water}$ in ‰ vs VSMOW. **(D)**: $\delta D_{alkenones}$ in ‰ vs. VSMOW. **(E)**: $\alpha_{alkenones\text{-}water}$. **(F)**: estimated sea surface salinities. Solid line indicates onset of sapropel deposition as indicated by elevated C_{org} contents. The bar next to the depth scale indicates the pre-sapropel layer (white) and sapropel layer (black).

Further clues on the cause of the depletion in δD of C_{37} alkenones can be obtained by examining the $\delta^{18}O$ of foraminiferal carbonate shells which depends on both $\delta^{18}O$ of the sea water ($\delta^{18}O_{water}$) and temperature (e.g., Erez and Luz, 1983; Bemis et al., 1998) whereby the ^{18}O of the sea water co-varies with salinity. By combining the $\delta^{18}O$ record of the surface dwelling planktonic foraminifer *Globerigerinoides ruber* with sea surface temperature (SST) estimates from long-chain alkenones (the $U^{k'}_{37}$ index, with SST (°C) = ($U^{k'}_{37}$ -0.044)/0.033, Müller et al., 1998; Figure 2.1B) we obtain estimates of $\delta^{18}O_{water}$ using the temperature-^{18}O fractionation equation of Bemis et al.(1998):

$$T(°C) = 16.5 - 4.80\ (\delta^{18}O_{carbonate\ shell} - \delta^{18}O_{water}) \qquad (1)$$

The results suggest that $\delta^{18}O_{water}$ was around 1.5‰ and shifted, prior to

sapropel deposition, to lighter values of about 1.0‰ (Figure 2.1C). At the onset of sapropel deposition there was large shift of about 1.5‰ towards even lighter values (Figure 2.1C). During sapropel deposition, $\delta^{18}O_{water}$ values slowly returned to just below pre-sapropel values. After sapropel deposition has ended the $\delta^{18}O_{water}$ values finally return to pre-sapropel values. The timing and direction of these shifts in $\delta^{18}O_{water}$ coincide in general with those in δD of alkenones, i.e., large shifts towards light values during the onset of sapropel deposition and gradual return to pre-sapropel values during sapropel deposition. This confirms that the alkenone δD record reflects changes in the δD of water and/or SSS. The two-step shift in $\delta^{18}O_{water}$ to lighter values is not evident in the δD record. We note that the initial $\delta^{18}O_{water}$ shift coincides with the start of an increase in the $U^{k'}_{37}$-derived SSTs. It is, therefore, unclear whether the decrease in $\delta^{18}O_{ruber}$ reflects an actual decrease in $\delta^{18}O_{water}$ or an even larger temperature shift for *G. ruber* compared to that experienced by haptophyte algae.

The δD of eastern Mediterranean surface water (δD_{water}) can be estimated from the $\delta^{18}O$ of the water using the eastern Mediterranean Meteoric Water Line (MMWL; Gat and Carmi, 1987; Bar-Matthews et al., 2003):

$$\delta D_{water} \cong (8 \times \delta^{18}O_{water}) + d \qquad (2)$$

with d = deuterium excess. For the MMWL d is 22‰ rather than the global average of 10‰ due to local circumstances (e.g., evaporation, water source, prevailing winds etc.). The deuterium excess (d) during the last interglacial has been shown to be similar to that of the present day MMWL (McGarry et al., 2004). For evaporative basins, such as the eastern Mediterranean, it has been shown that the ratio of changes in δD_{water} and $\delta^{18}O_{water}$ (i.e., $\Delta\delta D_{water}/\Delta\delta^{18}O_{water}$ or the slope of the meteoric waterline) is lower than that of the general meteoric waterline (Craig and Gordon, 1965; Gat, 1996). As a first approximation, we assume that the ratio was closer to 6 before and after S5 (when net evaporation was more dominant), and higher during S5 (when net evaporation was reduced). For our salinity estimations we assumed a constant slope of 7 and constant d of 22‰ (the effect of different slopes and intercepts on the SSS estimates is discussed below). The $\delta^{18}O$ - δD relationship of the eastern Mediterranean surface water thus becomes:

$$\delta D_{water} \cong (7 \times \delta^{18}O_{water}) + 22 \qquad (3)$$

At the onset of sapropel deposition, $\delta^{18}O_{water}$ decreased by 2.2‰ and thus the reconstructed changes in δD_{water} are at most 15‰, which cannot explain the entire 25‰ shift in the δD of alkenones (Figure 2.1D). Thus, fractionation between δD of alkenones and δD_{water} has substantially increased at the onset of the S5 sapropel deposition and, in view of the culture results (Schouten et al., 2006), salinities must thus have decreased substantially. The substantial lowering of SSS is

in agreement with results from many previous studies based on $\delta^{18}O$ ratios in carbonate tests of foraminifera (Rossignol-Strick et al., 1982; Rossignol-Strick, 1983, 1985; Rohling et al., 2002b; Chapter 1).

2.3.2. Estimation of paleosalinities of the Aegean Sea during S5 sapropel deposition

Based on the results reported above we can estimate paleosalinities from the hydrogen isotopic fractionation of alkenone-producing algae. The dominant haptophyte alga in the eastern Mediterranean during Marine Isotope Stage 5e (i.e., the last interglacial maximum) was *G. oceanica* (Giunta et al., 2006). We can estimate SSS using the isotopic fractionation factor α:

$$\alpha_{\text{alkenones - water}} = (1000 + \delta D_{\text{alkenones}}) / (1000 + \delta D_{\text{water}}) \quad (4)$$

and the results of Schouten et al. (2006) for hydrogen isotope fractionation by *G. oceanica*:

$$\alpha_{\text{alkenones - water}} = (0.0030 \times S) + 0.676 \quad (5)$$

where α (Figure 2.1E) is the fractionation factor and S is salinity (Figure 2.1F). The δD_{water} can be estimated from the combination of $\delta^{18}O$ ratios in the carbonate tests of *G. ruber* (see Chapter 1), the $U^{k'}_{37}$ SSTs (see Chapter 1) and the MMWL as described above. Our salinity reconstruction suggests absolute SSS at the base of the S5 sapropel to be about 39 followed by a 6 decrease at the onset of S5 sapropel deposition to about 33 (Figure 2.1F). After the initial freshening the SSS slowly returns to more or less pre-sapropel values (Figure 2.1F).

The estimated SSS values seem quite reasonable as they, for example, yield similar SSS as the present day Aegean Sea, i.e., 39, before sapropel deposition. Furthermore, the pattern and magnitude of change in SSS look remarkably similar to those modeled by Rohling et al. (2004) for the upper surface water layers during deposition of different S5 sapropels. Thus, it seems that the hydrogen isotopic composition of alkenones can yield reasonable estimates for the patterns and amplitudes of past SSS changes.

The absolute SSS estimates (Figure 2.1F), however, should be interpreted with care as they are subject to relatively large uncertainties. Besides the above assumptions that have been made in order to calculate the SSS estimates, error propagation, especially in the empirically determined correlation between α and salinity (Equation 5), results in a large error in the estimated SSS values. To investigate this we performed a sensitivity analysis of our salinity estimates for the different parameters used in our calculations. One uncertainty relates to the slope

in the MMWL which can range between 6 and 8 (see above). Changing the slope from 6 to 8 yields only relatively small changes in SSS estimates of less than 1. An uncertainty in the deuterium excess d of the MMWL of 1‰ results in an uncertainty of ±0.3 in the SSS estimates. Hence, the uncertainties in Equation 3 are leading to an error in the SSS estimates of <1. The by far largest uncertainty comes from the α salinity relationship because of the relatively large scatter (R^2=0.61). The uncertainty in the slope 0.003±0.001 results in uncertainty in SSS estimates of ±16 from the estimates presented here. The uncertainty in the intercept, 0.676±0.03 results in uncertainty in the salinity estimates of ±10. Thus, to reduce the uncertainties in our SSS estimates, the δD-salinity relationship has to be better constrained in cultures and also tested in field studies. Nevertheless, the reasonable SSS estimates calculated here for the S5 sapropel in the Aegean Sea show that the combined use of δD of alkenones, $U^{k'}_{37}$ of alkenones and $\delta^{18}O$ of the carbonate tests of planktonic foraminifera may be a promising tool for SSS reconstructions.

2.4. Conclusions

Our δD record of C_{37} alkenones, produced by haptophyte algae, from the eastern Mediterranean shows a large and abrupt shift towards more negative values at the onset of sapropel deposition. This change runs parallel with that of the $\delta^{18}O$ of the carbonate tests of surface dwelling planktonic foraminifer *Globigerinoides ruber* suggesting that δD of C_{37} alkenones accurately records the large decrease in sea surface salinity during freshwater flooding. Based on the δD of the water, calculated from the $\delta^{18}O$ of foraminifera and $U^{k'}_{37}$ sea surface temperatures, and the δD of C_{37} alkenones we can estimate that the salinity shift at the onset of S5 sapropel deposition was approximately 6, from about 39 to about 33.

Chapter 3

Early and middle Holocene in the Aegean Sea: interplay between high and low-latitude climate variability

Based on:
Gianluca Marino, Francesca Sangiorgi, Eelco J. Rohling, Angela Hayes, James L. Casford, André F. Lotter, Michal Kucera, and Henk Brinkhuis

To be submitted

Abstract

The Aegean region resides at the boundary between the high- to mid-latitude and the tropical/subtropical climate systems. The latitudinal shift with the seasons of this boundary controls the region's seasonal climate and hydrography. Obtaining co-registered season-specific proxy records for sea surface temperature (SST) and hydrography from the Aegean Sea may therefore be critical to advance our understanding of the large-scale climate interactions during past episodes of climate change. Here we focus on the early to mid Holocene interval of Northern Hemisphere insolation/monsoon maximum. We reconstruct the south-eastern Aegean $\delta^{18}O_{seawater}$ and note a distinct negative shift (1.5‰) between 10.6 and 9.6 ka BP. This decrease in surface-water $\delta^{18}O$ represents the regional expression of the intensification of the African monsoon and its related freshwater flooding, which affected the entire eastern Mediterranean during the early to mid Holocene. A virtually contemporaneous shift of similar magnitude has been noted in $\delta^{18}O_{speleothem}$ at Soreq Cave (northern Israel). Consequently, we suggest that the $\delta^{18}O_{speleothem}$ changes may not be due to changes in the amount of precipitation over the cave's catchment area, but instead may reflect our reconstructed changes in the isotopic composition of the moisture source region (Aegean-Levantine basin). Superimposed upon these long-term hydrographic changes are Aegean multicentennial episodes of winter cooling of maximum 1.8°C. These episodes display a positive correlation with non-seasalt K^+ series from the Greenland GISP2 ice core, suggesting that they were intimately linked to meridional displacements of the atmospheric polar vortex. The three main episodes of Aegean winter cooling at ~10.5 ka BP, 9.8-9.1 ka BP and 8.6-8.0 ka BP are found to coincide closely with previously described centennial-scale deteriorations of the Indian summer monsoon. We propose a linking mechanism by which Eurasian winters of increased severity led to more pronounced snow cover in the Asian highlands, causing delayed/weakened summer monsoons, and contemporaneous yet independent intensification of the Siberian High. Finally, we report the first indications of a particularly sharp Aegean cooling event between 8.3 and 8.15 ka BP, embedded within the general cooling episode of 8.6-8.0 ka BP. In both timing and duration, this sharp event agrees with the so-called 8.2 ka BP event reported from several records from the wider North Atlantic region, which has been related to a brief weakening of the Atlantic Meridional Overturning Circulation.

3.1. Introduction

During the current interglacial period (Holocene, since 11.5 thousand years Before Present, ka BP) the Earth's climate has experienced considerable fluctua-

tions on centennial to millennial timescales (for an overview, see Mayewski et al., 2004). A variety of studies has noted a close temporal relationship between these fluctuations and intervals of reduced solar output, as inferred from cosmogenic isotope series (among many others Denton and Karlén, 1973; O'Brien et al., 1995; Bond et al., 2001; Neff et al., 2001; Rohling et al., 2002a; Mayewski et al., 2004; Maasch et al., 2005). In addition, superimposed sharp climate anomalies have occurred in the wider North Atlantic region, especially during the early Holocene (e.g., Alley et al., 1997; von Grafenstein et al., 1998; Risebrobakken et al., 2003; Alley and Ágústsdóttir, 2005; Rohling and Pälike, 2005; Ellison et al., 2006; Thomas et al., 2007; Marshall et al., 2007; Kobashi et al., 2007; Rasmussen et al., 2007). These are thought to be related to reductions in the Atlantic Meridional Overturning Circulation (AMOC) (Ellison et al., 2006) due to meltwater injections into the northern North Atlantic (Barber et al., 1999; Hillaire-Marcel et al., 2007).

Model experiments suggest that the climate impacts of meltwater-forced AMOC disturbances may not have been restricted to the North Atlantic region, but were noticeable throughout the Northern Hemisphere (Renssen et al., 2001, 2002; Wiersma and Renssen, 2006; LeGrande et al., 2006). Rohling and Pälike (2005) collated data for the most extreme of such events, centred on 8.2 ka BP, and concluded that the sharp anomaly (~160 years in duration, Thomas et al., 2007) was superimposed upon a multi-centennial climate change and may have been considerably weighted towards winter. Accordingly, they called for season-specific and carefully constrained proxy records to trace the true extent of the sharp anomaly, and thus advance our understanding of the impacts of AMOC reductions on the wider Northern Hemisphere climate.

The present study follows the approach of establishing co-registered summer- and winter-specific proxy records obtained from a key region that is sufficiently distant and isolated from the North Atlantic not to be directly affected by its oceanic circulation: the Aegean Sea (north-eastern Mediterranean). By compiling a variety of season-specific and highly resolved sea-surface proxy records that are co-registered within the same archive/sample-set, we reconstruct changes in winter and summer sea-surface temperatures and hydrography of the Aegean Sea during the early to mid Holocene. The proxies employed are: qualitative winter sea surface temperature (SST) reconstructions based on organic-walled dinoflagellate cyst (dinocyst) abundances; quantitative (artificial neural network, ANN) summer and winter SST reconstructions based on planktonic foraminiferal census counts; and hydrographic reconstructions based on planktonic foraminiferal oxygen isotope ($\delta^{18}O$) data that together with the ANN SST data yield seawater $\delta^{18}O$. To assess causal relationships and large-scale climate interactions, we compare our (season-specific) Aegean Sea reconstructions with paleoclimate proxy records from

key high-to-low-latitude regions of the Northern Hemisphere, namely Greenland (Grootes et al., 1993; Mayewski et al., 1997; Rasmussen et al., 2007), the northern North Atlantic (Ellison et al., 2006), Northern Israel (Soreq Cave) (Bar-Matthews et al., 2000) and Southern Oman (Qunf Cave) (Fleitmann et al., 2003) (Figure 3.1).

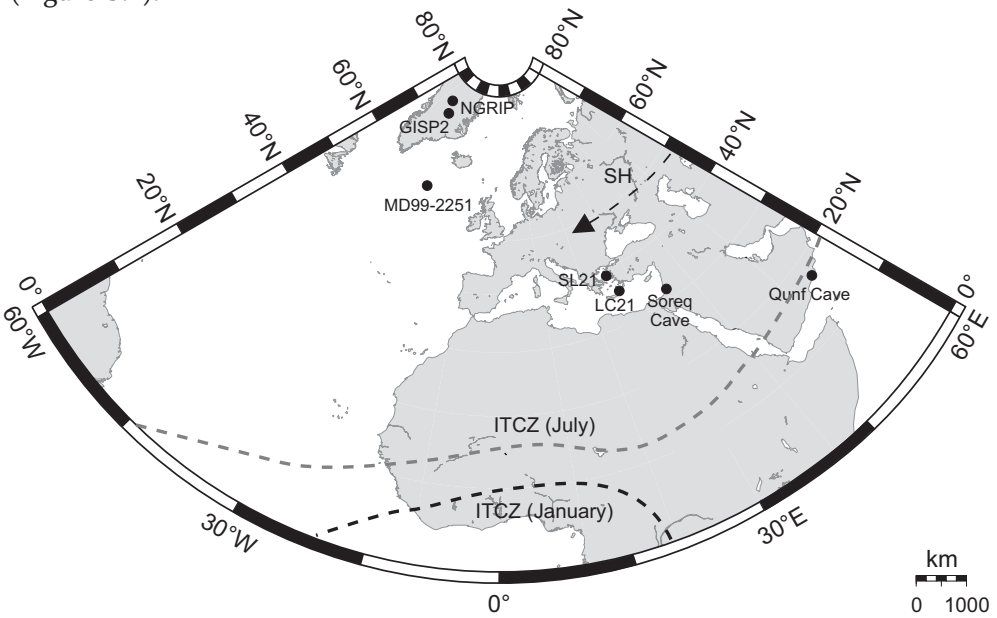

Figure 3.1: Map showing locations of the sites discussed in the text. Greenland Summit (GISP2 and NGRIP ice cores), the Aegean Sea (sediment cores LC21 and SL21) and the Middle East speleothems (Soreq and Qunf Caves). Black and dark grey dashed lines indicate the present day mean January and July latitudinal position of the Intertropical Convergence Zone (ITCZ), respectively. The dashed arrow tracks the westward ridging of the Siberian High (SH) towards northwest Europe and southern Scandinavia during winter/spring.

3.2. Rationale: Why the Aegean Sea?

The Aegean Sea is distant and virtually isolated from the North Atlantic oceanic circulation (Figure 3.1). Previous work has established that it is highly sensitive to high-latitude climate changes, through an intense atmospheric connection related to the meridional extent of the atmospheric polar vortex (Rohling et al., 2002a; Casford et al., 2003). During the early Holocene, the timing and magnitude of sea-surface temperature events in the Aegean may be compared to intervals of AMOC reduction, to test model-suggested atmospheric downstream impacts of these AMOC events (e.g., Renssen et al., 2001, 2002; LeGrande et al., 2006; Wiersma and Renssen, 2006). In addition, the Aegean Sea's surface-water oxygen isotope composition in the early to mid Holocene has been found to be pre-

dominantly influenced by changes in the eastern Mediterranean's overall freshwater budget due to fluctuations in the African monsoon intensity (Rohling, 1999; Casford et al., 2002, 2003; Rohling et al., 2002a). The present study combines this predominant impact on the surface water isotopes with new, co-registered Aegean records, to evaluate phase relationships between African monsoon fluctuations and northern high-latitude climate events.

The present-day winter regime in the Aegean Sea is dominated by westerly circulation, which drives a net eastward transport towards Turkey and the Levant of Mediterranean depressions that are formed by cyclogenesis over especially the northern sectors of the basin. These Mediterranean depressions commonly develop as secondary features to the larger Atlantic depressions that pass north of the Alps, and also rely on local cyclogenesis due to the relatively high Mediterranean sea-surface temperatures (for overviews, see Rohling and Hilgen, 1991; Rohling et al., 2008a). Occasionally, dry and cold polar/continental air masses break out over the basin through gaps in the mountainous southern European margin, producing episodes of severe cooling (for overviews, see Maheras et al., 1999; Casford et al., 2003; Rohling et al., 2008a). Reconstructions of Aegean climate during the Holocene have revealed the occurrence of these episodes of exceptional winter cooling also on multi-centennial to millennial timescales, with a strong apparent link to contemporaneous intensifications of the atmospheric polar vortex (Rohling et al., 2002a; Casford et al., 2003).

Today, summer conditions in the eastern Mediterranean are dominated by expansion of subtropical conditions from the south, and although there is some cyclogenesis over the basin, little precipitation develops as a consequence of descent in the upper troposphere (Rodwell and Hoskins, 1996; Ziv et al., 2004; Rohling et al., 2008a). During the early-mid Holocene orbitally induced insolation maximum, the influence of the African monsoon on the basin was enhanced through intensified flooding especially of the Nile River (Rossignol-Strick et al., 1982; Fontugne et al., 1994). In addition, effective moisture supply (precipitation) during summer may have been intensified all around the basin, as suggested by changes in pollen records; especially the enhanced presence of deciduous oak (Rossignol-Strick, 1987; Wijmstra et al., 1991; Rohling and Hilgen, 1991). Speleothem $\delta^{18}O$ data from Soreq Cave in northern Israel have been used to argue for enhanced precipitation - although not seasonally specified - during the early to mid Holocene. Combined oxygen and hydrogen isotope data in fluid inclusions within the speleothems suggest that at that time (as today) the moisture was sourced from the eastern Mediterranean (Matthews et al., 2000; McGarry et al., 2004). Reconstructions from stable oxygen isotopes in snail shells in the Negev Desert, southern Israel, corroborate the persistence of Mediterranean sourcing for the moisture that precipitated over the Levant (Goodfriend, 1991).

Studies of sediment cores retrieved throughout the eastern Mediterranean suggest that during the early to mid Holocene the main hydrological impacts on the basin, including the Aegean (Rohling et al., 2002a; Casford et al., 2002, 2003), were related to the African summer monsoon maximum, which caused an enhanced supply of freshwater to the entire eastern Mediterranean through especially the Nile River (Fontugne et al., 1994; Rohling and De Rijk., 1999; Emeis et al., 2000b; Scrivner et al., 2004).

3.3. Materials and methods

Descriptions of Aegean cores LC21 (35°40'N; 26°35'E; 1522 m water depth) and SL21 (39°01'N, 25°25' E; 317 m water depth) (Figure 3.1) are given in Casford et al. (2002, 2003). Both cores contain distinct organic-rich dark intervals representing the regional expression of sapropel S1 (Mercone et al., 2000, 2001; Casford et al., 2002, 2003; Rohling et al., 2002a). Cores SL21 and LC21 were sampled in a continuous sequence of 0.5 and 1 cm intervals, respectively, which allows investigation of the early to mid Holocene at multidecadal to centennial resolution.

3.3.1. Palynological processing

Seventy-five samples for dinocyst analyses were oven-dried at 60°C and spiked with *Lycopodium clavatum* spores to estimate palynomorph concentrations. Weighted sediment samples (from about 0.5 to about 2 g) were treated with 10% cold HCl to remove carbonates, 38% cold HF to remove silicates, and 30% cold HCl to remove the fluoride gel. After sieving over a 10 µm nylon mesh sieve, aliquots (40-60 µl) of the homogenized residue were placed on microscope slides, embedded in glycerine jelly and sealed with paraffin wax. Entire slides were counted for dinocyst abundances (about 250 cysts per sample) at 400X magnification. The taxonomy follows Williams et al. (2004) and Rochon et al. (1999). For the purpose of the present study, the abundance of one dinocyst species (*Spiniferites elongatus*) was selected to reconstruct relative SST changes.

3.3.2. SST reconstruction from planktonic foraminiferal abundances

Census counts of planktonic foraminifera from core LC21 (Casfords et al., 2002) were converted into summer and winter SST using artificial neural networks (ANN) developed by Hayes et al. (2005) specifically for application in the Mediterranean. ANN is a computer-intensive approach based on unsupervised learning of a relationship between two sets of variables. In comparison with other transfer

function techniques; ANN have the ability to characterise highly non-linear relationships and extract general relationships even in relatively small calibration datasets (Malmgren et al., 2001). Hayes et al. (2005) used ten different partitions of the calibration dataset into training and validation subsets to obtain ten neural networks for each SST definition. The reconstructed SSTs are then calculated as averages of SST estimates from these ten networks and the divergence among the ten estimates is used to estimate the reliability of each SST reconstruction. In the calibration by Hayes et al. (2005), the census counts were calibrated to winter (JFM) and summer (JAS) long-term SST averages at 10-m depth and calibration errors, expressed as average root mean square errors of prediction (RMSEP) in the test set of each of the ten partitions, were 1.14°C for summer SST and 0.79 °C for winter SST.

3.3.3. Chronological framework

The chronology for Aegean core SL21 benefits from a highly resolved multi-proxy correlation framework that was applied to 9 cores throughout the eastern Mediterranean with a total of 33 accelerator mass spectrometry (AMS) radiocarbon (^{14}C) datings, which constrains the total uncertainties for the calibrated timescale to within ±350 years (2σ, 95% variance) (Casford et al., 2007). This time-stratigraphic framework is particularly robust within the early to mid Holocene interval of sapropel S1 deposition because of the absence of bioturbation due to persistent bottom-water dysoxia. Core LC21 was used as benchmark against which the other Aegean records have been calibrated (Casford et al., 2007). The chronology for LC21 itself is based on 8 calibrated AMS ^{14}C datings (Mercone et al., 2000), and subsequently corroborated by the multi-proxy correlation framework (Casford et al., 2007). In addition, correlation of decreases in warm- versus cold-water planktonic foraminifera in LC21 to intervals of enhanced accumulation of potassium in GISP2 Greenland ice core (Mayewski et al., 1997), supported by the age of the Minoan ash layer, has allowed fine tuning of the LC21 chronology to a GISP2-equivalent chronology (Rohling et al., 2002a). A robust chronology, in calibrated ages, for the Aegean records is essential to discuss timing relationships with climate signals obtained from other well-dated, highly resolved archives, namely the Greenland ice cores (Meese et al., 1994; Rasmussen et al., 2007), the Qunf Cave speleothem record from Southern Oman (Fleitmann et al., 2007), and the Soreq Cave speleothem record from northern Israel (Bar-Matthews et al., 2000). All records discussed in this paper are considered versus calibrated (cal.) age in kiloyears (ka) before present (BP, which refers to the conventional benchmark of 1950 A.D.).

3.4. Paleoclimate proxy records

3.4.1. The high-latitude climate signal: Greenland ice cores

We compare our results with the oxygen isotope ($\delta^{18}O_{ice}$) and potassium ion concentration (K^+) records from the well-dated and finely resolved Greenland Ice Project Two (GISP2) ice core (Figure 3.1) (Grootes et al., 1993; Mayewski et al., 1997). The early Holocene $\delta^{18}O_{ice}$ record of the North Greenland Ice core Project (NGRIP) ice core (Figure 3.1) (NGRIP members, 2004) complements the GISP2 $\delta^{18}O_{ice}$ reconstruction, using the latest, layer-counted GICC05 timescale (Rasmussen et al., 2007). Down-core $\delta^{18}O_{ice}$ fluctuations predominantly reflect past changes in temperature (Dansgaard et al., 1964) and dynamics of the air masses advected over Greenland (Charles et al., 1994). Coolings (warmings) result in shifts to lighter (heavier) $\delta^{18}O_{ice}$ values (Dansgaard et al., 1964, 1989). Increases (decreases) in the continental-sourced non-seasalt (K^+) time-series from GISP2 have been found to covary with periods of winter/spring strengthening (weakening) of the Siberian anticyclone, the coldest and densest air mass in the Northern Hemisphere (Mayewski et al., 1997; Cohen et al., 2000; Meeker and Mayewski, 2002).

3.4.2. Season-specific reconstructions of Agean climate variability: organic-walled dinoflagellate cysts and planktonic foraminifera

Autotrophic dinoflagellates thrive in the upper photic zone and some of them produce cysts (e.g., Taylor, 1987). Several studies, based on both surface and down-core sediment samples, have revealed clear links between the occurrence of certain autotrophic dinocyst species and sea-surface parameters, including temperature (Wall et al., 1977; Edwards and Andrle, 1992, Rochon et al., 1999; de Vernal et al., 2001, 2002, 2005; Marret and Zonneveld, 2003). Temperature-sensitive dinocyst species data have provided qualitative paleo-temperature reconstructions for the eastern Mediterranean, using either calculations of a warm versus cold dinocyst ratio ($W/C_{dinocyst}$) (Sangiorgi et al., 2002), or changes in the relative abundance of warm-water dinocyst assemblages (Sangiorgi et al., 2003). $W/C_{dinocyst}$ ratios may be biased due to the systematic dominance of warm taxa in the eastern Mediterranean during the Holocene (Sangiorgi et al., 2003). On the other hand, reconstructions based on cumulative percentages of all warm-water dinocysts may be biased by the different responses of the various warm species to parameters other than temperature, as is often the case with biological proxies (Sangiorgi et al., 2003; Kucera et al., 2005). Here, we reduce the potential for such complications in the assessment of relative SST changes in the eastern Mediterranean by focussing on a single temperature-sensitive species, the cool-water

indicator *Spiniferites elongatus*.

In the Northern Hemisphere, *S. elongatus* is found in high percentages (up to 50%) in surface samples retrieved from cool temperate to polar regions and reveals no systematic responses to either nutrient availability or salinity (de Vernal et al., 1994; Rochon et al., 1999; Marret and Zonneveld, 2003). In the eastern Mediterranean, this taxon is relatively abundant (up to about 12%) in cold stadials of the last glacial cycle, while it is either found in very low percentages (> 2%) or completely absent in the Holocene (Zonneveld, 1995, 1996; Sangiorgi et al., 2002). We infer that the presence of *S. elongatus* within interglacials within the eastern Mediterranean represents considerably lowered (winter) SSTs.

We use shifts in the relative abundance of *S. elongastus* to assess relative SST changes through the early to mid Holocene in central-eastern Aegean core SL21. To avoid any bias in the reconstructions and interpretations by the high numbers of *Protoperidinium* cysts and their differential productivity/preservation issues in a sapropel-bearing sequence (Zonneveld et al., 2001, 2007; Versteegh and Zonneveld, 2002, Reichart and Brinkhuis, 2003), we calculate percentages of *S. elongatus* relative to both a total and a gonyaulacoid-only dinocyst sum (for an overview on the gonyaulacoid lineage see Fensome et al., 1996). Differences between these two records would highlight any potential bias from productivity and preservation issues.

Fluctuations in the relative abundance of warm versus cold water planktonic foraminifera in south-eastern Aegean core LC21 have been described previously, and were attributed to relative winter-spring SST changes (Rohling et al., 2002a). We refer to that study for a detailed discussion.

We supplement the above mentioned records of relative winter SST changes with absolute summer- and winter-specific SST reconstructions based on the ANN technique using planktonic foraminiferal census counts for core LC21. The ANN calibration and application to Mediterranean planktonic foraminiferal faunas has been described in detail by Hayes et al. (2005). Fluctuations in both summer and winter SSTs are discussed as departures expressed in degree Celsius (°C) from the early to mid Holocene average summer and winter values, respectively (Table 3.1).

Table 3.1: Modern and derived Holocene season-specific SST average values in south-eastern Aegean Sea

Time interval	Summer SST	Winter SST
Modern	23.5°C (Poulos et al., 1997)	16.0°C (Poulos et al., 1997)
late Holocene (0.7-4 ka BP)	24.1±0.5°C (1σ)	15.6±0.4°C (1σ)
early/mid Holocene (4-10.9 ka BP)	24.8±0.7°C (1σ)	16.0±0.8°C (1σ)
Holocene (0.7-10.9 ka BP)	24.6±0.8°C (1σ)	15.9±0.7°C (1σ)

3.4.3. The eastern Mediterranean freshwater budget: Aegean Sea $\delta^{18}O_{ruber}$ and $\delta^{18}O_{seawater}$

Processes such as the glacial concentration effect on the (modified) Atlantic waters entering the basin, the temperature of the water to carbonate fractionation, and changes in the basin's freshwater budget affect the oxygen isotope signature of foraminiferal calcite ($\delta^{18}O_{foraminifera}$) in the eastern Mediterranean (Rohling, 1999; Rohling et al., 2004). During intervals of sapropel formation, the input of large volumes of isotopically light (monsoon-sourced) freshwater along the North African margin greatly controlled the $\delta^{18}O$ of the (eastern) Mediterranean sea surface waters (Rohling, 1999; Rohling and de Rijk, 1999; Scrivner et al., 2004; Rohling et al., 2004). The consequent sea surface freshening has been found to propagate rapidly through the wider eastern Mediterranean away from the sites of freshwater discharge, including the Aegean Sea (Chapter 1). This signal was most likely transmitted through the basin by the efficient large scale counter-clockwise circulation of the surface waters (Pinardi and Masetti, 2000; Theocharis et al., 2002). The south-east Aegean site of core LC21 sits directly within the inflow of these surface waters into the Aegean Sea, at a considerable distance 'downstream' of the North African sites of freshwater discharge into the open eastern Mediterranean. Accordingly, the oxygen isotope composition of the surface waters ($\delta^{18}O_{seawater}$) at this specific site is expected to reflect a well-mixed expression of the changes in the surface-water $\delta^{18}O$ in the wider eastern Mediterranean, rather than a merely local signal (Chapter 1).

We reconstruct $\delta^{18}O_{seawater}$ during the early to mid Holocene by combining the stable oxygen isotope record for the (planktonic) summer mixed-layer dwelling foraminifer *Globigerinoides ruber* white ($\delta^{18}O_{ruber}$) (Rohling et al., 2002a) with summer SST reconstructions from ANN calculations within the same sample set of core LC21. Estimates of $\delta^{18}O_{seawater}$ are based on the temperature: $\delta^{18}O_{ruber}$ fractionation equation of Bemis et al. (1998):

$$T(°C)=16.5 - 4.80 (\delta^{18}O_{ruber} - \delta^{18}O_{seawater})$$

3.4.4. The tropical and subtropical precipitation signal: the speleothem records

Soreq Cave, northern Israel (Figure 3.1), resides in a semi-arid region where most of the annual rainfall derives from winter-time Mediterranean cyclogenesis (Bar-Matthews et al., 1996; Matthews et al., 2000). It has been established that the oxygen isotope composition of speleothem calcite ($\delta^{18}O_{speleothem}$) in Soreq Cave depends on the annual precipitation and evaporation balance in the epikarst zone. Lighter (heavier) $\delta^{18}O_{speleothem}$ corresponds to enhanced (reduced) net precipitation

over Soreq Cave (Bar-Matthews et al., 1996).

Qunf Cave (Figure 3.1) is located in Southern Oman at the northern boundary of the Indian summer monsoon penetration over the Arabian Peninsula, which accounts for 90% of the annual rainfall in the region. Given its location, the Qunf Cave $\delta^{18}O_{speleothem}$ record is expected to be very sensitive to even minor reorganizations of the Intertropical Convergence Zone (ITCZ) and associated Indian summer monsoon (Fleitmann et al., 2003). The amount effect causes the $\delta^{18}O$ of precipitation, and consequently speleothem calcite, to shift towards lighter values as rainfall increases (Dansgaard, 1964). Qunf Cave $\delta^{18}O_{speleothem}$ thus represents a key archive of changes in Indian summer monsoon rainfall.

3.5. Results

3.5.1. The early to mid Holocene monsoon maximum

Our record of ANN-based summer SSTs in LC21 (Figure 3.2b) suggests that warm Holocene values were first attained around 10.9 ka BP, and that summer SST was higher than the present-day value of 23.5°C between 10.1 and 6.6 ka BP (Poulos et al., 1997). Overall, during the early to mid Holocene, LC21 summer SSTs oscillated around an average value of 24.8±0.7°C (see Table 3.1).

Regarding the $\delta^{18}O$ of *G. ruber* and seawater in the Aegean Sea cores LC21 and SL21, we note a virtually synchronous rapid decrease of about 1.8‰ of $\delta^{18}O_{ruber}$ in cores LC21 (Figure 3.2c) and SL21 (Figure 3.2a) and of about 1.5‰ in $\delta^{18}O_{seawater}$ in LC21 (Figure 3.2d) between 10.6 and 9.6 ka BP. The close similarity in timing and magnitude of the negative $\delta^{18}O$ changes observed in both foraminifer calcite (*G. ruber*) and seawater provides strong support to the hypothesis that the negative $\delta^{18}O_{ruber}$ shift in the Aegean cores prior to sapropel S1 deposition is dominated by the inflow of isotopically light fresher surface waters into the Aegean Sea (Casford et al., 2002, 2003) with a negligible role of summer SSTs (i.e., temperature of calcification of *G. ruber* shells). Moreover, this reconstruction proves that fresher surface waters spread as far north as the central-eastern Aegean site of core SL21.

From about 9.5 ka BP onwards, the $\delta^{18}O_{ruber}$ records of cores LC21 and SL21 show fairly different developments. In LC21, $\delta^{18}O_{ruber}$ (Figure 3.2c) shows low amplitude fluctuations (~0.5‰) around an average of about 0.15‰ until 7.2 ka BP, followed by a gradual decrease towards modern values. In core SL21 (Figure 3.2a), $\delta^{18}O_{ruber}$ is more variable. Between 9.2 and 5.6 ka BP it oscillates around a mean of 0.7‰, which is heavier by ~0.5‰ than $\delta^{18}O_{ruber}$ between 10.6 and 9.6 ka BP at the same location. At ~5.6 ka BP, SL21 $\delta^{18}O_{ruber}$ shifts back to lighter values, which then continue until about 4.2 ka BP.

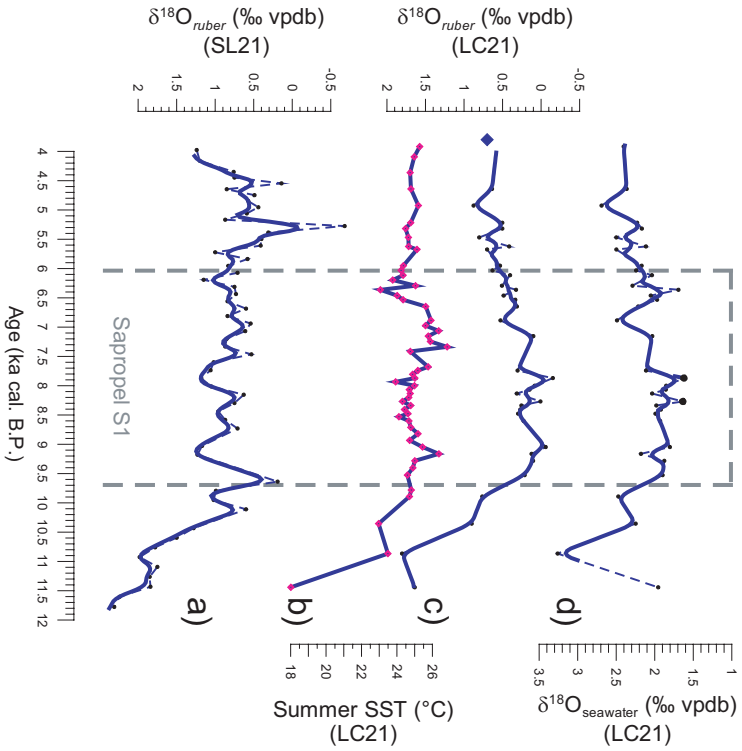

Figure 3.2: Stable oxygen isotope and summer sea surface temperature (SST) records from Aegean Sea cores SL21 and LC21. Grey dashed lines represent the visual extent of the dark interval associated with the sapropel S1 deposition in the Aegean Sea. **(a)** and **(c)** $\delta^{18}O$ of the summer mixed layer dwelling planktonic foraminifer *Globigerinoides ruber* (white) for Aegean Sea cores SL21 and LC21, respectively (Casford et al., 2002, 2003; Rohling et al., 2002a). Blue solid lines represent the 200 years moving average across the $\delta^{18}O_{ruber}$ profiles. Blue solid diamond indicates the Holocene $\delta^{18}O_{ruber}$ background values for core LC21 (Rohling et al., 2002a). **(b)** ANN-based summer SSTs for core LC21. The SST axis is calibrated relative to the $\delta^{18}O$ axis so that every 1°C change in temperature corresponds to 0.23‰ in $\delta^{18}O$ (Kim and O'Neil, 1997). **(d)** $\delta^{18}O$ of sea surface waters at site of core LC21.

Comparing the Aegean records with that from the Middle East (Figure 3.3), we note a general resemblance between the LC21 $\delta^{18}O_{seawater}$ (Figure 3.3a) and $\delta^{18}O_{speleothem}$ from Soreq Cave (Figure 3.3b) (Bar-Matthews et al., 2000) throughout the early to mid Holocene. Both records display virtually contemporaneous - within the chronological uncertainties (Bar-Matthews et al., 200) - and similar magnitudes shifts of to lighter $\delta^{18}O$. This similarity is especially apparent on millennial time scales as indicated by the lagged cross-correlation test shown in Figure 3.3d; between 9.6 and 4 ka BP, LC21 $\delta^{18}O_{seawater}$ and Soreq Cave $\delta^{18}O_{speleothem}$ are positively correlated and share 65% of the variance for a lag of 450 years (i.e., within chronological 2σ uncertainty).

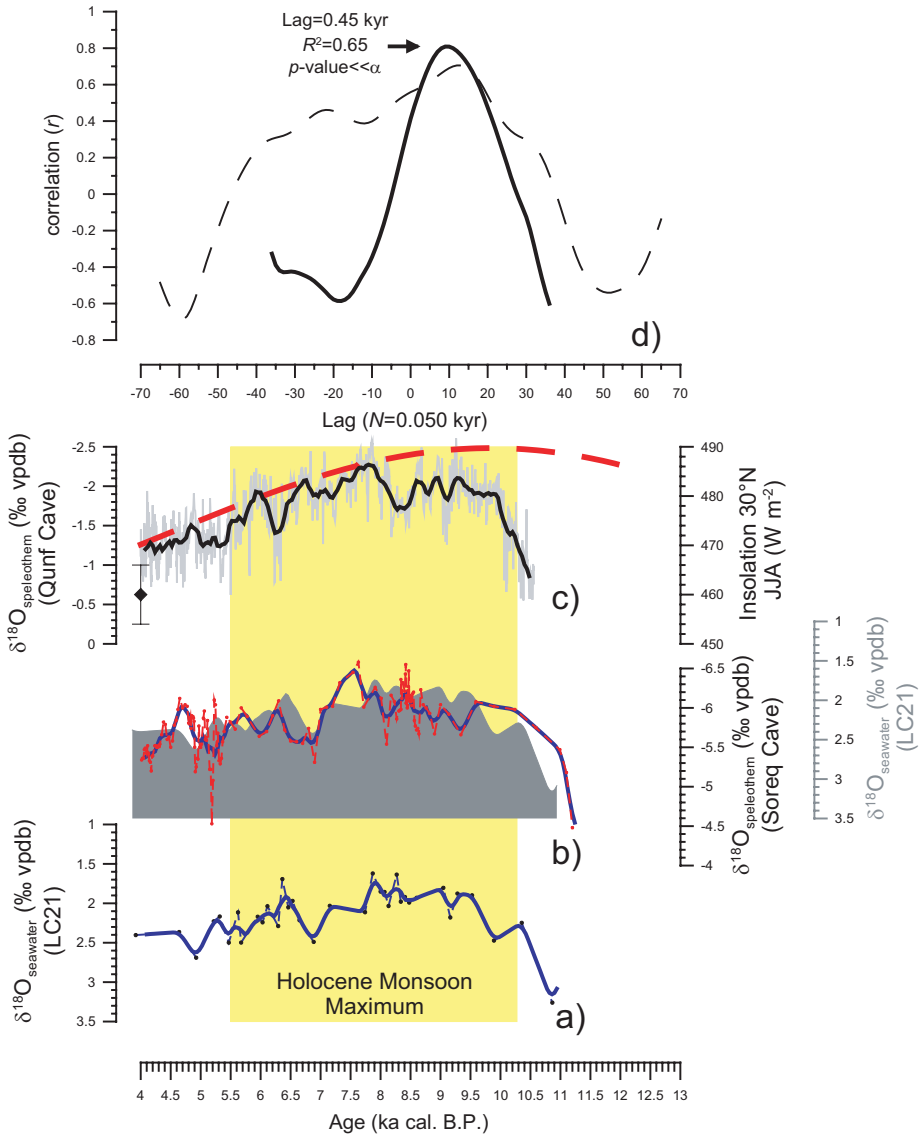

Fig**ure 3.3:** Oxygen stable isotope records from the eastern Mediterranean and Middle East regions. **(a)** $\delta^{18}O$ of sea surface waters at site of core LC21. **(b)** $\delta^{18}O_{speleothem}$ from Soreq Cave (Northern Israel) (Bar-Matthews et al., 2000). Soreq Cave profiles are overlain on the ~200 year moving average of LC21 $\delta^{18}O_{seawater}$ (grey shaded area). **(c)** $\delta^{18}O_{speleothem}$ from Qunf Cave (Southern Oman) (Fleitmann et al., 2003). This record is overlain on the 30°N insolation averaged from June to August (dashed red line) (Paillard et al., 1996; Laskar, 1990). The yellow horizontal band spans an interval of overall increased monsoonal activity in the boreal tropics/subtropics, commonly referred to as Holocene monsoon maximum. **(d)** Lagged cross-correlation analysis of the 500 year running averages of the LC21 $\delta_{18}O_{seawater}$ and Soreq Cave $\delta^{18}O_{speleothem}$ across the 9.6-6 (solid line) and 10.5-4 ka BP (dashed line) intervals.

It has been previously proposed, based on Soreq Cave $\delta^{18}O_{speleothem}$ data, that precipitation over Israel was much enhanced between 10 and 7 ka BP, relative to the present, effectively interpreting the light $\delta^{18}O_{speleothem}$ values as an expression of the so-called "amount-effect" on the $\delta^{18}O$ of precipitation (Bar-Matthews et al., 2000). Our records, however, suggest that there may be an alternative explanation, given that deuterium excess values of fluid inclusions in the speleothems imply that precipitation in the Soreq Cave region at that time (as today) was sourced from the eastern Mediterranean (Matthews et al., 2000; McGarry et al., 2004). The similarity in the developments of LC21 $\delta^{18}O_{seawater}$ and Soreq Cave $\delta^{18}O_{speleothem}$ may then be equally well explained in terms of a change in the source $\delta^{18}O$ (seen in LC21 $\delta^{18}O_{seawater}$) for the eastern Mediterranean vapour that eventually precipitated over the Levant. Following that argument, Soreq Cave $\delta^{18}O_{speleothem}$ would mostly be passively recording the changes in eastern Mediterranean surface water $\delta^{18}O$ caused by African monsoon flooding. Given that there are no considerable changes in the relative offset between LC21 $\delta^{18}O_{seawater}$ and Soreq Cave $\delta^{18}O_{speleothem}$ (Figure 3.3b) on millennial time scales, the amount of Rayleigh distillation away from the moisture-source $\delta^{18}O$ does not seem to have changed a lot, suggesting that there were no significant variations in the amount effect, and hence no reasons to assume that precipitation over the Soreq Cave catchment was greatly increased between 10 and 7 ka BP. We cannot exclude, however, that on shorter (centennial) timescales, changes in the temperature of the air masses advected over the eastern Mediterranean (see section 3.5.2) may have affected the Rayleigh distillation processes thereby accounting for shorter-term fluctuations in the offset between LC21 $\delta^{18}O_{seawater}$ and Soreq Cave $\delta^{18}O_{speleothem}$.

3.5.2. Early to middle Holocene Aegean winter climate variability: a tight link to high-latitude climate

To reconstruct the short-term (centennial- to millennial-scale) winter SST variability in the Aegean Sea during the early to mid Holocene, we focus on the *Spiniferites elongatus* record for core SL21 (Figure 3.4d) and the ANN winter SST calculations based on planktonic foraminiferal census counts in core LC21 (Figure 3.4f). Interpretations of large-scale processes influencing the early to mid Holocene Aegean (winter) climate are then provided by comparing these new winter-specific proxy records, along with the previously published LC21 warm versus cold (planktonic) foraminiferal record (Figure 3.4d) (Rohling et al., 2002a), with key northern high-latitude ice and sediment core records (Figure 3.4a, b, c) (Grootes et al., 1993; Mayewski et al., 1997; Ellison et al., 2006; Rasmussen et al., 2007).

The relative abundance records of *S. elongatus* calculated with respect to a

total (dashed line in Figure 3.4d) and a gonyaulacoid-only (solid line in Figure 3.4d) dinocyst sum are virtually identical to one another. Hence, we can exclude that, at this specific site, the relative abundances of *S. elongatus* are biased by changes in the primary productivity at the sea surface and/or preservation of the dinocyst assemblages at the sea floor. Consequently, we will hereafter refer exclusively to the relative abundances of *S. elongatus* calculated with respect to the gonyaulacoid-only sum.

At 10.9 to 10.7 ka BP the *S. elongatus* record for SL21 (Figure 3.4d) approaches the early to mid Holocene average values at this site (2.6±1.5%). Between 10.7 and 8.9 ka BP, SL21 *S. elongatus* displays more variability than the warm versus cold foraminiferal ratio in LC21 (Figure 3.4e). The *S. elongatus* record shows a sharp peak (~6.5%) centred on ~10.5 ka BP and a broader maximum between 9.8 and 9.1 ka, which culminates at a value of 4.7% at around 9.6 ka BP. Despite the much lower resolution of the LC21 winter SST data (Figure 3.4f) in this specific segment of the record, we find a decrease of 1.8°C with respect to the early to mid Holocene average value (Table 1), coinciding with the peak of abundance of *S. elongatus* at ~10.5.

The *S. elongatus* fluctuations in SL21 show reasonable similarity to the centennial-scale variability in GISP2 (K^+) through the 10.7 to 8.9 ka BP interval. Main peaks in the GISP2 (K^+) time series, centred on 10.5 and 9.4 ka BP, appear younger by ~200 yr (i.e., within 2σ uncertainty of the SL21 chronology) than similar events recorded by *S. elongatus* in SL21 (see following). The foraminiferal ratio in core LC21 also tracks the GISP2 (K^+) fluctuations, but this agreement is limited to the millennial scale (Rohling et al., 2002a). Given that the time resolution of the two records in this interval is roughly the same, it would appear that a greater sensitivity of the *S. elongatus* fluctuations allows a better signal comparison on all timescales with the ice-core ion series.

Through the 8.9 to 5.0 ka BP interval, *S. elongatus* and GISP2 (K^+) covary to a remarkable extent (100-year interpolated values are linearly correlated with R^2=0.75 for N = 40) (Figure 3.5). At 8.8 to 8.0 and 6.0 to 5.2 ka BP, the SL21 record of *S. elongatus* also reveals clear expressions of two multi-centennial fluctuations (centred on 8.4 and 5.9 ka BP) that are similarly apparent in the LC21 foraminiferal ratio (Figure 3.4e), and which were previously related to excursions in the GISP2 (K^+) series (Rohling et al., 2002a). However, the precise timing of the younger of these events in south-eastern Aegean core LC21 remains controversial, as the chronostratigraphic framework in this specific interval is not as well constrained as in the rest of the Holocene of LC21 (see Rohling et al., 2002a). The ANN-based winter SST reconstructions for core LC21 also display fluctuations coinciding with the foraminiferal ratio for the same core (Figure 3.4f). Up to 1 and

2°C cool departures from mean early to mid Holocene winter SST values are apparent in LC21 at 8.6-7.9 and 6.5-6.2 ka BP, respectively.

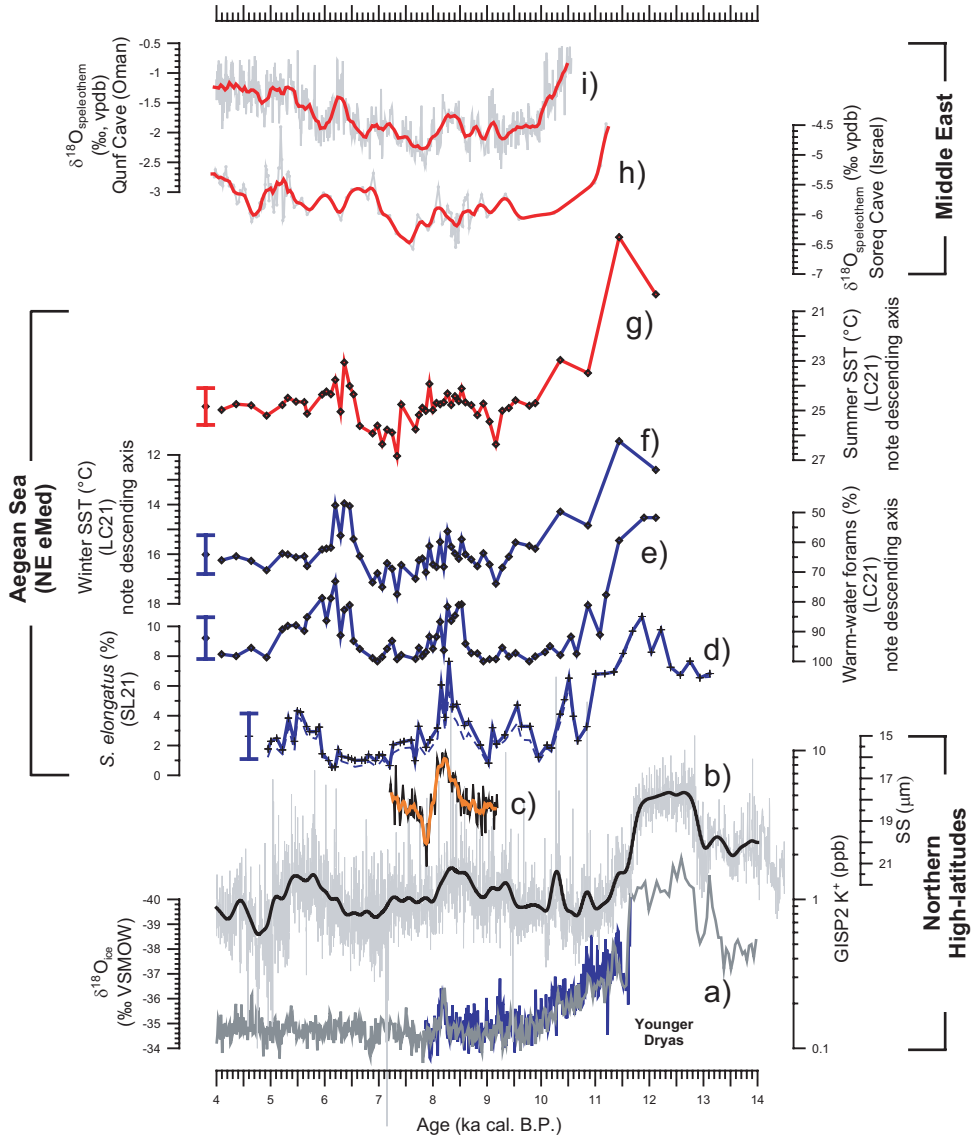

Figure 3.4: Array of paleoclimate proxy records along a north-south transect in the Northern Hemisphere. **(a)** GISP2 $\delta^{18}O_{ice}$ (‰, VSMOW) (Grootes et al., 1993) overlain onto the NGRIP $\delta^{18}O_{ice}$ (‰, VSMOW) (NGRIP members, 2004) on the new layer counted chronology 2005 (GICC05) timescale (Rasmussen et al., 2007). **(b)** GISP2 potassium series (K^+, ppb). Black solid line represents a 200 year moving Gaussian to highlight the main trends (Mayewski et al., 1997). **(c)** paleocurrent flow speed based on the variations of the mean size of the sortable silt (SS) in core MD99-2251, where higher mean reflects stronger AMOC (Ellison et al., 2006). Orange solid line represents a 90 year running average. **(d)** Relative abundances

(%) of *S. elongatus* in core SL21 with respect to a total (dashed line) and a gonyaulacoid-only (solid line) dinocyst sum. **(e)** Relative abundances (%) of warm-water planktonic foraminifera on the timescale corrected to match the Minoan eruption of Santorini to its actual age (Rohling et al., 2002a). **(f)** ANN-based winter SSTs for core LC21. **(g)** ANN-based summer SSTs for core LC21. **(h)** $\delta^{18}O_{speleothem}$ from Soreq Cave (Northern Israel) (Bar-Matthews et al., 2000). **(i)** $\delta^{18}O_{speleothem}$ from Qunf Cave (Southern Oman) (Fleitmann et al., 2003). Bars displayed on the top of the profiles d, e, f, and g, represent the 1σ (68%) band of variability for the early to mid Holocene background values.

The strong overall signal similarity between the Aegean winter/spring SST proxy records and GISP2 (K^+) is supported by the significant linear correlation (R^2=0.57 for N = 54) of the 100-year interpolated values across the 10.3 to 5ka BP interval (Figure 3.5). This similarity may be taken to suggest that the small ~200 yr offset between *S. elongatus* and GISP2 (K^+) in the earliest Holocene does not reflect an actual phase offset, but may simply result from time-scale uncertainties in SL21 (see Casford et al., 2007) and/or different time resolutions of the two records.

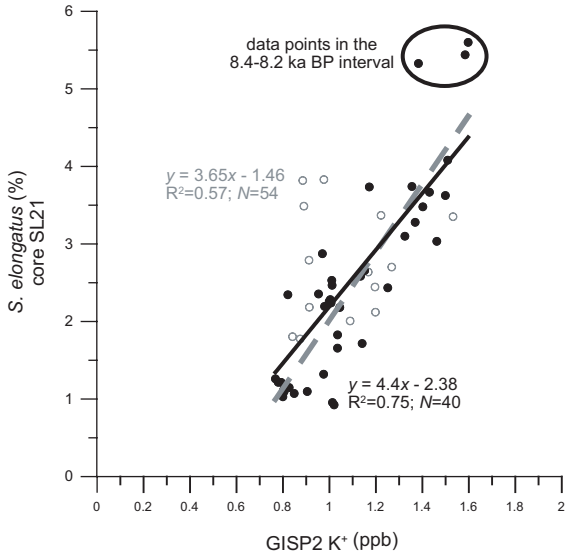

Figure 3.5: Cross-correlation analysis of GISP2 (K^+) (Mayewski et al., 1997) and the *Spiniferites elongatus* relative abundances (solid line in Figure 3.4d) in central eastern Aegean core SL21 through the early to mid Holocene. The two records have been first linearly interpolated, to read values at evenly spaced intervals of 100 years. Next, the records have been cross-correlated across the intervals 10.3-5 ka BP (grey open dots, grey dashed line represents the linear fit) and 8.9-5 ka BP (black solid dots, black line represents the linear fit).

Our findings corroborate the previous notion of a coherent in-phase response of the Aegean winter/spring climate to strengthening of the atmospheric polar vortex on multi-centennial to millennial time scales, which may have been modulated by changes in solar irradiation (Rohling et al., 2002a; Mayewski et al., 2004). Moreover, the new *S. elongatus* record in SL21 offers information at higher (centennial) resolution, with the largest peaks for each of the aforementioned events exceeding the 1σ (68%) interval of the variability in the early to mid Holocene background (see 1σ bar in Figure 3.4d).

Next, we exploit the apparent sensitivity of the SL21 *S. elongatus* record to assess the Aegean responses to sharp climate anomalies related to AMOC disturbances, such as the 8.2 ka BP event (Alley et al., 1997; von Grafenstein et al., 1999; Ellison et al., 2006; Thomas et al., 2007; Marshall et al., 2007; Rasmussen et al., 2007). The agreement between the Aegean *S. elongatus* and Greenland GISP2 (K^+) records between 8.9 and 8.0 ka BP would be consistent with a longer-term (multi-centennial) summer cooling in the North Atlantic region as reported by Ellison et al. (2006) and highlighted in several other (mostly summer-biased) records spanning the Northern Hemisphere (Rohling and Pälike, 2005). Superimposed upon this broad change are two sharp *S. elongatus* peaks centred on 8.3 and 8.15 ka BP, which exceed the 2σ (95%) band of the variability around the early to mid Holocene mean (Figure 3.4d). At about 8.3 ka BP also the LC21 winter SSTs display a distinct decrease (~1°C), which stands out from the millennial-scale change that started at 8.9 ka BP (Figure 3.4f). These sharp changes in the Aegean cores are within age uncertainties coeval with negative $\delta^{18}O_{ice}$ anomalies in the Greenland ice cores (Figure 3.4a) (8.25-8.15 in GISP2, 8.15-8.05 in NGRIP) (Grootes et al., 1993; NGRIP members, 2004; Rasmussen et al., 2007; Thomas et al., 2007). In addition, the composite structure of a broad *S. elongatus* maximum with superimposed sharp peaks bears a remarkable similarity with North Atlantic sortable silt records that suggest an AMOC disturbance (Figure 3.4c) (Ellison et al., 2006). However, this signal similarity does not extend to the interval younger than 8 ka BP.

The coincidence in time, duration, and structure of the *S. elongatus* anomaly to the AMOC reduction, combined with the close agreement between the magnitude of cooling observed in LC21 and the model-predicted SST decrease at this site in response to a freshwater disturbance in the North Atlantic (Wiersma and Renssen, 2006), lends support to the hypothesis that AMOC disturbances have affected the Aegean climate. Given the virtual isolation of the Aegean Sea from the North Atlantic circulation, this points to an efficient transmission of the high-latitude climate signal via abrupt intensifications of the atmospheric circulation following AMOC reductions (Renssen et al., 2002). Allowing for chronological uncertainties, two other early Holocene winter events recorded in the Aegean Sea cores at 10.5 and 9.6 ka BP (Figure 3.3d, f) would also seem to correspond to short-lived anomalies that were previously reported from several records from the wider North Atlantic region (Bond et al., 1997; Björk et al., 2001; Came et al., 2007; Rasmussen et al., 2007) and which may also have been related to meltwater forced reductions of the AMOC (Nesje et al., 2004; Marshall et al., 2007; Hillaire-Marcel et al., 2007).

3.6. A wider perspective

Our new $\delta^{18}O_{seawater}$ record from south-eastern Aegean core LC21 points to substantial hydrographic changes in the basin during the early to mid Holocene, in agreement with previous reconstructions based on $\delta^{18}O_{ruber}$ (Casford et al., 2002, 2003). The timing reported here (10.6 to 9.6 ka BP) for the early Holocene decrease in the $\delta^{18}O$ of *G. ruber* and seawater in Aegean cores LC21 and SL21 (Figure 3.2a, c, d) coincides with a negative shift (~2.0‰) of $\delta^{18}O_{ruber}$ in a south-eastern Levantine Sea site close to the Nile River discharge (see Figure 3 of Sperling et al. 2003). These shifts in surface-water $\delta^{18}O$ appear virtually coeval with a distinct increase of Nile-sourced clay minerals in another south-eastern Aegean sediment core (10.5-9 ka BP) (Ehrmann et al., 2007). The timing of these changes in the Aegean Sea agrees with age estimates for the onset of the so-called "greening of the Sahara" (Gasse, 2000; Ritchie et al., 1985). Combined, these observations corroborate the previous notion that, during the early Holocene, Aegean surface waters freshened primarily in response to the enhanced monsoon-fuelled freshwater flooding into the open eastern Mediterranean (Casford et al., 2002, 2003). The eastern Mediterranean-wide decrease in surface-water $\delta^{18}O$ may in turn explain the similar isotope shift in $\delta^{18}O_{speleothem}$ in Soreq Cave (see section 3.4.1, and Figure 3.3b).

The onset of monsoon flooding into the eastern Mediterranean would appear to lag by ~1 kyr behind the abrupt shift to wetter conditions in the western Sahel (Weldeab et al., 2005, 2007), which is located at the present day northern edge of the ITCZ penetration over NW Africa (Ramel et al., 2006). This apparent lag suggests a time-transgressive northward shift of the mean latitudinal position of the monsoon front (in association with the ITCZ) over Northern Africa. Near the South Atlantic, in the NW Sahel, there would be a direct response of the ITCZ to insolation changes. The delayed northward shift over central and eastern North Africa might then be related to a vegetation-albedo feedback process (Kutzbach et al., 1996; Brovkin et al., 1998), requiring some time for a progressive increase in the vegetation cover following the change to more humid conditions.

Despite its location on the present-day northernmost limit of the ITCZ (Fleitmann et al., 2003, 2007), the earliest Holocene transition to wetter conditions over Southern Oman (Figure 3.3c) occurs around the same time as the changes in Northern Africa and in the eastern Mediterranean hydrography, and thus also lags by about 1 kyr behind the change in the western Sahel (Weldeab et al., 2005, 2007). This suggests a delayed response of the Indian monsoon to insolation change, relative to the African monsoon. Such a time lag might be explained in terms of the negative relationship between Eurasian snow cover and Indian monsoon intensity in the earliest Holocene (Barnett et al., 1998; Gupta et al., 2003; Fleitmann et al., 2003, 2007). Enhanced snow cover over Eurasia reduces the (sensible) heating of

the Eurasian landmass, which weakens the pressure gradient between the Indian Ocean and the Tibetan Plateau (Overpeck et al., 1996), the engine of the Indian summer monsoon circulation (Webster et al., 1998).

Regarding centennial-scale climate fluctuations, our qualitative and quantitative SST reconstructions for the Aegean Sea reveal a distinct pattern of climate deteriorations that in part agrees with the previously reported pattern of millennial-scale fluctuations in the region (Rohling et al., 2002a), but which in addition enriches that picture with centennial-scale details. Winter SST reconstructions for cores SL21 and LC21 show a remarkably good match with the GISP2 (K^+) series on all timescales, strengthening the view that the Aegean events represent episodes of enhanced incursion of polar air influences related to changes in the atmospheric polar vortex (Rohling et al., 2002a; Casford et al., 2003). For the early Holocene, the new Aegean winter-specific proxies reveal a climate evolution that is more complex than was previously appreciated. Two marked climate deteriorations centred on about 10.5 and 9.6 ka BP have been found in addition to the one at 8.6-8.0 ka BP that was also reported by Rohling et al. (2002).

Allowing for chronostratigraphic uncertainties, these changes in both Greenland and Aegean records (Figure 3.4b, d, e, f) would seem to agree in both timing and structure with early Holocene Indian monsoon deteriorations at ~10.1 and between 9.3 and 7.9 ka BP in Qunf Cave (Figure 3.4l). To further test this visual similarity and account for the small chronostratigraphic inconsistencies of the records we performed a lagged cross-correlation analysis on GISP2 (K+) (Mayewski et al., 1997) and Qunf Cave $\delta^{18}O_{speleothem}$ (Fleitmann et al., 2003) time series through the early to mid Holocene period (Figure 3.6). The Qunf Cave $\delta^{18}O_{speleothem}$ record has been first detrended (Figure 3.6c) by removing the long-term (frequency 0.1±0.01 kyr-1) trend (Figure 3.6b). Next, we used a lagged cross-correlation test between the 200 year smoothed detrended Qunf Cave $\delta^{18}O_{speleothem}$ and GISP2 (K^+) records (Figure 3.6d).

This exercise shows that the two time-series are positively correlated, sharing 62% of their variance across the 10.3-8 ka BP interval for a lag of 200 years of Qunf Cave $\delta^{18}O_{speleothem}$ behind GISP2 (K^+), which is within the uncertainties of the two chronologies (Meese et al., 1994; Fleitmann et al., 2007). Importantly, fluctuations time-equivalent to GISP2 (K^+) events were here recognised also in the Aegean Sea and previously in other North Atlantic records. This finding suggests that the early Holocene multi-centennial climate perturbations may have been virtually synchronous throughout the Northern Hemisphere, with substantial impacts on both winter and summer proxies. Superimposed on these changes are sharp anomalies, tied to AMOC reductions, which are recorded in both Greenland $\delta^{18}O_{ice}$ and in other winter-specific proxies (Rohling and Pälike, 2005), although their occurrence in summer-specific proxies cannot be ruled out (Fleitmann et al., 2007).

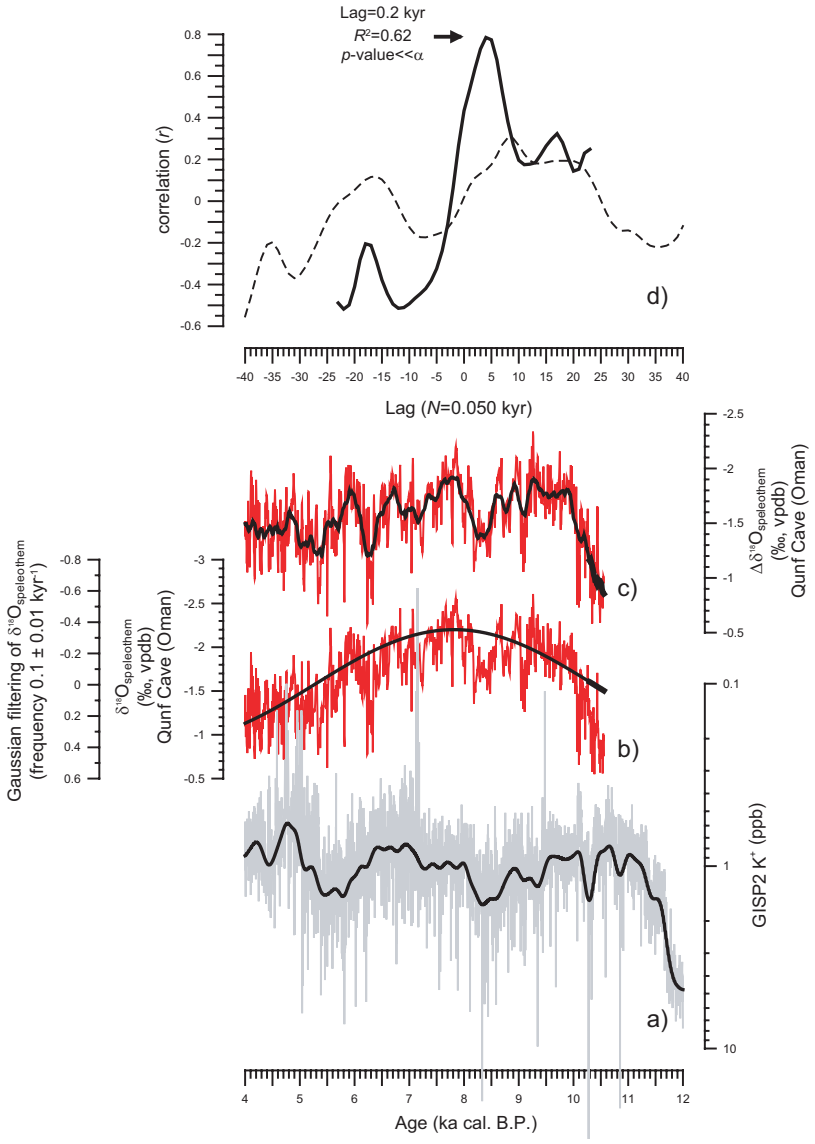

Figure 3.6: Comparison between GISP2 (K^+) and Qunf Cave $\delta^{18}O_{speleothem}$ through the early to mid Holocene. **(a)** GISP2 (K^+). Black solid line represents a 200 year moving Gaussian to highlight the main trends (Mayewski et al., 1997). **(b)** $\delta^{18}O_{speleothem}$ from Qunf Cave (Southern Oman) (Fleitmann et al., 2003). Black line represents the Gaussian 10±1 kyr bandpass filtering through the early to mid Holocene portion of the record to highlight the long-term (orbital) component of the signal. **(c)** detrended Qunf Cave $\delta^{18}O^{speleothem}$ record obtained by removing the long-term (orbital) component from the raw $\delta^{18}O_{speleothem}$ data. Black line represents a 200 years moving average through the detrended record. **(d)** Lagged cross-correlation analysis of GISP2 (K^+) and the Qunf Cave $\delta^{18}O_{speleothem}$ detrended record across the 10.3-8 (solid line) and 8-4 ka BP (dashed line) intervals.

We suggest a speculative scenario for the broad similarity in both timing and structure of both winter and summer proxy records in the early Holocene, which proposes an important role for the Eurasian snow cover. Besides its aforementioned effects on the Indian monsoon, increased Eurasian snow cover would also be associated with increases in the intensity and spatial extent of the winter/spring Siberian High (Cohen et al., 2000 and references therein).

Changes in the Eurasian snow cover may therefore have caused virtually synchronous, yet independent, responses of the winter/spring Siberian High and the summer Indian monsoon systems during the early Holocene. The disappearance of signal similarities between Aegean/GISP2 winter records and the Qunf Cave record after 8.0 ka BP (Figure 3.6d) may be explained by the eventual development of full interglacial conditions during the mid Holocene, removing this inferred common forcing of high and low latitude systems. Thereafter, the tropics are thought to have responded more directly to solar variation (Fleitmann et al., 2003; Dykoski et al., 2005). In their review of Holocene climate variability across the globe, Mayewski et al. (2004) also noted that Holocene events after 8 ka BP displayed reasonably common spatial characteristics, whereas earlier events showed different patterns, which corroborates our inference of a change in low versus high latitude responses to climate forcing from 8 ka BP onwards.

3.7. Conclusions

The study presented here shows that the Aegean Sea represents a valuable archive for paleoclimate investigations. Past changes in the Aegean's freshwater budget and winter sea surface temperature regime were controlled by the fluctuations in the tropical/subtropical and high- to mid-latitude climate systems, respectively. Accordingly, by providing a set of highly resolved season-specific proxy records co-registered within the same archive/sample-set we have tackled the centennial (suborbital) to multi-millennial (orbital) climate/hydrographic changes occurred in the Aegean region during the early to mid Holocene period of Northern Hemisphere insolation maximum.

A sound reconstruction of seawater $\delta^{18}O$ from south-eastern Aegean core LC21 has corroborated previous notions that during the earliest Holocene (10.6 to 9.6 ka BP), the Aegean Sea was invaded by large volumes of isotopically light fresher open eastern Mediterranean surface waters, which spread (at least) as far north as the central sector of the Aegean Sea. This change in the Aegean Sea is virtually coeval with a widespread perturbation in the eastern Mediterranean hydrography due to orbitally induced intensification of the African monsoon and consequent enhanced discharge of North African rivers (i.e., Nile River).

We find that the change to lighter $\delta^{18}O$ in eastern Mediterranean surface waters was coeval and similar in magnitude to a decrease in the $\delta^{18}O$ of speleothem calcite in Soreq Cave, northern Israel. This leads us to reconsider the previously reported explanation for the light $\delta^{18}O$ values in Soreq Cave during periods of sapropel deposition, which centered on enhanced precipitation over northern Israel. Instead, we suggest that the changes in Soreq Cave $d^{18}O_{speleothem}$ were primarily caused by changes in the isotopic composition of the source of moisture for Soreq Cave, the eastern Mediterranean surface waters.

Superimposed upon these long-term changes due to intensification of the African monsoon, we note Aegean centennial- to multicentennial-scale episodes of (winter) climate instability that appear intimately linked to meridional displacements of the atmospheric polar vortex. These events are apparent in two independent winter-specific proxy records from central-eastern and south-eastern Aegean cores SL21 and LC21; the fluctuations in the relative abundances of the cold water dinocyst *Spiniferites elongatus* and the ANN-based winter SST reconstructions from planktonic foraminiferal census counts, respectively. Three early Holocene episodes of winter cooling of up to 1.8°C are found at ~10.5, between 9.8 and 9.1, and between 8.6 and 8 ka BP. Superimposed upon the latter, the SL21 *S. elongatus* record reveals a sharp peak between 8.3 and 8.15 ka BP. This short-lived cooling event in the Aegean Sea coincided in timing and duration with a sharp climate anomaly in several records from the wider North Atlantic region and a reduction in the Atlantic Meridional Overturning Circulation.

Chapter 4

Reconstructing changes in marine productivity at the time of S1 deposition in the eastern Mediterranean; a marine palynological approach

Based on:
Gianluca Marino, Francesca Sangiorgi and Henk Brinkhuis

To be submitted

Abstract

Reconstruction of the primary productivity patterns during sapropel deposition remains problematic. Fluctuations in the heterotrophic dinoflagellate cysts (dinocysts) due to the dietary preference of their motile counterparts have been used to reconstruct past changes in the eukaryotic primary productivity patterns at the sea surface. Recently, some studies have warned that aerobic degradation under oxic conditions may affect abundances of heterotrophic dinocysts in the sediments and high abundances of these dinocysts in anoxic sediments may thus reflect enhanced preservation at the sea floor rather than increased sea surface productivity. To further investigate this issue, dinocyst data from early to mid Holocene sedimentary records (including time of sapropel S1) of the Strait of Sicily, Adriatic and Aegean Seas are here discussed in the context of recently published contemporaneous oxyphillic benthic foraminifer records as indicators of bottom water ventilation. We note a 4 kyr maximum in the absolute abundance of heterotrophic dinocysts in the Aegean Sea starting at ~10 ka BP. Similar changes in the concentration of heterotrophic dinocysts in the Adriatic Sea occurred much later (at ~8.5 ka BP) and terminated earlier, at ~7.1 ka BP. An increase in the concentration of heterotrophic dinocysts between 10 and 6.5 ka BP is also reported for the Strait of Sicily, albeit absolute values are much too low to allow conclusive speculations. Given the presence of oxyphillic benthic foraminifera in Adriatic and Aegean Seas during sapropel S1 deposition and the lack of significant correlations between changes in the deep sea ventilation of the two basins and fluctuations in the concentrations of heterotrophic dinocysts, we contend that the latter most likely reflect changes in the sea surface productivity. Interestingly, the onset and the spatial trends of the productivity increase at times of sapropel S1 deposition, imply that the presence of a reservoir of nutrients at intermediate depths, likely tied to weakening of the basin's thermohaline circulation, boosted productivity.

4.1. Introduction

Sapropels are organic-rich layers punctuating much of the Neogene sedimentary record of the (eastern) Mediterranean (see extensive reviews in Rohling, 1994, Cramp and O'Sullivan, 1999, Emeis et al., 2003). A wealth of evidence supports the hypothesis that sapropels formed in response to major perturbations of the physical process controlling the supply of oxygen to the deep sea, i.e., the deep water formation. During periods of Northern Hemisphere precession minima/ insolation maxima the intensification of the African monsoon increased the river discharge along the North African margin (Rossignol-Strick et al., 1982, Rossignol-

Strick, 1983, 1985, Rohling et al., 2002b, 2004). This reduced the density of the surface waters, thereby weakening (in some instances ceasing) the bottom water ventilation via failures in the deep water overturning process (e.g., Myers et al., 1998; Chapter 1) and enhancing the potential preservation and burial of organic matter. An alternative hypothesis postulates that an increase in sea surface primary productivity and the subsequent export of organic carbon would have enhanced the aerobic oxygen consumption and thus contributed to the bottom water anoxia/dysoxia, even without dramatic disruptions of the ventilation system (de Lange and Ten Haven, 1983; Calvert, 1983; Boyle and Lea, 1989; Pederson and Calvert, 1990; Van Os et al., 1994).

This controversy may be reconciled by invoking a combination of the two scenarios (Rohling and Gieskes, 1989, Howell and Thunnell, 1992; Nijenhuis et al., 1996). Yet, the current understanding of the sea surface productivity patterns during sapropel formation (Sancetta, 1994; Kemp et al., 1999; Sachs and Repeta, 1999; Struck et al., 2001; Weldeab et al., 2003) is not as well constrained as the impact of the monsoon-related shifts in the basin's freshwater budget on the Mediterranean water mass dynamics (e.g., Rohling, 1991; Myers et al., 1998; Casford et al., 2002, 2003; Rohling et al., 2004, 2006; Chapter 1). The difficulties encountered in assessing sea surface productivity are mostly due to the limitations of paleoproductivity proxies (e.g., biological proxies such as diatoms and calcareous nannoplankton, and geochemical proxies such as, barium and total organic carbon contents) available for paleoceanographic reconstructions (e.g., Rühlemann et al., 1999; Gingele et al., 1999; Versteegh and Zonneveld, 2002).

One way to at least qualitatively assess past changes in the eukaryotic primary productivity at the sea surface is to look at down-core fluctuations in the abundances of the organic-walled dinoflagellate cysts (dinocysts) likely formed by heterotrophic dinoflagellates and mostly belonging to the genus *Protoperidinium* (e.g., Reichart and Brinkhuis, 2003). The vast majority of *Protoperidinium* dinoflagellates is heterotrophic and feeds on other microplankton (e.g., diatoms) or organic matter (Jacobson and Anderson, 1986; Gaines and Elbrächter, 1987; Dale, 2001). Higher abundances of heterotrophic dinocysts in the sediments have been inferred to reflect enhanced eukaryotic sea surface primary productivity (Dale, 1996; Dale and Fjellså, 1994; Reichart and Brinkhuis, 2003). However, some studies have suggested that in well oxygenated settings the heterotrophic cysts become quickly degraded, being more sensitive to aerobic degradation than other cysts, notably those of autotrophic dinoflagellates (Zonneveld et al., 2001, 2007; Versteegh and Zonneveld, 2002). Following that argument, these authors conclude that high abundances of heterotrophic dinocysts in anoxic sediments might not necessarily reflect an increase of the primary productivity at the sea surface but rather an en-

hanced preservation at the sea floor. To circumvent these issues they propose to use only the so-called "oxygen resistant" dinocysts (a subgroup of the autotrophic dinocysts), which can be found in some highly productive areas around the globe (Zonneveld and Brummer, 2001), to reconstruct paleoproductivity (Zonneveld et al., 2001, 2007; Versteegh and Zonneveld, 2002). More recently, the study by Reichart and Brinkhuis (2003) established that the sensitivity of the heterotrophic dinocysts to oxic degradation potentially affects absolute abundances only when oxygen concentration of the bottom waters exceeds 2.5 ml/l, and, below that threshold, heterotrophic cyst concentrations can still be used as a valuable paleoproductivity proxy.

The present study aims to further test the potentialities of dinoflagellate cysts to reconstruct changes in sea surface productivity during the early to mid Holocene period of sapropel S1. By comparing changes in the some major dinocyst groups from well dated sediment cores from key locations in the eastern Mediterranean, namely the Aegean and Adriatic Seas and the Strait of Sicily (Figure 4.1) with previously published reconstructions of bottom water ventilation (benthic foraminifer assemblages, Casford et al., 2003; Abu-Zied et al., in press) and productivity changes (Ba_{excess}/Al; Mercone et al., 2001) from the same cores, we aim at circumventing issues related to potential preservation effects.

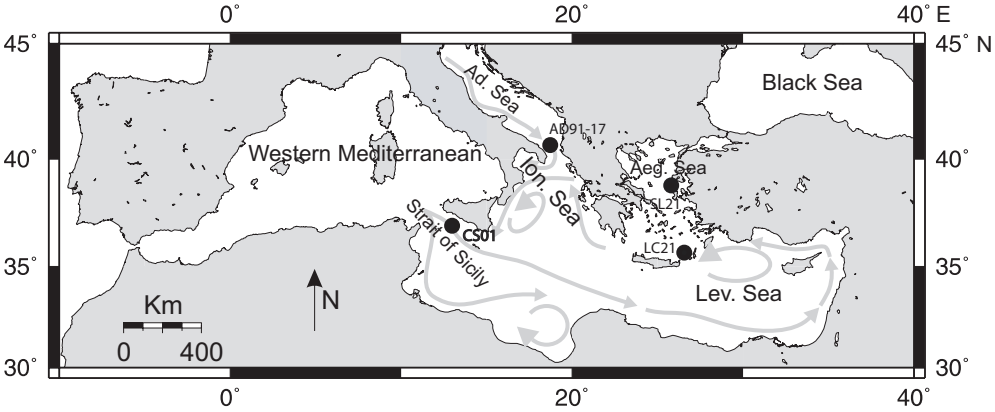

Figure 4.1: Map of the Mediterranean showing the main patterns of surface circulation (grey arrows) (Pinardi and Masetti, 2000) and locations (black dots) of the Aegean cores SL21 (39°01'N, 25°25' E; 317 m water depth) and LC21 (35°40'N; 26°35'E; 1522 m water depth), the Adriatic core AD91-17 (40°52'N, 18°38'E, 845 m water depth), and the Strait of Sicily's core CS01 (37°02'N, 13°09'E; 470 m water depth). Aeg. Sea = Aegean Sea; Lev. Sea = Levantine Sea; Ad. Sea = Adriatic Sea; Ion. Sea = Ionian Sea; Sic. Chan = Sicily Channel.

4.2. Materials and Methods

Lithological descriptions of the Aegean cores SL21 (39°01'N, 25°25' E; 317

m water depth) and LC21 (35°40'N; 26°35'E; 1522 m water depth) and Adriatic core AD91-17 (40°52'N, 18°38'E, 845 m water depth) are given in Casford et al. (2002, 2003) and Sangiorgi et al. (2003), respectively. Core CS01 (37°02'N, 13°09'E; 470 m water depth) was recovered in 2001 from the Sicily Channel by R/V Urania (Figure 4.1). The CS01 core site is located on a low ridge between the Gela Basin and Adventure Bank, a few km away from the ODP site 963D. Core CS01 is 436 cm long and consists of homogenous brown grey mud with no evidence of turbidites, erosional surfaces or tephra layers. No lithological expression of sapropel is evident in core CS01, likely due to the fact that the core location is shallower than the minimum depth where anoxic/dysoxic conditions developed in that area (Muerdter, 1983; Sprovieri et al., 2003).

4.2.1 Palynological processing

In total, hundred and sixty-nine samples were processed for dinocyst analyses. They were oven-dried at 60°C and, before chemical treatment was started, a known amount of *Lycopodium clavatum* spores was added to each sample to estimate palynomorph concentrations. Exactly weighted sediment samples (between 0.5 and 2 g) were treated with 10% cold HCl to remove carbonates, 38% cold HF to remove silicates and with 30% cold HCl to remove the fluoride gel. After sieving over a 10 μm nylon mesh sieve, known amounts (40-60 μl) of homogenized residue were placed on microscope slides, embedded in glycerine jelly and sealed with paraffin wax. Entire slides were counted for dinocysts (~250 cysts per sample) at 400X magnifications. The taxonomy follows Rochon et al. (1999), Head (2002), and Fensome and Williams (2004). All dinocyst data presented in this study are available on request.

4.2.2 Chronology

Chronology for core CS01 is constrained by six accelerator mass spectrometry (AMS) radiocarbon (^{14}C) dating of pteropod (upper 3 datings) and planktonic foraminifer (lower 3 datings) shells (Table 4.1). All measurements were performed at the Van de Graaff Laboratorium, Utrecht University, The Netherlands. These ^{14}C ages, expressed as years (yr) before present (BP, which refers to the conventional benchmark of 1950 A.D.), have been converted into calibrated ages (cal. yr BP) using Calib 5 with 1σ (68%) range (Stuiver et al., 1998), which incorporates a reservoir correction ΔR = 400 years (Siani et al., 2001) (Table 4.1). The average cal. age has been calculated and used to develop the chronology of the core (Figure 4.2).

Table 4.1: AMS ^{14}C measurements for core CS01

Depth (cmbsf)	Dated material	^{14}C Conventional Age (years BP)	Average Cal. Age (years BP)
70.0	Pteropods	4,200 ± 45	4,290
117.5	Pteropods	6,236 ± 46	6,678
170.0	Pteropods	8,300 ± 50	8,816
260.0	Planktic forams	12,000 ± 60	13,412
321.0	Planktic forams	13,010 ± 60	14,807
430.0	Planktic forams	15,950 ± 90	18,458

Chronological frameworks for the southern Adriatic core AD91-17 and the Aegean cores SL21 and LC21 are reported in Sangiorgi et al. (2003) and Casford et al. (2007), respectively. Specifically, the LC21 chronology used in this study derives from eight AMS ^{14}C datings (Mercone et al., 2000), supported by the multi-proxy correlation framework (Casford et al., 2007). For the middle and late Holocene the LC21 age model has been corrected to match the Minoan eruption of Santorini to its actual age (Rohling et al., 2002a).

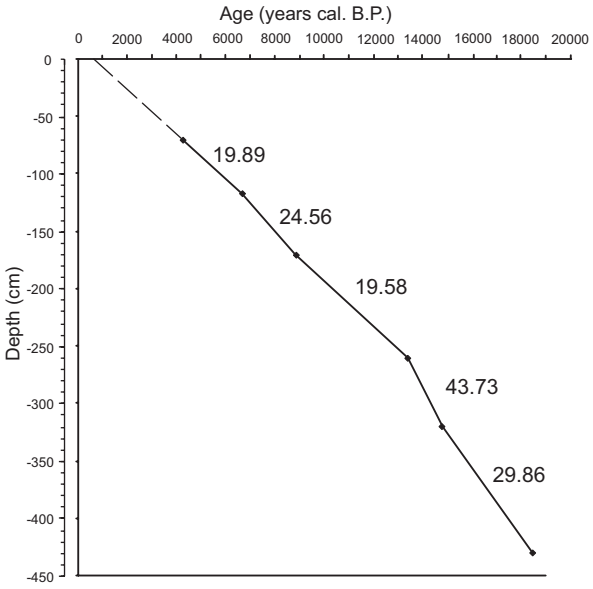

Figure 4.2: Age control points used to derive the age model in core CS01. Calibrated years have been calculated using Calib 5 (Stuiver et al., 1998). Sedimentation rates are also reported (cm kyr^{-1}).

4.3. Results

For the purpose of this study, dinocyst species have been grouped in four main categories, namely total heterotrophic, total autotrophic, "oxygen resistant", and total dinocysts. The "total heterotrophic dinocysts" include all the cysts produced by the dinoflagellate belonging to *Protoperidinium* that have a heterotrophic lifestyle (Jacobson and Anderson, 1986; Gaines and Elbrächter, 1987; Dale, 1996; Dale and Fjellså, 1994), plus *Echinidinium* cysts, which are likely to be produced

by heterotrophic dinoflagellates (see Head, 2003). The total autotrophic dinocysts include all the dinocyst species belonging to the gonyaulacoid lineage, and the peridinioid dinocyst produced by the dinoflagellate *Pentapharsodinium dalei* (for an overview on the gonyaulacoid and peridinioid lineages see Fensome et al., 1996). Following Versteegh and Zonneveld (2002), the dinocysts *Impagidinium* spp., *Nematosphaeropsis labyrinthus*, *Operculodinium centrocarpum*, and the cysts of *Pentapharsodinium dalei* are here grouped and referred to as "oxygen resistant". To avoid potential biases caused by different water depth at the different sites, the abundance of oxygen resistant dinocysts has been calculated both including and excluding the *Impagidinium* spp. as this genus is characteristics of open water/ oceanic environments (Wall et al., 1977; Marret and Zonneveld, 2003; Pross and Brinkhuis, 2005). Finally, the total amount of all dinocysts found is referred to as total dinocysts. Variations in these four main dinocyst groups during the early to mid Holocene, which includes time of sapropel S1 deposition, are reported in the following sections for the Aegean Sea (4.3.1), Adriatic Sea (4.3.2), and Strait of Sicily (4.3.3).

4.3.1. The Aegean Sea

In the early to mid Holocene interval of core SL21 from the central-eastern Aegean Sea, *Brigantedinium* spp. and *Echinidinium zonneveldiae* dominate the heterotrophic dinocyst assemblage, accounting for ~64% of it. Among the autotrophic dinocysts, species belonging to the genus *Spiniferites* are dominant.

We record an abrupt shift in the concentration of total heterotrophic dinocysts from values < 100 cysts g^{-1} during the Younger Dryas and the earliest Holocene to values higher than 700 cysts g^{-1} at ~10 ka BP in core SL21 (Figure 4.3a). In the same sample, increases in both the relative abundances of the total heterotrophic (up to ~30%, Figure 4.3b) and total autotrophic dinocyst concentrations (up to ~1700 cysts g^{-1}, dashed line in Figure 4.3c) occur. Conversely, there is no synchronous substantial change in the oxygen resistant dinocysts (Figure 4.3d). Between ~10 ka BP and ~6 ka BP concentrations of total heterotrophic dinocysts in central-eastern Aegean core SL21 remain generally higher than the early to mid Holocene (11.5 to 5 ka BP) mean value (450 cysts g^{-1}), with few intervals of lower abundance at ~9.2, 8.3 and 7.4 ka BP. From ~6 ka BP concentrations of total heterotrophic dinocysts decrease to values as low as ~200 cysts g^{-1}. Decreases at 8.4 and 7.4 ka BP are apparent in all the dinocyst records of core SL21, including the oxygen resistant dinocysts, which overall show very low amplitude oscillations around a mean value of ~500 cysts g^{-1} throughout the studied interval. Overall, throughout the 12 to 5 ka BP interval in SL21, relative

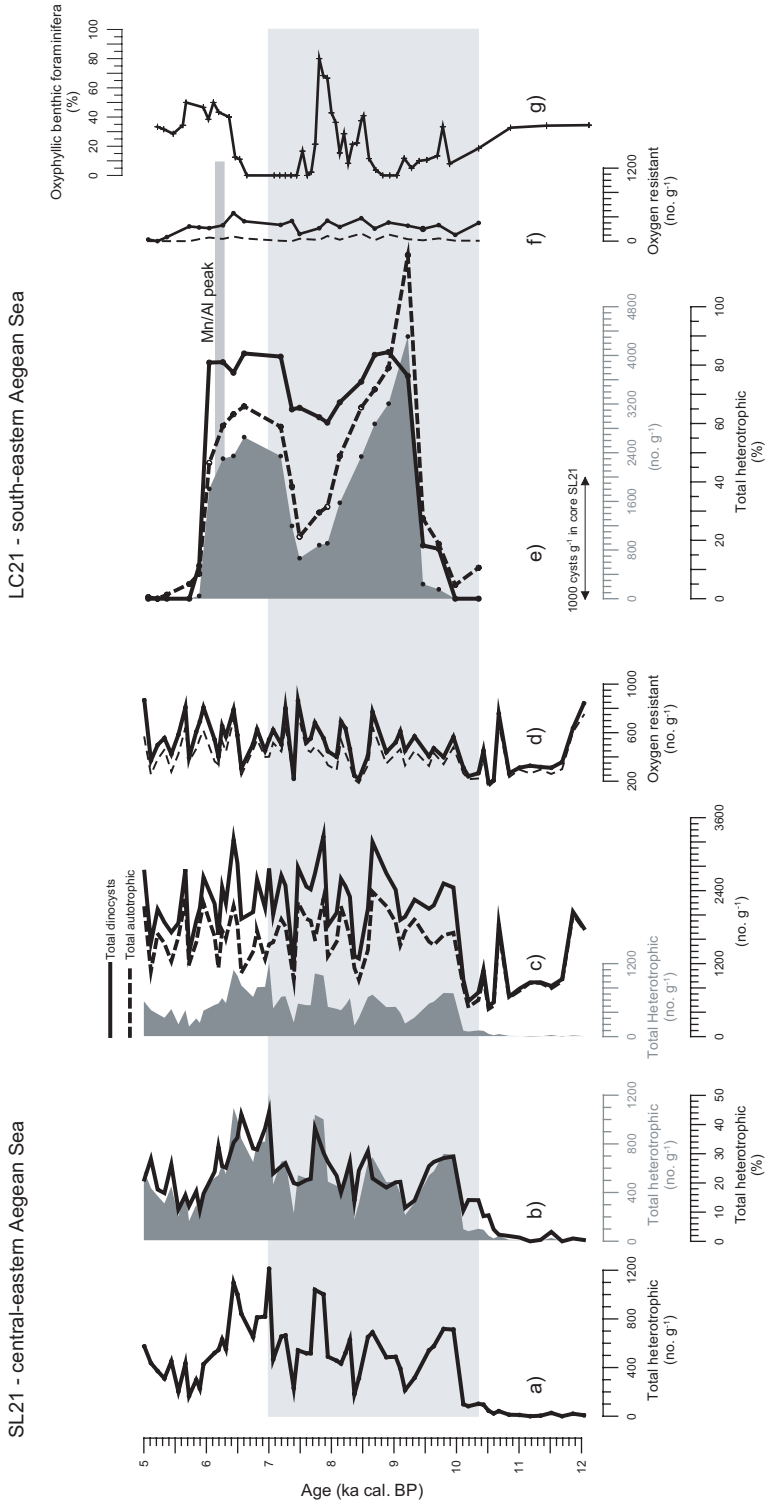
SL21 - central-eastern Aegean Sea
LC21 - south-eastern Aegean Sea
Oxyphyllic benthic foraminifera (%)
Mn/Al peak
Total dinocysts
Total autotrophic
1000 cysts g-1 in core SL21
a)
b)
c)
d)
e)
f)
g)
Total heterotrophic (no. g-1)
Total Heterotrophic (no. g-1)
Oxygen resistant (no. g-1)
Total heterotrophic (%)
Age (ka cal. BP)

abundances of heterotrophic dinocysts and the total dinocyst concentrations are very similar to the concentrations of total heterotrophic dinocysts.

In south-eastern Aegean core LC21 we note that both the total heterotrophic and total dinocysts show two lobes of very high abundances separated by a ~500 year interval of lower values (< 1000 cysts g^{-1}). The lower lobe occurs between 9.5 and 8 ka BP while the upper one between 7.4 and 6 ka BP. This structure is not apparent in the "oxygen resistant" record from the same core, which rather displays a virtually flat profile throughout the early to mid Holocene interval (Figure 4.3f). Total heterotrophic dinocyst concentrations show a net increase at the base of the lower lobe between 9.5 and 9.2 ka BP, with a peak value of ~4300 cysts g^{-1} at 9.2 ka BP, which stands out as the highest of the entire early to mid Holocene interval in LC21. This concentration is one order of magnitude greater than the early to mid Holocene mean value in the nearby core SL21. Given that sedimentation rates at site of core LC21 are about twice as high as in core SL21 (Casford et al., 2003), the observed difference in the concentrations of total heterotrophic dinocysts cannot obviously be explained in terms of dilution effect at site of core SL21 site. In agreement with several studies from both the eastern Mediterranean (Zonneveld et al., 2001; Versteegh and Zonneveld, 2002) and other regions (Zonneveld et al., 2007), it might be argued that more severe anoxic conditions experienced at the deeper site (LC21) during sapropel S1 deposition could have favoured the preservation of the oxygen sensitive *Protoperidinium* cysts relative to the shallower site (SL21) where long-term anoxia never developed (Abu-Zied et al., in press).

Figure 4.3 (left): Distribution versus age of total heterotrophic, total, and oxygen resistant dinocysts in Aegean cores SL21 (a, b, c, d) and LC21 (e, f), and oxyphillic benthic foraminifera (Casford et al., 2003) in core LC21. **(a)** concentrations (no. g^{-1}) of total heterotrophic dinocysts. **(b)** relative abundances (%) (black solid line) overlain onto the concentrations (dark grey shaded profile) of heterotrophic dinocysts. **(c)** concentrations (no. g^{-1}) of total (solid line) and autotrophic (dashed line) dinocysts overlain onto the concentrations (grey shaded profile) of heterotrophic dinocysts. **(d)** concentrations (no. g^{-1}) of oxygen resistant dinocysts including (solid line) not including (dashed line) *Impagidinium* spp. **(e)** concentrations (no. g^{-1}) of total dinocysts (dashed line) and relative (solid line) and absolute (grey shaded profile) abundances of heterotrophic dinocysts. **(f)** concentrations (no. g^{-1}) of oxygen resistant dinocysts including (solid line) not including (dashed line) *Impagidinium* spp. g) percentages of oxyphillic benthic foraminifera in LC21 (Casford et al., 2003). Light grey shaded area represents the sea surface freshening accompanying the sapropel S1 deposition as reconstructed by foraminifer and seawater oxygen stable isotopes (Casford et al., 2002, 2003; Rohling et al., 2002a; Chapter 3). Grey inset indicates the Mn/Al peak in core LC21 (Mercone et al., 2001).

However, at least three lines of evidence suggest that fluctuations in the absolute abundances of total heterotrophic dinocysts in core LC21 are more likely to truly reflect changes in the primary productivity at the sea surface rather than enhanced preservation at the sea floor. Firstly, LC21 concentrations of total heterotrophic dinocysts are found to significantly covary with two other paleoproductivity indicators, namely the Ba_{excess} (R^2=0.78, N=28) and the C_{org} (R^2=0.65, N=28) previously reported from the same core (Figure 4.4b) (Mercone et al., 2001). Secondly, if compared to the pattern of extinctions/repopulations of oxyphillic benthic foraminifera in LC21 (Figure 4.3g) the heterotrophic dinocyst record for the same core does display neither visual nor statistical similarity (R^2=0.16, N=20). Overall, decreases (increases) in the oxyphillic benthic foraminifer record do not correspond to increases (decreases) in the concentration of the total heterotrophic dinocysts, thereby suggesting that a strong overprint of bottom water ventilation effects on the structure of the heterotrophic dinocyst concentration signal is rather unlikely. This is clearly visible at the onset of the lower lobe of sapropel S1 in LC21, where the increase in heterotrophic dinocysts occurs when oxyphillic benthic foraminifera are still present with abundances of ~5%. And it is even clearer in the interval between the two lobes when the absence of benthic foraminifera between ~9.0 and 8.5 ka BP corresponds to a decrease in the heterotrophic dinocyst concentrations, which hence follow an independent trend. Finally, the downward diffusion of the oxygen front in core LC21 postdating the sapropel event, which is indicated by a distinct peak in Mn/Al at 6.3 ka BP (see yellow inset in Figure 4.3) (Mercone et al., 2001), does not seem to affect the trend of the total heterotrophic dinocysts that still shows high concentrations until ~6 ka BP.

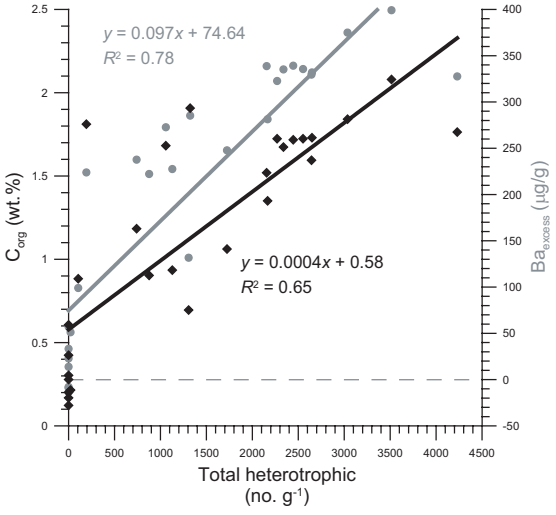

Figure 4.4: Correlations between the concentrations of total heterotrophic dinocysts with and Ba_{excess} (grey dots) and C_{org} (black diamonds) in core LC21 (geochemical data from Mercone et al., 2001).

With respect to the onset of the Aegean sea surface freshening as recorded by the $\delta^{18}O$ of the planktonic foraminifer *Globigerinoides ruber* prior to sapropel S1 deposition (see grey band in Figure 4.3) (Casford et al., 2002, 2003) the major shift in the SL21 dinocyst assemblages centred on 10 ka BP appears to post-date such an event by ~600 years. In south-eastern Aegean core LC21 the net increase in concentration of total heterotrophic dinocysts occurs up to ~800 years later than in SL21 core. LC21 seawater $\delta^{18}O$ data (Chapter 3) indicate that fresher sea surface conditions in the Aegean persisted until 7.2 ka BP when the basin's hydrography initiated a gradual return towards modern conditions (Casford et al., 2002, 2003). This gradual change in the surface waters, however, is not reflected in any of the dinocyst groups presented for cores SL21 and LC21, let alone in the heterotrophic dinocyst concentrations (Figure 4.3a, b, e) that show a broad maximum until 6 ka BP.

4.3.2. The southern Adriatic Sea

The main dinocyst species occurring in southern Adriatic core AD91-17 have been previously reported in Giunta et al. (2003) and Sangiorgi et al. (2003). Likewise in the Aegean Sea, the heterotrophic dinocyst assemblage in the Adriatic core AD91-17 through the early to mid Holocene is dominated by *Brigantedinium* spp. and *Echinidinium zonneveldiae*, which on average account for ~62% of the of the total heterotrophic cyst counts.

In core AD91-17, the first sharp increase in the heterotrophic dinocysts concentration (Figure 4.5a) occurs at ~8.5 ka BP, accompanied by a marked shift in their percentages from values lower than 30% to about 55% (Figure 4.5b). At 8 ka BP the heterotrophic dinocyst concentrations reach a maximum of 2700 cysts g^{-1}. The concentrations of total heterotrophic dinocysts are always relatively high (> 1000 cysts g^{-1}) between 8.5 and 7.1 ka BP with the exception of two lows centred at 7.9 (< 231 cysts g^{-1}) and 7.4 ka BP (< 820 cysts g^{-1}). Both autotrophic and oxygen resistant dinocysts markedly increase only in the interval between 7.6 and 7.1 ka BP, where they reach values comparable to the earliest Holocene. The decrease to background values starts at 7.1 ka, in parallel with the heterotrophic dinocyst decline.

In general, the Adriatic core AD91-17 shows heterotrophic dinocysts concentrations slightly higher than those in the Aegean core SL21 and lower than those of Aegean core LC21, with a more variable signal than in the Aegean records. However, similar to the Aegean records, also in the Adriatic core AD91-17 decreases in the heterotrophic dinocyst concentrations do not correspond to increases in the oxyphillic benthic foraminifer percentages and therefore in the bottom water

oxygenation (Figure 4.5e). Importantly, the highest peak in the heterotrophic dinocyst concentration at 8.0 ka BP rather corresponds to a peak percentage of oxyphillic benthonic foraminifera, suggesting that also in core AD91-17 heterotrophic dinocysts are unlikely to be affected by the bottom water oxygenation.

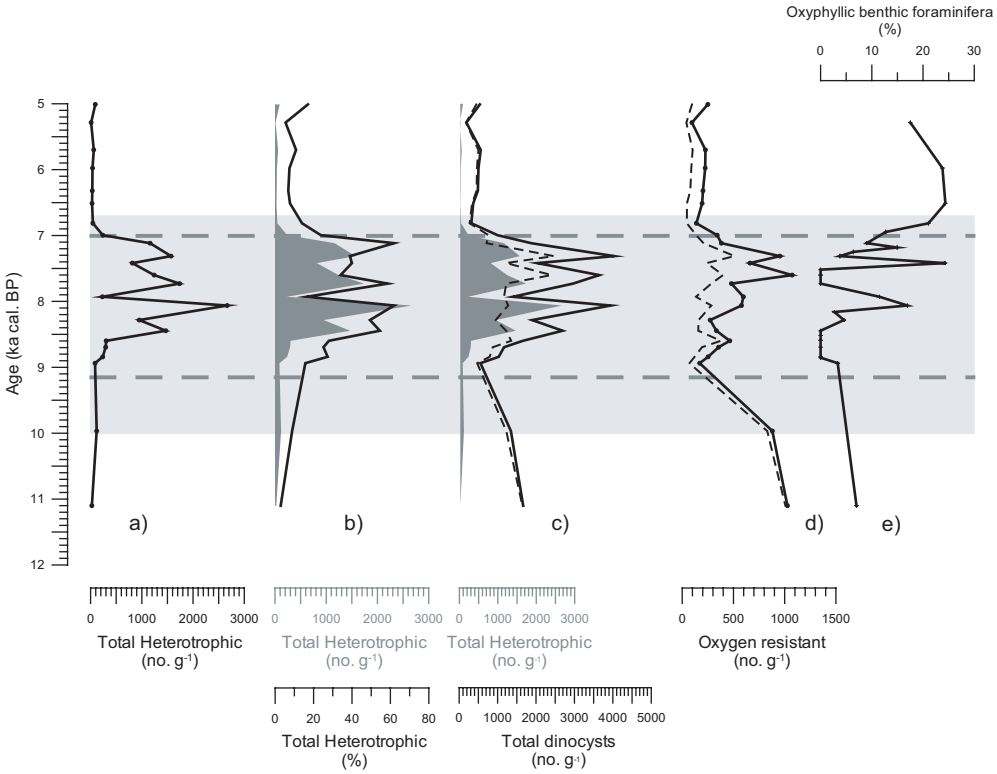

Figure 4.5: Distribution versus age of total heterotrophic, total, and oxygen resistant dinocysts, and oxyphillic benthic foraminifera in southern Adriatic core AD91-17. **(a)** concentrations (no. g^{-1}) of total heterotrophic dinocysts (black solid line). **(b)** relative abundances (%) of heterotrophic dinocysts (black solid line). These profiles are overlain onto the concentrations (grey shaded profile) of heterotrophic dinocysts. **(c)** concentrations (no. g^{-1}) of total dinocysts (black solid line). These profiles are overlain onto the concentrations (grey shaded profile) of heterotrophic dinocysts. **(d)** concentrations (no. g^{-1}) of oxygen resistant dinocysts including (solid line) not including (dashed line) *Impagidinium* spp. **(d)** oxyphillic benthic foraminifera (Giunta et al., 2003). Grey shaded area represents the sea surface freshening accompanying the sapropel S1 deposition as reconstructed by foraminifer and oxygen stable isotopes (Sangiorgi et al., 2003).

Overall, the increase in dinocyst abundances in the Southern Adriatic core AD91-17 occurs much later (~1.5 kyr BP) than the surface water freshening as recorded by the $\delta^{18}O$ of the planktonic foraminifer *Globigerina bulloides* in this sector of the basin (Siani et al., 2001, Sangiorgi et al., 2003). The decrease in all the

dinocyst records (Figure 4.5) begins at ~7.1 ka BP, thereby preceding the termination of the sea surface freshening by a few centuries. However, the termination of the sea surface freshening in the Adriatic Sea cores is generally less well defined than in the Aegean Sea record due to the different habitat of the planktonic foraminifer species used to reconstruct surface salinity.

4.3.3. Strait of Sicily

In the early to mid Holocene interval of core CS01 from the Sicily Channel, the total heterotrophic dinocyst assemblage is again dominated by *Brigantedinium* spp. and *Echinidinium zonneveldiae*, which together account for on average the ~63% of the total heterotrophic group. Brigantedinium spp. is usually dominant in highly productive regions (Marret and Zonneveld 2003) and is the most abundant heterotrophic dinocyst in the eastern Mediterranean records spanning the last deglaciation (Zonneveld, 1995; Sangiorgi et al., 2002). On the other hand, *E. zonneveldiae* is commonly not reported as one of the most occurring species in the eastern Mediterranean records. Notably, given that this taxon has been described and defined only recently (Head, 2003), its absence in previous studies may not necessarily imply the actual absence of *E. zonneveldiae* from the eastern Mediterranean records. *E. zonneveldia*e has been recently found in assemblages of the last interglacial period from the Baltic Sea, when the region underwent an abrupt change (decrease) in salinity (Head et al., 2005). This evidence combined with the occurrence of *E. zonneveldiae* in records from different locations of the eastern Mediterranean during the early to mid Holocene period of widespread sea surface freshening (Rohling and De Rijk, 1999) hints to the euryhaline character of this species.

It is worth noting that dinocysts in the Strait of Sicily core are never abundant, and in the early and middle Holocene, the total dinocyst concentration never exceeds ~450 cysts g^{-1} (Figure 4.6). In this respect, if shift in the dinocyst concentrations from the Strait of Sicily core were scaled to the shifts in the Adriatic and the Aegean records (see Figure 4.7 and section 4.4), they would be hardly detectable.

Heterotrophic dinocyst concentrations (Figure 4.6a) and percentages (Figure 4.6b) synchronously start to increase at ~10.5 ka BP, culminating at ~8.1 ka BP, with values of 205 cysts g^{-1} and ~60%. The increase of heterotrophic dinocysts in the interval between 10 and 6.5 ka BP is roughly coeval to the estimated time of sapropel S1 deposition in the wider eastern Mediterranean Sea (e.g., Mercone et al., 2000). Moreover, the peaks in heterotrophic dinocyst concentrations and percentages at 8.1 ka BP is synchronous (within the same sample) with ~1°C sea surface cooling reported from alkenone-based reconstructions at the same site

(data not shown here and available upon request). This cooling is likely linked to an episode of centennial-scale cooling widespread to the entire Northern Hemisphere (see Chapter 3 and references therein), which in the eastern Mediterranean was associated to a reventilation interlude that interrupted the anoxic/dysoxic sedimentation of sapropel S1 (Rohling et al., 1997; De Rijk et al., 1999; Myers and Rohling, 2000; Casford et al., 2003; Abu-Zied et al., in press). Accordingly, we speculate that the recorded peak in heterotrophic dinocysts in CS01 could reflect an increase in productivity following stronger mixing of the water column during time of sapropel S1 interruption, in support of previous reconstructions based on planktonic foraminifera and calcareous nannoplankton from the nearby ODP core 963D (Sprovieri et al., 2003; Di Stefano and Incarbona, 2004).

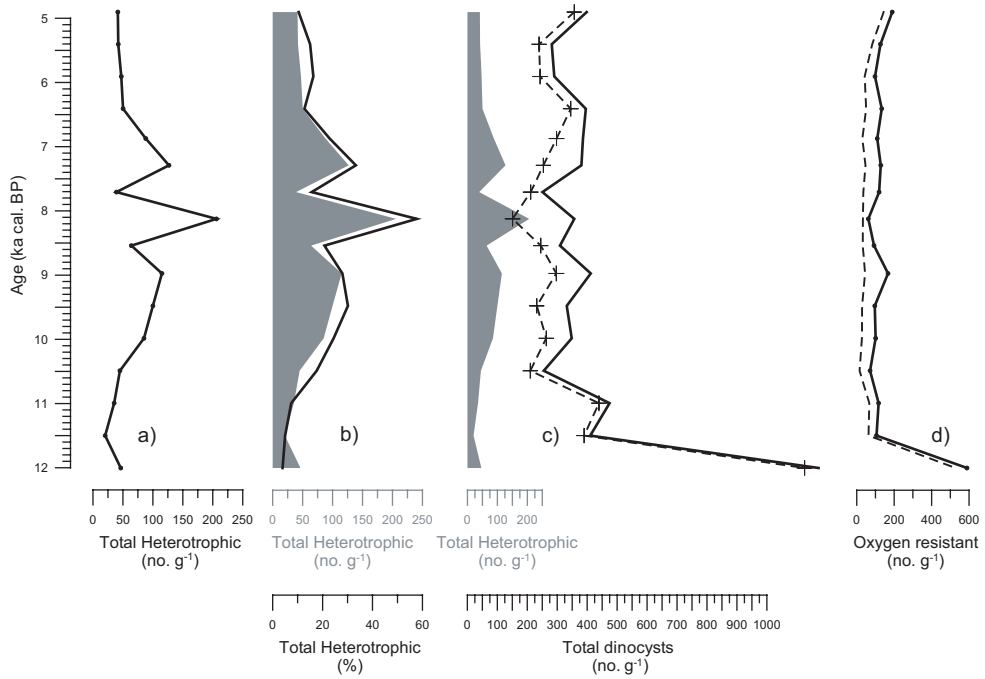

Figure 4.6: Distribution versus age of total heterotrophic, total, and oxygen resistant dinocysts in Strait of Sicily's core CS01. **(a)** concentrations (no. g^{-1}) of total heterotrophic dinocysts. **(b)** relative abundances (%) (black solid line) overlain onto the concentrations (grey shaded profile) of heterotrophic dinocysts. **(c)** concentrations (no. g^{-1}) of total dinocysts overlain onto the concentrations (grey shaded profile) of heterotrophic dinocysts. **(d)** concentrations (no. g^{-1}) of oxygen resistant dinocysts including (solid line) not including (dashed line) *Impagidinium* spp.

Instead, no significant increase is recorded in either the autotrophic or in the oxygen resistant dinocyst profiles (Figure 4.6 c, d) during the early to middle Holocene. The oxygen resistant dinocysts show a large decrease in abundance culmi-

nating at 11.5 ka BP followed by a remarkably flat trend throughout the remnant early to mid Holocene section. In the autotrophic dinocysts we note a two-step decrease terminating at 11.5 and 10.5, respectively, followed by low amplitude oscillations. Those marked decreases in the oxygen resistant and in the autotrophic dinocysts seem to be rather mirroring a complex climatic signal (which include a warming trend) occurring at the Younger Dryas/Holocene transition rather than a change in productivity at the sea surface.

4.4. Discussion and concluding remarks

Four sediment cores retrieved from three key sectors of the eastern Mediterranean Sea (Aegean and Adriatic Seas, Strait of Sicily) have been investigated for dinocyst abundances to assess the potentiality of dinocysts as sea surface productivity indicators at times of probable increased organic matter preservation due to overall decreased bottom water oxygenation. Our discussion will be mostly focused on heterotrophic dinocysts, as their reliability as productivity indicators has been - and still is - a matter of discussion (Zonneveld et al., 2001, 2007; Versteegh and Zonneveld, 2002, Reichart and Brinkhuis, 2003) and on oxygen resistant dinocyst, taken in some studies (Zonneveld et al., 2001, 2007; Versteegh and Zonneveld, 2002) as the ideal proxy for paleoproductivity reconstruction.

During sapropel S1 deposition both the Aegean and Adriatic cores display distinct maxima in both concentrations and percentages of heterotrophic dinocysts, although differences in the timing (onset), duration and magnitude of these changes between the different sites exist. Core CS01 from the Strait of Sicily also displays an increase in the concentration of heterotrophic dinocysts between 10 and 6.5 ka BP but absolute numbers are here much too low to allow conclusive speculations. Concerning the Aegean and Adriatic Seas, comparison between records of heterotrophic dinocyst concentrations and oxygen demanding benthic foraminifera obtained from within the same cores are of particular interest. Overall, the results reveal that fluctuations in the ventilation regime as reflected by oxyphillic benthic foraminifera (see, e.g., Casford et al., 2003; Abu-Zied et al., in press) unlikely have substantially affected the structure of the absolute heterotrophic dinocyst signal through the early to mid Holocene. Furthermore, in core LC21 concentrations of heterotrophic dinocysts and the productivity indicator Ba_{excess}/Al (e.g., Gingele et al., 1999) are positively correlated (R^2=0.78, N=28), suggesting a strong control of productivity changes on the structure of the (absolute) heterotrophic dinocyst signal. Taken together these evidences suggest that in the Aegean and Adriatic Seas the heterotrophic dinocyst concentrations seem to genuinely reflect changes in the productivity patterns at the sea surface rather than representing

preservation overprint effects at the sea floor, in support to previous studies from other highly productive regions (Reichart and Brinkhuis, 2003).

The present study hence does show that heterotrophic organic walled dinoflagellate cysts records may be used - with some minor caveats - to reconstruct past productivity patterns at the sea surface.

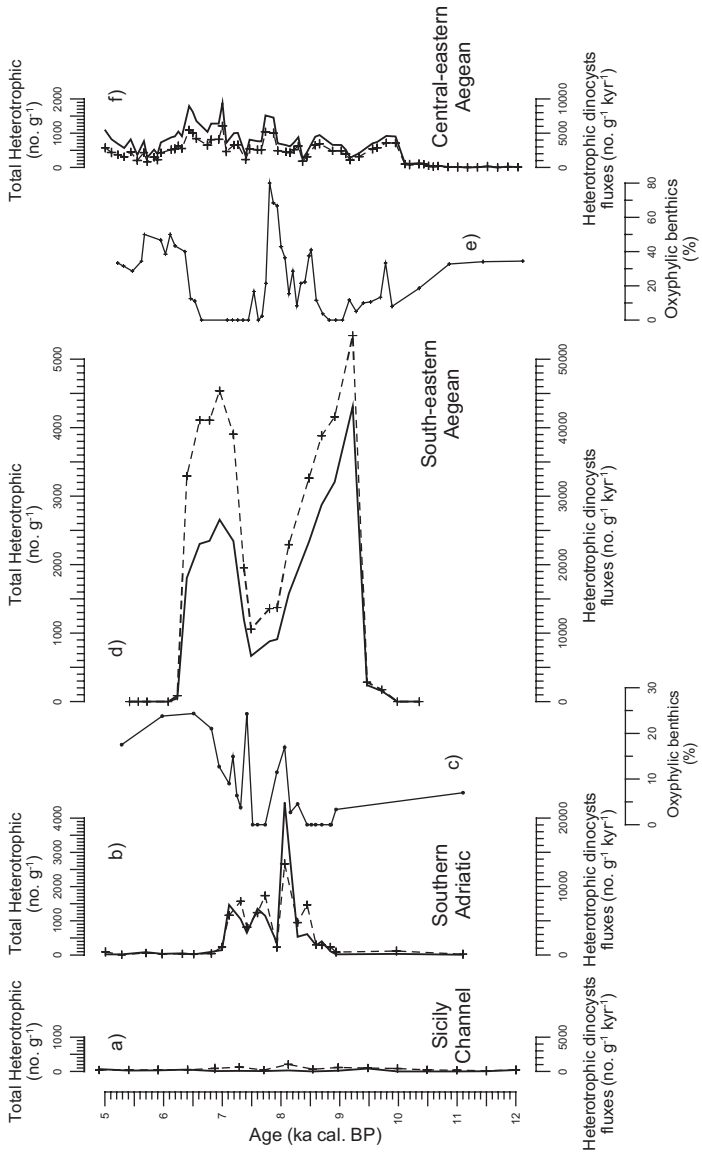

Figure 4.7: paleofluxes of total heterotrophic dinocysts (no. g^{-1} kyr^{-1}) in cores CS01 **(a)**, AD91-17 **(b)**, LC21 **(d)**, and SL21 **(f)**. Dashed lines with + symbols overlain onto profiles in a, b, d, and f represent the concentrations of total heterotrophic dinocysts in the Strait of Sicily's, Adriatic, and Aegean cores. Oxyphillic benthic foraminifer records are shown in c for core AD91-17 and in e for core LC21, respectively.

Interestingly, the onset of more productive sea surface waters in central-eastern Aegean core SL21 at 10 ka BP as detected with heterotrophic dinocysts precedes by up to ~800 and ~1500 years similar changes in south-eastern core LC21 (Figure 4.3) and the Adriatic sea (Figure 4.5), respectively. Casford et al. (2002) have proposed that nutrient supply needed to account for the organic carbon buried during S1 deposition may only be explained by isolation of the intermediate/deep water masses for ~1000 years prior to the sapropel inception and consequent storage of nutrients at depth. Accordingly, the increase in sea surface productivity at site of core SL21 appears coincident with the shoaling of the pycnocline in the Aegean and with subsequent injections of nutrients at shallow depths. It is also worth reminding that heterotrophic dinoflagellate can thrive deeper than autotrophic dinoflagellates and other photosynthetic phytoplankton as they do not require light to survive. Given the above, and the dominant cyclonic circulation of the central Aegean Sea, persistent also during S1 deposition (Myers et al., 1998; Casford et al., 2002), a speculative scenario would suggest that this (intermediate) reservoir of nutrients was most likely closer to the surface waters in the central sector of the basin than in its south-eastern sites. Our results thus seem to suggest that sea surface productivity increase during sapropel S1 deposition was likely favoured by a weakened intermediate water circulation that acted as nutrients trap at intermediate depths (Sarmiento et al., 1988).

The hypothesis of nutrient-enriched intermediate water during S1 time deposition would agree with a peak in sea surface productivity detected in records from the Strait of Sicily and coinciding with a centennial-scale episode of severe winter cooling and deeper mixing, which allowed interaction of the surface and nutrient rich intermediate waters (Sprovieri et al., 2003; Di Stefano and Incarbona, 2004, this study).

To conclude we provide evidences that trends in the concentrations of heterotrophic dinocysts reported here are not linked to changes in the sedimentation rates through time. This is apparent if fluctuations in the heterotrophic dinocysts are discussed in terms of dinocyst accumulation rates, expressed as cysts g-1 kyr-1 (Figure 4.7). Reconstructed dinocyst accumulation rates for the different sites presented in this study clearly indicate that changes in the sedimentation rates minimally affected the structure of the heterotrophic dinocyst record. It is however worth noting that, if considered on the same scale, dinocyst accumulation rates at the Aegean and Adriatic sites are more than two orders of magnitude larger than in the Strait of Sicily, with the currently markedly oligotrophic area of south-eastern Aegean (Psarra et al., 2000) showing the highest dinocyst accumulation rates (Figure 4.7d).

Chapter 5

Amplified response of the eastern Mediterranean to insolation changes; insights from the last two interglacial periods

Based on:
Gianluca Marino, Eelco J. Rohling, Francesca Sangiorgi, Jaap S. Sinninghe Damsté, and Henk Brinkhuis

To be submitted

Abstract

The sensitivity of the Mediterranean marine system to climate forcing is still a matter of debate. Here we test the long-term sensitivity of the eastern Mediterranean circulation to insolation forcing over the last two intervals of peak interglacial conditions, at times of substantial hydrological perturbations when extensive hydrographic changes led to the widespread deposition of organic-rich sediments (sapropels). To this purpose for the first time a set of highly resolved paleoceanographic proxy records are analyzed within the same sediment core (south-eastern Aegean core LC21) through both the last and the current (Holocene) interglacial peak periods of sapropel S1 and S5 deposition, respectively. Oxygen ($\delta^{18}O$) and carbon ($\delta^{13}C$) isotopes for surface water (*Globigerinoides ruber*) and sub-thermocline dwelling (*Neogloboquadrina pachyderma*) planktonic foraminifera and total organic carbon (C_{org} wt%) data are used to reconstruct the water mass dynamics and the magnitude of C_{org} burial during these two peak interglacial periods. We find overall more pronounced environmental changes in the last interglacial records than during the Holocene. During deposition of the last interglacial sapropel S5, C_{org} mass accumulation rates (MAR) reached ~3 g C m^{-2} yr^{-1}, an order of magnitude higher than the highest C_{org} MAR for the Holocene sapropel S1. In addition, the negative shift in the $\delta^{18}O$ record of the summer mixed layer dwelling planktonic foraminifer *Globigerinoides ruber* at the onset of S5 deposition is twice as large as the shift occurred at the S1 onset. $\delta^{13}C$ gradients in surface to intermediate waters during deposition of S5 are larger than during deposition of S1, and similar to the intermediate to deep waters $\delta^{13}C$ gradients for S1. This suggests that intermediate waters during S5 were as poorly ventilated (thus strongly isolated) as the deep waters during S1. Taken together, the datasets suggest a greater insolation forcing during the last interglacial period caused stronger water mass stratification during sapropel S5, with a significantly shallower depth of the chemocline and higher C_{org} MARs, relative to S1.

5.1. Introduction

The current (Holocene, since 11.5 thousand years Before Present, ka BP) and the last interglacial (~130 to 116 ka BP) periods have similar precession and obliquity configurations but markedly different eccentricities (Harrison et al., 1995). This resulted in higher peak summer insolation at the latitude of 30°N during the last interglacial (~13% larger than today) period than during the early Holocene (~8% larger than today) (Laskar, 1990). These insolation differences are thought to have produced slightly warmer conditions during the last interglacial period (Lozhkin et al., 1995; Harrison et al., 1995; Cortijo et al., 1999) and, in turn,

substantial retreat of continental ice at both poles (Duplessy et al., 2007) leading to sea level that exceeded the present day level by a few meters (Otto-Bliesner et al., 2006; Rohling et al., 2008b).

In the (eastern) Mediterranean, episodes of precession minima/insolation maxima of the last two interglacial periods are featured by the deposition of organic-rich layers deposited under dysoxic/anoxic conditions of the bottom waters (sapropels) (Mercone et al., 2000, 2001; Casford et al., 2002, 2003; Cane et al., 2002; Rohling et al., 2002b, 2004, 2006). These have been linked to positive shifts of the basin's freshwater budget in response to increases in African monsoon-fuelled river discharge along the North African margin (Rossignol-Strick et al., 1982; Rossignol-Strick, 1983, 1985; Rohling et al., 2002b, 2004; Scrivner et al., 2004).

The last interglacial sapropel S5 appears to be more intensively developed than the early to mid Holocene S1, as evidenced by larger organic carbon contents (Fontugne and Calvert, 1992), and a more extreme freshwater disturbance (Rohling, 1999; Rohling et al, 2004). To date, however, no detailed assessments of the differences in magnitude of response between the two events, which rely on high resolution records of sapropels S1 and S5 from the same site, are available. Here we compare for the first time several sets of foraminiferal stable isotope and organic geochemical paleoceanographic proxy records performed on the same sample series (i.e., co-registered) through both S1 and S5 from one and the same sediment core (south-eastern Aegean Sea core LC21, see Figure 1.1), with the aim of understanding the responses at the same location to different magnitude forcings.

The south-eastern Aegean Sea is ideally suited for the purpose of this study, as it is relatively remote from the North African sites of freshwater discharge into the open eastern Mediterranean (Fontugne et al., 1994; Rohling et al., 2002b, 2004). In addition, in this region substantial winter-time sea surface buoyancy loss occurs, with associated deep winter mixing (D'Ortenzio et al., 2005) and water-column instability (Georgopoulos et al., 1989). Consequently, records from the site of core LC21 are expected to (1) provide a basin-integrated record of the monsoon-fuelled freshwater discharges into the eastern Mediterranean, rather than the strong variability that affects sites close to these inputs such as ODP Site 971 (Rohling et al., 2002b) and ODP Site 967 (Scrivner et al., 2004); and (2) be highly sensitive to changes in water mass dynamics associated with winter-cooling induced buoyancy loss from the basin (Chapter 1).

5.2. Materials and methods

Core LC21 was recovered in the south-eastern Aegean Sea (35°40'N;

26°35'E; 1522 m water depth) in 1995 by RV *Marion Dufresne* for the EC-MAST2 (Marine, Science, and Technology Programme) PALEOFLUX (Biogeochemical Fluxes in the Mediterranean Water-Sediment System) program. Core LC21 consists of calcareous microfossil rich hemipelagic ooze punctuated by distinctly defined dark bands of sapropelic material (Rothwell, 1995). LC21 contains a distinct 10 cm thick ash layer of the late Holocene that is related to the Minoan eruption of Santorini. Accordingly, the depth scale presented has been adjusted to account for it (Rohling et al., 2002a).

Core LC21 has been sampled at 1 cm resolution throughout and subsequently sub-sampled for foraminiferal censuses/stable isotopes, marine palynology, and organic geochemistry. In the present paper, we discuss foraminiferal stable isotope and organic geochemistry data for intervals 0-234 and 826-1035 centimetres below the seafloor (hereafter cm), containing sapropel S1 and S5, respectively. Details on the chronological frameworks for the studied intervals are reported in Chapter 1 (sapropel S5) and Chapter 3 (sapropel S1 and Holocene; see also Casford et al., 2007).

5.2.1. Foraminiferal oxygen and carbon stable isotopes ($\delta^{18}O$ and $\delta^{13}C$)

Sediment samples have been weighed, oven-dried, and subsequently disaggregated and wet sieved over 63, 125, 150 and 600 μm meshes, using demineralised water. The various fractions have been oven dried and weighed. The 150-600 μm fraction has been split with a random ("Otto") microsplitter, into an aliquot for the isotope studies and an aliquot reserved for faunal abundance studies. Using a binocular light microscope, clean and well-preserved adult specimens of *Globigerinoides ruber* (*N*=15 per sample) and *Neogloboquadrina pachyderma* (*N*=20 per sample) have been hand-picked in a narrow size-window (300-350 μm for *G. ruber* and 250-300 μm for *N. pachyderma*) constrained using a measurement eyepiece. Species selection was based on habitat reconstructions reported in Rohling et al. (2004).

Foraminiferal $\delta^{18}O$ and $\delta^{13}C$ analyses have been performed at the National Oceanography Centre (Southampton, UK) with a Europa Geo2020 dual inlet mass spectrometer following individual acid-bath reaction of foraminiferal calcite samples. Isotope ratios are expressed as $\delta^{13}C$ and $\delta^{18}O$, in per mil (‰) values relative to Vienna PeeDee Belemnite (VPDB). External precision was better than 0.06 ‰ for both $\delta^{13}C$ and $\delta^{18}O$.

5.2.2. Organic geochemistry

Organic geochemical analyses through the last interglacial section of core

LC21 were performed at the NIOZ Royal Netherlands Institute for Sea Research (Den Burg, Texel, The Netherlands). The total organic carbon (C_{org} wt%) contents were determined by elemental analysis (EA)/isotope-ratio-monitoring mass spectrometry (EA/irmMS). EA/irmMS analyses were performed on decalcified (by reaction with 1 N HCl for 18 h) sediments using a Carlo Erba Flash elemental analyzer coupled to a Thermofinnigan DeltaPLUS irmMS system. The C_{org} contents were determined using external standards with known carbon content. Details on the organic geochemical analyses performed on the Holocene section of core LC21 are reported in Mercone et al. (2000, 2001).

C_{org} mass accumulation rates (MARs) (g C m^{-2} yr^{-1}) have been then calculated according to the equation:

$$C_{org}\ \text{MAR}\ (\text{g C m}^{-2}\ \text{yr}^{-1}) = C_{org}\ (\text{g C}/100\text{g}) \times \text{sediment accumulation rate (cm kyr}^{-1}) \times \text{bulk dry density (g cm}^{-3})/100$$

Bulk dry densities of the sediment equal 1.2 g cm^{-3} for non-sapropel sediments and 0.8 g cm^{-3} for sapropel intervals (Robertson et al., 1996).

5.3. Results

The oxygen and carbon stable isotope records for the planktonic foraminiferal species *Globigerinoides ruber* and *Neogloboquadrina pachyderma* and the C_{org} contents through the last (S5) and the current (S1) interglacial periods in southeastern Aegean core LC21 are shown in Figure 5.1. The sapropels are visually distinct as dark intervals between 995 and 875 cm and between 185 and 128 cm (see light grey shaded areas in Figure 5.1).

The dark interval between 995 and 875 cm represents last interglacial sapropel S5 (Chapter 1) (Figure 5.1, panel II). It consists of a 120 cm thick continuous organic carbon-rich layer devoid of benthic fauna with preserved sedimentary lamination in some intervals (Chapter 1). At 995 cm a synchronous increase in C_{org} concentrations and the extinction of benthic fauna mark the onset of the anoxic event (Chapter 1) (Figure 5.1a, panel II). Following that change, C_{org} steadily increases to attain high values (>12%) between 980 and 970, with a maximum of ~14% centred on 955 cm. Starting at 865 cm, C_{org} returns to the typical eastern Mediterranean non-sapropel concentrations (~0.3%).

The dark interval between 185 and 128 cm represents Holocene sapropel S1 (Mercone et al., 200, 2001; Casford et al., 2002, 2003; Rohling et al., 2002a), and it includes two benthic azoic intervals. In between these azoic intervals, a 10 cm thick lighter-coloured section containing a repopulation of benthic foraminifera that reflects a centennial-scale re-oxygenation of the bottom waters (De Rijk et

al., 1999; Mercone et al., 2001; Casford et al., 2003; Abu-Zied et al., in press). The C_{org} profile for S1 shows two lobes of enhanced values (~2%) and a drop in Corg concentrations (<1%) during the reventilation event (Mercone et al., 2001) (Figure 5.1a, panel I).

Information regarding surface-water responses to hydrological forcing in the eastern Mediterranean can be obtained from the oxygen isotope records of the summer mixed layer dwelling planktonic foraminifer *Globigerinoides ruber* ($\delta^{18}O_{ruber}$) (Rohling, 1999; Rohling et al., 2004). Before the onset of sapropel S5, $\delta^{18}O_{ruber}$ in LC21 reveals an abrupt negative shift of ~1.7‰ that connects two distinct plateaus at 1035-1013.5 (2±0.17‰, 1σ bounds) and 1009-996 cm (0.2±0.13‰) (Figure 5.1d, panel II). Starting at 996 cm, $\delta^{18}O_{ruber}$ markedly decreases again through the onset of S5, towards a value as light as -1.7‰ at 983 cm (within S5). This is the lightest $\delta^{18}O_{ruber}$ peak found in LC21 throughout the last interglacial (Chapter 1) and it represents a feature that is common to several coeval eastern Mediterranean $\delta^{18}O_{ruber}$ records (Cane et al., 2002; Rohling et al., 2002b, 2004, 2006). It has been previously interpreted as a maximum in the monsoon-fuelled freshwater flooding (Rohling et al., 2002b, 2004, 2006), and its onset appears to slightly precede the onset of anoxic sedimentation in LC21 (Chapter 1).

A roughly similar structure is apparent in the $d^{18}O_{ruber}$ at the early Holocene pre-sapropel to sapropel S1 transition; two plateaus at 226.5 to 191.5 (1.8±0.1‰) and 186.5 to 181.5 cm (0.9-0.8‰) followed by a 0.8‰ shift to lighter values that terminates within S1 (~172 cm) (Figure 5.1d, panel I). Along with the structural similarity of the $\delta^{18}O_{ruber}$ records prior to and at the onset of sapropel S5 and S1 in LC21, we emphasize that the pre-sapropel $\delta^{18}O_{ruber}$ values from 1013.5 to 10035 cm and between 226.5 and 191.5 cm are identical to one another within the 1σ bounds of the variance of these specific intervals of the LC21 $\delta^{18}O_{ruber}$ record (see bars in Figure 5.1d). This markedly contrasts starkly with the different values attained at the onset and throughout the sapropel intervals, with the last interglacial values much lighter than the Holocene values, by 1.6 and 1.1‰, respectively.

Figure 5.1 (right): Foraminiferal stable isotope and total organic carbon contents (C_{org}) through the current (panel I) and the last interglacial (panel II) section of core LC21. **(a)** C_{org} (wt%). **(b)** oxygen isotope record for the top intermediate water dwelling planktonic foraminifer *Neogloboquadrina pachyderma* ($\delta^{18}O_{pachyderma}$) (black solid diamonds). **(c)** carbon isotope record for *N. pachyderma* ($\delta^{13}C_{pachyderma}$). **(d)** oxygen isotope record for the summer mixed layer dwelling planktonic foraminifer *Globigerinoides ruber* ($\delta^{18}O_{ruber}$) (black solid dots). **(e)** carbon isotope record for *G. ruber* ($\delta^{13}C_{ruber}$). Dark grey shaded envelope represents the 1σ variance with respect to the 5 points running average smoothers (solid lines). Light grey shaded areas represent the visual extent of the dark-coloured sapropels S1 (panel I) and S5 (panel II) in LC21. Bars in d) and e) are 1σ of the variance through the pre-sapropel sections.

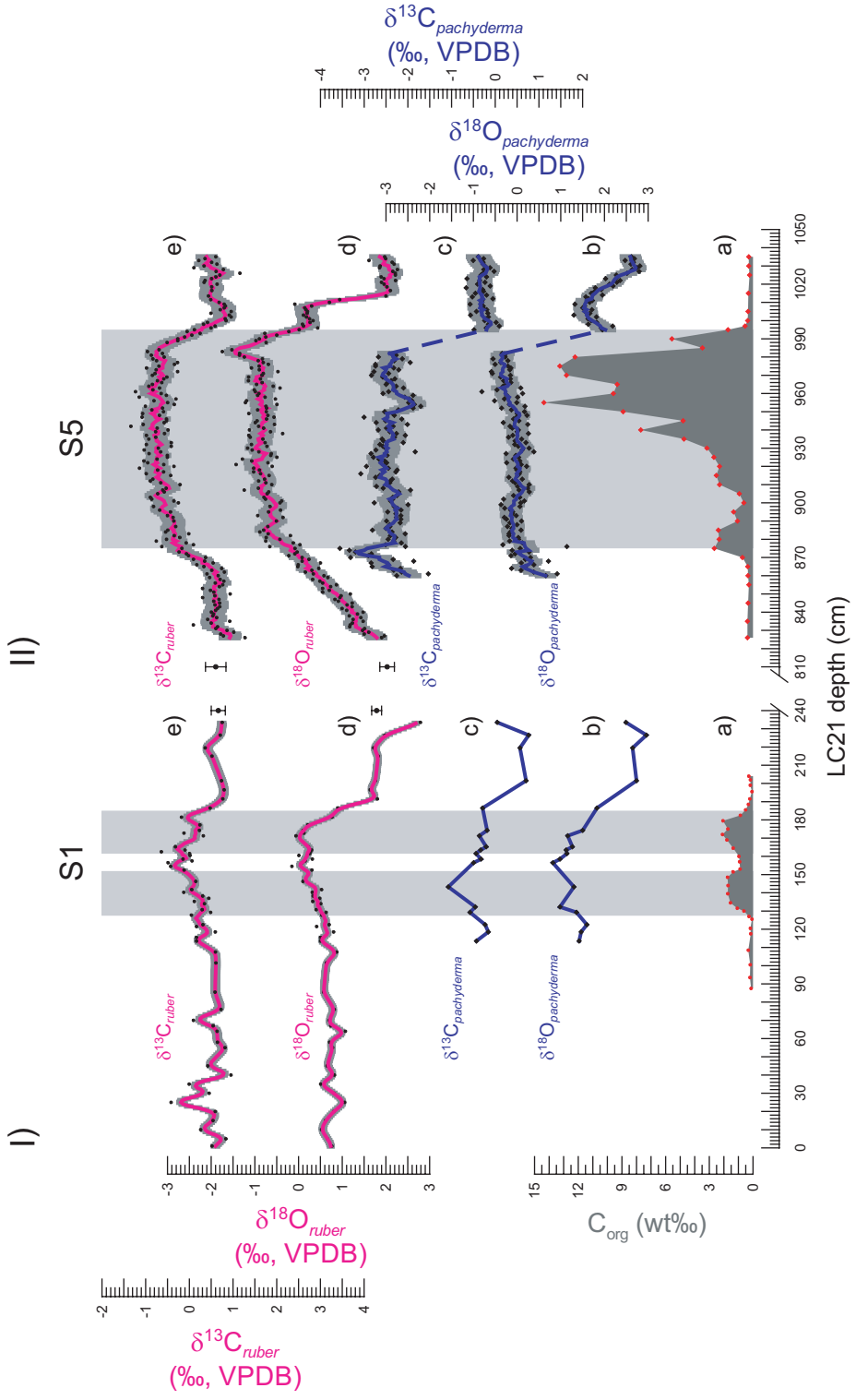
I)
II)
S1
S5
a)
b)
c)
d)
e)
LC21 depth (cm)
C_{org} (wt‰)
$\delta^{18}O_{ruber}$ (‰, VPDB)
$\delta^{13}C_{ruber}$ (‰, VPDB)
$\delta^{13}C_{pachyderma}$ (‰, VPDB)
$\delta^{18}O_{pachyderma}$ (‰, VPDB)

Information regarding the (top) intermediate-water responses to hydrological forcing can be obtained from the oxygen isotope records of the planktonic foraminifer *Neogloboquadrina pachyderma* ($\delta^{18}O_{pachyderma}$) (Rohling et al., 2004). The $\delta^{18}O_{pachyderma}$ record for the last interglacial shows a prominent shoulder in the pre-S5 section between 1028 and 996 cm, which is followed by a jump to values as low as -0.4‰ at 982 cm and, in turn, by a long-term plateau (-0.04±0.3‰) that continues throughout S5 and beyond (Figure 2b, panel II). Absolute $\delta^{18}O_{pachyderma}$ values within S5 are lighter than the ones found within S1, which reaches a minimum of 0.8‰ at 157 cm (Figure 2b, panel I). The exact timing and structure of the negative $\delta^{18}O_{pachyderma}$ shift towards the light values recorded within S5 are obscured by a short (~400 years) absence of *N. pachyderma* from 995 to 982 cm (Chapter 1). The latter event correlates with the disappearance of another sub-thermocline planktonic foraminifer species (*Globorotalia scitula*) at the onset of S5 in LC21 and in several eastern Mediterranean records of the last interglacial period (Cane et al., 2002; Rohling et al., 2002b, 2004, 2006). In the early Holocene section, the transition from heavy pre-sapropel (2.6±0.2‰) to relatively light sapropel (<1.8‰) values appears rather gradual (Figure 5.1d).

Both for S5 and for S1 in core LC21, $\delta^{13}C_{ruber}$ is lighter within the sapropel than in the pre- and post-sapropel sections (Figure 5.1e). This agrees with the typical $\delta^{13}C_{ruber}$ signature found in a range of Quaternary sapropels throughout the eastern Mediterranean (Fontugne and Calvert, 1992; Struck et al., 2001; Cane et al., 2002; Casford et al., 2002, 2003; Rohling et al., 2004, 2006). The typically negative $\delta^{13}C_{ruber}$ values within sapropels have been interpreted as driven by larger influxes of freshwater-borne isotopically light dissolved inorganic carbon during periods of precession minima (Fontugne and Calvert, 1992; Rohling et al., 2004). Looking at the last interglacial record in LC21, we note two plateaus with $\delta^{13}C_{ruber}$ values of 0.6±0.2‰ in the pre- and post-S5 sections (Figure 5.1e, panel II). Interestingly, these are virtually identical to the $\delta^{13}C_{ruber}$ values found in the Holocene between 234 and 192 cm (0.7±0.2‰) and from 108 to 76 cm (0.6±0.1‰) (Figure 5.1e, panel I). Absolute $\delta^{13}C_{ruber}$ values within S5 vary around a mean of -0.65‰, while they are heavier (~0.1‰) through S1. Also the LC21 $\delta^{13}C$ records for *N. pachyderma* reveal lighter values within both sapropels than in the pre-sapropel sections (Figure 5.1c). The $\delta^{13}C_{pachyderma}$ values found within S5 (-2.4±0.3‰) (Figure 5.1c), panel II are much lighter than the ones found through S1, which range between -0.3 and -1‰ (Figure 5.1c, panel I).

5.4. Organic carbon accumulation rates and water mass stratification

Comparison of the different paleoceanographic proxy records used in this

study reveals that environmental changes were more pronounced through S5 than through S1. Specifically, S5 in LC21 contains much higher C_{org} levels, reaching up to ~14% (Figure 5.1a, panel II) (Chapter 1). These are the highest Corg concentrations known from Quaternary marine records from the Mediterranean Sea, and they dwarf the values of up to 2% found in the relatively weakly developed sapropel S1 in the same core (Figure 5.1a, panel I) (Mercone et al., 2000, 2001). Still, even the high C_{org} values of S5 in LC21 are notably lower than those recorded in some Pliocene sapropels (30%), which are regarded as the result of extreme perturbations of the basin's biogeochemical and physical processes (Passier et al., 1999; Nijenhuis and de Lange, 2000).

High detrital inputs at sites of high sedimentation rates, such as core LC21, dilute C_{org} concentrations and so produce values that may not be representative of the actual C_{org} fluxes to the seafloor (Mercone et al., 2001). To eliminate any such bias, we have calculated the C_{org} mass accumulation rates (MARs) through the current and last interglacial sections of core LC21 (Figure 5.2). Sapropel S5 is thought to have developed over a period of 5 kyr (Figure 3a, panel II) (Cane et al., 2002; Rohling et al., 2002b, 2006), which corresponds in LC21 to an average sedimentation rate of 25.2 cm kyr^{-1} (see Chapter 1 for details). According to the new GISP2-tuned chronology developed for the Holocene section of LC21 (see Chapter 3 for details), S1 formed over a period of ~4.2 kyr (Figure 5.2a, panel I) with an average sedimentation rate that amounts to 13.6 cm kyr^{-1}.

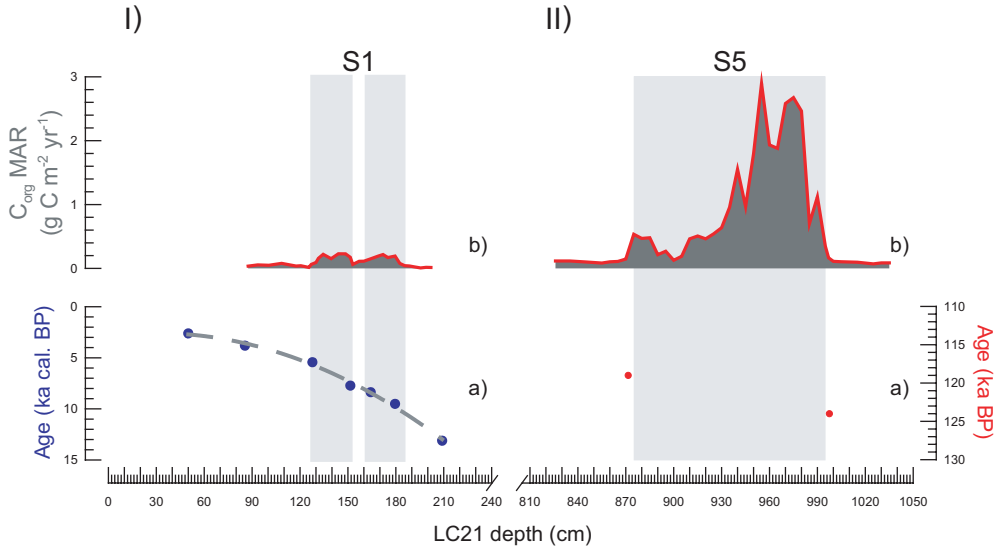

Figure 5.2: Total organic carbon mass accumulation rates (C_{org} MARs) through the current (panel I) and last interglacial (panel II) sections of core LC21. **(a)** chronologies for the current (see Chapter 3 and Casford et al., 2007) and last interglacial (see Chapter 1) intervals. **(b)** C_{org} MARs for sapropels S1 and S5.

We find that through most of the lower half of S5 C_{org} MARs vary between 1 and 2 g C m^{-2} yr^{-1} with a distinct maximum that approaches ~3 g C m^{-2} yr^{-1} (Figure 5.2b, panel II). The latter exceeds the peak values (~0.2 g C m^{-2} yr^{-1}) recorded during S1 at the same site by more than one order of magnitude (Figure 5.2b, panel I), but it is of the same order of magnitude as the average C_{org} MAR values (4 g C m-2 yr-1) inferred for the Pliocene sapropels (Passier et al., 1999). Clearly, the C_{org} MARs recorded for S5 in south-eastern Aegean core LC21 are very high, in particular when taking into account that the core derives from an area that today is distinctly oligotrophic (Psarra et al., 2000).

The burial flux of organic carbon depends on the balance between primary production in the photic zone (de Lange and Ten Haven, 1983; Calvert, 1983; Pederson and Calvert, 1990; Van Os et al., 1994) and aerobic/anaerobic degradation of the organic matter throughout the water column and at the seafloor, where aerobic degradation is thought to be most important (Moodley et al., 2005). Evidence exists that during S5 the eastern Mediterranean thermohaline circulation was substantially weakened (Rohling et al., 2006; Chapter 1). Ventilation processes in the Aegean Sea likely were restricted to the top ~200 m, overlaying a truly euxinic water column, as indicated by the appearance of high concentrations of the biomarker isorenieratene several centuries after the onset of the anoxic layer (Chapter 1). The almost completely euxinic water column will have considerably minimised the degradation of organic matter, in turn increasing the potential preservation of C_{org} in the sediments (Arthur et al., 1994; Sinninghe Damsté and Koster, 1998; Moodley et al., 2005). Conversely, benthic foraminifer assemblages from relatively shallow sites (260 to 430m) in the Aegean Sea reveal that intermediate depths during S1 never experienced persistent anoxia (Abu-Zied et al., in press; Kuhnt et al., 2007), which was likely only restricted to the deeper waters (>1500 m) (Mercone et al., 2001; Casford et al., 2003). Based on these evidences, it would appear that the chemocline (i.e., the oxic/anoxic interface) resided at significantly shallower depths during S5 than during S1, suggesting that during S5 the intermediate water ventilation may have collapsed as well as the deep water ventilation, whereas some intermediate water ventilation persisted during the deposition of S1.

To assess the ventilation state of intermediate waters in the south-eastern Aegean during the Holocene and the last interglacial, we consider surface to intermediate water $\delta^{13}C$ gradients. The $\delta^{13}C_{\Sigma CO2}$ of intermediate water is primarily controlled by the interplay between ventilation processes and remineralisation of organic products at intermediate depths (Pierre, 1999; Rohling et al., 2004, 2006). Long-term (centennial- to millennial-scale) isolation of intermediate waters from the surface would lead to an increase of ^{13}C depleted CO_2 at intermediate depths due to steady build-up of ^{12}C-rich remineralisation products (Rohling et al., 2004).

Conversely, homogenized surface and intermediate waters result in very similar to one another $\delta^{13}C_{\Sigma CO2}$ values, i.e., the production of isotopically light respired CO_2 due to remineralisation is balanced by "fresh" CO_2, which is advected downward by an effective overturning. A modern analogue for the latter scenario is the Rhodes Gyre's convection centre (Malanotte-Rizzoli and Hecht, 1988; Buongiorno Nardelli and Salusti, 2000) where the surface to intermediate $\delta^{13}C_{\Sigma CO2}$ gradient amounts to only 0.1‰ (Pierre, 1999).

The $\Delta\delta^{13}C_{ruber\text{-}pachyderma}$ found through the early Holocene pre-S1 interval at the site of core LC21 amounts to -0.1±0.1‰ (Figure 5.3b, panel I), whereas the transition to S1 is marked by an increase in $\Delta\delta^{13}C_{ruber\text{-}pachyderma}$ to 0.5±0.3‰. A much more pronounced $\Delta\delta^{13}C_{ruber\text{-}pachyderma}$ increase of about 1‰ is observed at the pre-S5 to S5 transition (Figure 5.3b, panel II), despite the fact that pre-S5 values (0.9±0.3‰) were already higher than the pre-S1 ones (Figure 5.3b). Similar to a recently reported record from the open eastern Mediterranean (Rohling et al., 2006), the $\Delta\delta^{13}C_{ruber\text{-}pachyderma}$ developments within S5 in LC21 appear primarily driven by the very light $\delta^{13}C_{pachyderma}$ values attained within S5, and to a much lesser extent by $\delta^{13}C_{ruber}$ (Figure 5.3a, panel II). This indicates strong accumulation of respiration products in (and/or aging of) the intermediate waters during the last interglacial anoxic event. Although absolute values should be considered with caution due to the scarce knowledge of the vital effects of the various foraminifer species with respect to the $\delta^{13}C$ in the Mediterranean Sea (Rohling et al., 2004), the absolute $\delta^{13}C_{pachyderma}$ values in S5 are virtually identical to the $\delta^{13}C$ measured on the low-oxygen tolerant benthic foraminifera *Chilostomella mediterranensis* ($\delta^{13}C_{benthic}$) through S1 at the same site (~1500 m depth) (Figure 5.3a, panel I). Accordingly, $\Delta\delta^{13}C_{ruber\text{-}pachyderma}$ during S5 equals the $\Delta\delta^{13}C_{pachyderma\text{-}benthic}$ during S1 (Figure 5.3b), suggesting that intermediate waters during S5 were experiencing comparable poorly ventilated (isolated) conditions as the deep waters during S1.

Our finding implies a strongly stratified south-eastern Aegean water column during S5, in which continuous supply of oxygen was limited to the surface (winter) mixed layer only. This stratification during S5 appears to have been much stronger than during S1. It is widely acknowledged that the water column stability associated with the deposition of sapropels S5 and S1 was primarily due to enhanced freshwater flooding into the basin and subsequent buoyancy gain at the sea surface (Williams et al., 1978; Rossignol-Strick et al., 1982; Thunell and Williams, 1989; Kallel et al., 1997a, b; Rohling, 1999; Rohling and De Rijk, 1999; Rohling et al., 2002b, 2004; Chapter 1, 3), as best exemplified by $\delta^{18}O_{ruber}$ (Rohling et al., 2004). Comparison of the $\delta^{18}O_{ruber}$ records through S1 and S5 in core LC21 reveals that, starting from virtually identical pre-sapropel values, the shift to light $\delta^{18}O_{ruber}$ at the onset of S5 was twice as large as that at the onset of S1.This agrees

with previous suggestions of a more extreme monsoon-fuelled freshwater disturbance during S5 than during S1 (Rohling, 1999; Rohling et al., 2004), in turn forced by the effects of a stronger summer insolation forcing on the African summer monsoon during the last interglacial period. However, while previous studies were more speculative as based on records from different locations, here, for the first time, we can directly compare the strength and the effect of freshwater disturbance from the unique perspective of high-resolution $\delta^{18}O_{ruber}$ data for the two sapropels at one and the same location.

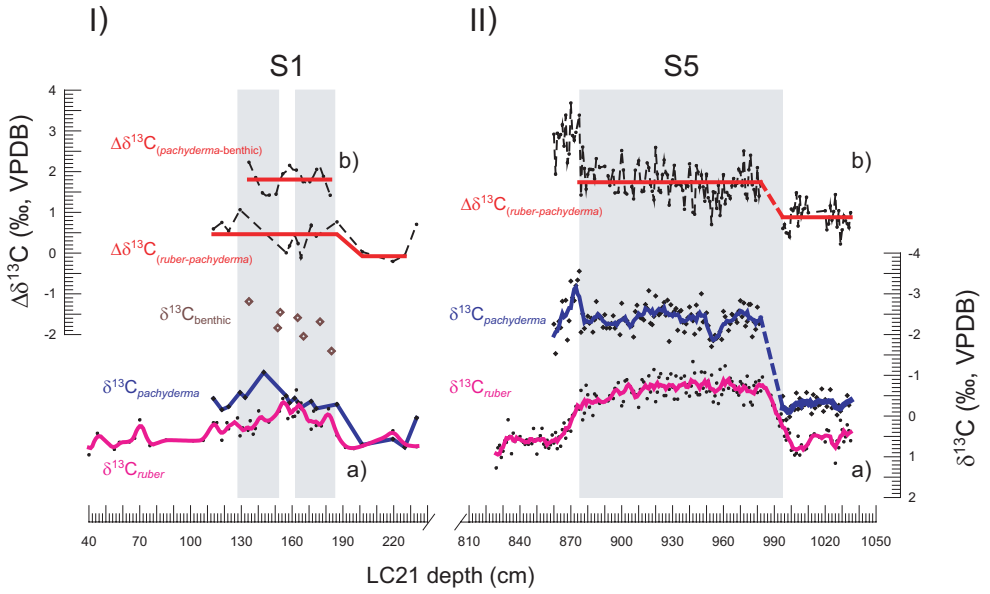

Figure 5.3: Foraminiferal carbon isotope records and gradients through the current (panel I) and the last interglacial (panel II) section of core LC21. **(a)** carbon isotope record for the summer mixed layer planktonic foraminifer *Globigerinoides ruber* (black dots and magenta solid lines), for the top intermediate water dwelling *Neogloboquadrina pachyderma* (black solid diamonds and blue solid line), and for the low-oxygen tolerant benthic foraminifer *Chilostomella mediterranensis* (dark brown open diamonds). **(b)** isotopic differences between carbon isotopic values of *G. ruber* and *N. pachyderma* and *N. pachyderma* and *Chilostomella mediterranensis*.

5.5. Conclusions

The investigation of integrated stable oxygen and carbon isotope in surface (*Globigerinoides ruber*) and intermediate (*Neogloboquadrina pachyderma*) water dwelling foraminifers and of the organic carbon content in records of the current (Holocene) and last interglacial periods from within the same site (south-eastern Aegean core LC21) provides evidence of much more pronounced environmental

changes following the insolation maximum of the last interglacial period. Particularly, we find, in agreement with previous studies (Rohling, 1999; Rohling et al., 2004), a more extreme freshwater perturbation, which triggered a stronger water mass stratification during last interglacial sapropel S5. The latter was coupled to considerably shallower depth of the chemocline, relative to the Holocene sapropel S1. In addition, the highest total organic carbon mass accumulation rates in S5 (MARs up to 3 g C m^2 y^{-1}) exceed peak values found in S1 by more than an order of magnitude.

These findings imply that: (1) summer insolation forcing 8% (peak current interglacial) and 13% (peak last interglacial) stronger than at present both promoted pronounced responses of the Mediterranean marine system; (2) substantially different responses can be however detected at the same location following those different magnitude forcings, which suggests the existence of a threshold that during the last interglacial period that was most likely crossed.

Samenvatting

De mate van gevoeligheid van het huidige interglaciale klimaat voor de toenemende antropogene uitstoot van broeikasgassen is een fundamenteel probleem voor de moderne samenleving. Voor bijvoorbeeld het Mediterrane gebied laten historische instrumentele waarnemingen een duidelijke trend zien van steeds sterker toenemende droogte en warmte, zelfs meer dan het mondiale gemiddelde (IPCC, 2007). Een bijkomend probleem in deze regio is het feit dat er steeds sterkere indicaties zijn dat de huidige milieu- en klimaatveranderingen zeer snel (binnen decennia) worden doorgegeven aan de diepere delen van de Middellandse Zee via een zeer effectieve thermohaline circulatie, wat vervolgens leidt tot dramatische veranderingen in het gehele Mediterrane mariene ecosysteem (Béthoux et al., 1990, 1998; Roether et al., 1996; Skliris et al., 2007).

De toenemende behoefte het effect van 'Global Warming' op het complex gekoppelde Mediterrane atmosfeer-oceaan systeem beter te begrijpen vormt de inspiratie van dit proefschrift. Het is inmiddels uitgebreid aangetoond dat gedurende het Holoceen (de afgelopen 10,000 jaar), de huidige interglaciale periode, maar ook tijdens eerdere interglacialen, enorme veranderingen in de hydrologische, ecologische en oceanografische omstandigheden hebben plaatsgevonden in de Middellandse Zee. Gezamenlijk leidden deze tot de vorming van zgn. 'sapropelen'; organisch rijke sedimentlagen in de diepere delen van vooral de oostelijke Middellandse Zee (zie bv., Cita en Grignani, 1982; Mangini en Schlosser, 1986; Rohling, 1994, Cramp en O'Sullivan, 1999, Emeis et al., 2003). Deze pelagische, onder anoxische tot suboxische condities afgezette lagen vormen een excellent, vaak gelamineerd, archief van de Mediterrane milieu- en klimaatveranderingen aangezien ze niet doorgraven noch op andere wijze aangetast of verstoord zijn. De sapropelen gevormd tijdens het Holoceen (S1) en het voorlaatste belangrijke interglaciaal (Eemien; S5, ~125,000 jaar geleden) zijn voor dit proefschrift gebruikt als voornaamste natuurlijke archieven. Deze afzettingen, afkomstig van kernen genomen op oceanografisch belangrijke locaties in het oostelijke Mediterrane bekken (Egeïsche Zee, Adriatische Zee, en het Kanaal van Sicilië) zijn in detail onderzocht met een breed spectrum van gecombineerde moderne palaeomariene milieu- en klimaat 'proxies', zoals mariene palynologie (vooral dinoflagellatencysten met een organische wand), stabiele isotopen van kalkig microplankton en benthos, en organisch geochemische 'biomarker' gegevens.

In dit proefschrift worden deze gegevens gecombineerd, en ingezet om te komen tot een sterk verbeterd inzicht in de veranderingen van de gekoppelde atmosferische en oceanische circulatie, en de daaraan gerelateerde mariene ecologische veranderingen ten gevolge van (interglaciale) opwarming.

Synopsis

De afgelopen decennia hebben zich grote veranderingen voorgedaan in de diepe circulatie van de oostelijke Middellandse Zee, met o.a. een verschuiving van de belangrijkste locatie van de vorming van oostelijk Mediterraan diepwater van de Adriatische naar de Egeïsche Zee. Dit fenomeen, wat bekend staat als de 'Eastern Mediterranean Transient' (EMT), was waarschijnlijk geconditioneerd door toename van de netto evaporatie, waardoor het zoetwater budget van het bekken veranderde. De kennelijke gevoeligheid van de oostelijke Mediterrane thermohaline circulatie ten gevolge van veranderingen in het zoetwater budget van het bekken is aan de orde in **Hoofdstuk 1**. Soortspecifieke stabiele isotopen metingen van resten van planktonische foraminiferen ($\delta^{18}O$, $\delta^{13}C$) en organisch geochemische gegevens (alkenonen, isorenierateen, en totaal organische koolstof data) van kern LC21 uit de zuidoost Egeïsche Zee worden gecombineerd voor een gedetailleerde reconstructie van de diepe circulatie tijdens het jongste interglaciaal. Resultaten worden vergeleken met vergelijkbare gegevens afkomstig van open oostelijke Middellandse Zee kern Ocean Drilling Program (ODP) 971A. De gegevens wijzen op het ineenstorten van de diepe ventilatie van de Egeïsche Zee ~40±20 jaar na een grote influx van zoetwater dat leidde tot anoxische condities van het bodem- en intermediair water. Binnen ~650±250 jaar resulteerde dit proces tot fotische zone anoxia. Weer 300±120 jaar later hadden deze condities zich uitgebreid tot de gehele oostelijke Middellandse Zee. Deze studie benadrukt de zeer grote mate van gevoeligheid van het Egeïsche gekoppelde klimaat-oceaan systeem voor zelfs geringe klimaatsveranderingen, die dan vervolgens tot enorme, bekken-wijde, veranderingen kunnen leiden in het oostelijke Mediterrane mariene systeem.

Sapropelen zijn organisch rijke sedimenten die de afgelopen ~13,5 miljoen jaar episodisch werden afgezet in de Middellandse Zee, vooral in het oostelijke bekken. De anoxische fases die leidden tot submariene sapropelvorming worden vooral toegeschreven aan de invloed van maxima in de Afrikaanse Moesson op de hydrologie en oceanografie van het Mediterrane Bekken. Sterke verschuiving naar zwaardere waarden in de samenstelling van stabiele zuurstof-isotopen ($\delta^{18}O$) gemeten aan planktonische foraminiferen voorafgaand aan de sapropel depositie suggereert dat een sterke influx van zoetwater resulteerde in lage saliniteit van het oppervlakte water en sterke stratificatie van de waterkolom. Absolute kwantificering van de hoeveelheid zoetwater, en de bijbehorende saliniteits-veranderingen is echter nog een groot probleem. Een innovatieve techniek om zeeoppervlakte saliniteit te bepalen is gebaseerd op het meten van de samenstelling van waterstof-isotopen (δD) van alkenonen die worden geproduceerd door haptophyte algen. Deze compositie wordt vooral beïnvloed door de δD van het omringende water en door de saliniteit. In **Hoofdstuk 2** wordt deze techniek

toegepast op alkenonen van Sapropeel S5 van de Egeïsche Zee, gevormd tijdens het voorlaatste grote interglaciaal. De resultaten omvatten een sterke daling van δD waarden tijdens het begin van de Sapropel vorming, duidend op een daling van de zeeoppervlakte saliniteit met ~6 PSU, van 39 naar 39 PSU. Hoewel de absolute waarden met enige voorzichtigheid moeten worden benaderd en verder moeten worden getest, zijn ze realistisch in de zin dat de pre-Sapropeel waarden vergelijkbaar zijn met die van de huidige Egeïsche Zee. Deze studie toont het grote potentieel aan van gecombineerd gebruik van de δD van alkenonen, de $U^{k'}_{37}$ van dezelfde alkenonen, en van de $\delta^{18}O$ van planktonische foraminiferen.

De Egeïsche Zee bevindt zich zowel op de grens van de hoge- en midden breedte graden, als op de grens van de tropische en subtropische klimaatssystemen. De seizoens gebonden verschuiving van deze gordels bepalen in belangrijke mate het regionale klimaat en de hydrografie. Het genereren van seizoens-specifieke milieu- en temperatuur gegevens, onttrokken aan één en het zelfde archief, kan aldus een belangrijke bijdrage leveren aan ons inzicht in de dynamiek van klimaatsvariaties uit het verleden. Dit proces staat centraal in **Hoofdstuk 3**, waarin wordt ingegaan op het vroeg tot midden Holocene maximum van zonneinstraling en moesson activiteit op het Noordelijk Halfrond. Gereconstrueerde Zuid Egeïsche Zee $\delta^{18}O_{zeewater}$ variaties laten een sterke daling zien rond 10.6 en 9.6 BP. Deze daling wordt gezien als de regionale expressie van de intensificatie van de Afrikaanse Moesson, en gerelateerde toename van zoetwater influx in de Egeïsche Zee, en zelfs in het totale Mediterrane mariene systeem. Een vergelijkbare daling is gerapporteerd in speleothems van de Soreq Grot in Noord Israël. Daarom wordt gesuggereerd dat dit fenomeen niet gerelateerd is aan veranderende precipitatie, maar samenhangt met isotopen variaties in het evaporatie brongebied, t.w. het Levantijnse - Egeïsche bekken. Gesuperponeerd op deze lange-termijns respons zijn centennia-durende episodes gereconstrueerd met koudere winters (tot 1.8 graden C kouder) in de Egeïsche regio. Deze perioden zijn positief gecorreleerd met de concentratie Kalium-ionen gemeten in de Groenlandse GISP II ijskernen, wat suggereert dat deze variaties verband houden met meridionale verplaatsingen van de polaire atmosferische vortex. De drie belangrijkste perioden van koele winters in de Egeïsche regio, rond ~10,5 ka BP, 9.8-9.1 ka BP, en 8.6-8.0 ka BP, correleren goed met beschreven verzwakkingen van het Indische zomer Moesson systeem. Er wordt aldus een samenhang voorgesteld tussen sterkere Eurasiatische winters en sterkere sneeuw-bedekking in de Himalaya's dat leidde tot vertraagde en/of verzwakte zomer Moesson. Tegelijkertijd, maar onafhankelijk, versterkte het Siberisch atmosferisch hoge luchtdruk gebied, een van de componenten van de Polaire Vortex. Daarnaast worden de eerste indicaties van een bijzonder sterke afkoeling in de Egeïsche Zee gerapporteerd, te weten tussen 8.3 en 8.15 ka BP,

binnen de in het algemeen koelere periode van 8.6-8.0 ka BP. Zowel de ouderdom, als de duur van deze koude periode lijkt goed te correleren met de bekende 8.2 ka BP afkoeling gerapporteerd uit kernen vanuit de Noord Atlantische regio. Deze afkoeling wordt algemeen gezien als gevolg van een kortstondige verzwakking van de Atlantische meridionale circulatie.

De reconstructie van variaties in primaire productie tijdens de vorming van sapropelen blijft problematisch omdat bestaande geochemische of palaeobiologische technieken geen eenduidige resultaten geven. De toepassing van de kwantitatieve analyse van organische dinoflagellatencysten is onderwerp van **Hoofdstuk 4**. Vooral variaties in concentratie van cysten van heterotrofe dinoflagellaten in het sediment zijn potentieel geschikt voor de reconstructie van variërende hoeveelheden eukaryoot fotosynthetisch plankton, aangezien de laatste de belangrijkste voedselbron vormt van deze groep. Er is echter discussie over de toepasbaarheid van deze techniek aangezien er aanwijzingen zijn dat deze variaties gedeeltelijk toe te schrijven zouden zijn aan variaties in preservatie, en geen goede reflectie biedt van de hoeveelheden primaire producenten. Om deze toepassing verder te testen worden kwantitatieve dinoflagellaten gegevens afkomstig van uitstekend gedateerde, vroeg, tot midden Holocene kernen uit het Straat van Sicilië, de Egeïsche Zee, en de Adriatische Zee met elkaar vergeleken. Bovendien is van deze kernen ook andere belangrijke informatie met betrekking tot paleoproductiviteit (zoals Barium-concentraties) en zuurstof-beschikbaarheid (benthische foraminiferen) beschikbaar. De studie laat zien dat, mits de zuurstof-beschikbaarheid in het water niet te hoog is, zoals in het geval van de onderzochte afzettingen, concentraties van cysten van heterotrofe dinoflagellaten wel degelijk een bruikbare basis vormt voor realistische reconstructies van de eukaryotische primaire productie. Aldus worden in detail verschillen in productiviteit gereconstrueerd over het gehele oostelijk Mediterrane bekken.

In het afsluitende **Hoofdstuk 5** worden de sapropelen S1 en S5, gevormd tijdens maximale interglaciale condities, met elkaar vergeleken in een poging de gevoeligheid van het gekoppelde Mediterrane gekoppelde atmosfeer-oceaan systeem te documenteren. Voor deze studie is met name gebruikt gemaakt van kern LC21 uit de zuidoost Egeïsche Zee, een kern die zowel het S1 interval, als het S5 interval bevat. Soortspecifieke stabiele isotopen metingen ($\delta^{18}O$, $\delta^{13}C$) van zowel oppervlakte (*Globigerinoides ruber*) als sub-thermocline (*Neogloboquadrina pachyderma*) planktonische foraminiferen, en totaal organische koolstof (C_{org}) data worden ingezet om de watermassa dynamiek, en de omvang van de koolstof accumulatie vast te stellen. Tijdens de vorming van Sapropeel S5 blijken de milieuveranderingen drastischer te zijn geweest dan die tijdens S1; S5 accumulatie snelheden bereikten ~3g C m^{-2} yr^{-1} , een verschil van een orde van grootte met de

hoogste waarden bereikt tijdens de vorming van de S1. Bovendien is de verschuiving naar meer negatieve $\delta^{18}O$ waarden van *Globigerinoides ruber* aan de basis van de S5 twee keer zo groot als hetzelfde fenomeen aan de basis van de S1. Ook de $\delta^{13}C$ gradiënten van het oppervlakte naar intermediaire watermassa's ten tijde van de afzetting van S5 zijn groter dan vergelijkbare S1 waarden; ze zijn zelfs vergelijkbaar met de gradiënt tussen de intermediaire en de diepe watermassa's tijdens de vorming van de S1. Dit duidt op het feit dat de intermediaire watermassa's ten tijde van de S5 precies zo slecht geventileerd werden als de diepe watermassa's tijdens S1. In het algemeen laat deze studie zien dat hoe sterker en hoe warmer de piek-interglaciale condities zijn, hoe intenser de respons van het geïntegreerde systeem wordt, en des te sterker de milieu- en ecologische verandering zal zijn.

Aangezien het Mediterrane gebied in toenemende mate te maken krijgt met steeds sterker toenemende droogte en warmte (IPCC, 2007) houdt de conclusie van Hoofdstuk 5 (en feitelijk van het gehele proefschrift) een belangrijke waarschuwing in ten aanzien van de te verwachten ontwikkelingen in de onmiddellijke toekomst.

Riassunto e sinossi

La sensibilità climatica del presente interglaciale al continuo aumento dei gas serra in atmosfera cdi origine antropica costituisce un serio problema per la società moderna. Ad esempio, per le regioni Mediterranee, ricostruzioni basate su registrazioni strumentali di serie storiche rivelano un chiaro cambiamento del clima verso condizioni di maggiore siccità e di aumento delle temperature, mentre i modelli climatici prevedono che questo andamento continuerà nel prossimo futuro, diventando addirittura più elevato della media globale (IPCC, 2007). Inoltre, nell'area mediterranea, gli effetti del presente clima interglaciale, probabilmente aumentati dalle attività antropiche (Rohling e Bryden, 1992), vengono velocemente (nell'arco di pochi decenni) trasmesse al mare profondo attraverso una efficiente circolazione termoalina (Béthoux et al., 1990, 1998; Roether et al., 1996; Skliris et al., 2007). Questo mostra l'eccezionale sensibilità delle dinamiche del sistema oceano-atmosfera ai forzati naturali e antropogenici in questa regione.

Questa tesi nasce dalla necessità di aumentare le nostre conoscenze sulla sensibilità delle regioni mediterranee alle perturbazioni che interessano il sistema atmosfera/oceano durante gli interglaciali. Oggi esistono forti evidenze che sia durante il presente interglaciale (Olocene) che durante il penultimo interglaciale (Eemiano), il Mediterraneo abbia subito drastici cambiamenti nell'idrologia. Ciò ha provocato cambiamenti idrografici ed ecologici di grande entità che nei sedimenti sono testimoniati dalla deposizione di livelli ricchi di sostanza organica detti sapropels (vedi ad esempio, Cita e Grignani, 1982; Mangini e Schlosser, 1986; Rohling, 1994; Cramp e O'Sullivan, 1999; Emeis et al., 2003). Questi depositi sono associati ad anossia delle acque profonde e quindi rappresentano archivi pressoché ideali, in quanto non soggetti a a bioturbazione, dei cambiamenti climatici ed ambientali avvenuti nel Mediterraneo durante periodi relativamente caldi. In particolare, in questa tesi vengono utilizzati gli archivi sedimentari offerti dal sapropel S1 (depositatosi durante l'Olocene) e sapropel S5 (depositatosi durante il penultimo interglaciale). I sapropel S1 e S5 vengono qui investigati generando un ampio ventaglio di ricostruzioni paleoceanografiche principalmente basate su indicatori derivanti dalla palinologia marina (cisti di dinoflagellate a parete organica), da isotopi stabili misurati su gusci calcarei dei foraminiferi planctonici, e dalla geochimica organica, ed ottenuti studiando carote di sedimento ubicate in posizioni strategiche del bacino mediterraneo orientale (mar Egeo, mar Adriatico, Stretto di Sicilia).

Sinossi

Negli ultimi decenni, le acque profonde del Mediterraneo hanno evidenziato un importante cambiamento; lo spostamento del luogo preferenziale di formazione delle acque profonde del Mediterraneao orientale dal mare Adriatico al mare Egeo.

Questo fenomeno, anche conosciuto come transiente del mediterraneo orientale (EMT) è stato molto probabilmente pre-condizionato da un aumento nella evaporazione netta del bacino (quindi da un cambiamento nel bilancio di acqua dolce del bacino). L'apparente estrema sensibilità della circolazione termoalina del Mediterraneo (orientale) a cambiamenti nel bilancio delle acque dolci del bacino è argomento del **Capitolo 1**. In questo capitolo, gli isotopi stabili ($\delta^{18}O$ e $\delta^{13}C$) di alcune specie di foraminiferi planctonici e dati di geochimica organica (alchenoni, isorenieratene e carbonio organico totale), misurati su campioni di sedimento derivanti dalla carota LC21, prelevata nel mar Egeo sud orientale, vengono integrati per fornire una dettagliata ricostruzione del sistema di circolazione delle acque profonde durante il penultimo interglaciale. Tali indicatori vengono poi confrontati con gli stessi indicatori provenienti dalla carota 971A, prelevata nel bacino Mediterraneo orientale aperto. In seguito ad un largo flusso di acqua dolce nel bacino Levantino, la ventilazione delle acque sub-superficiali dell'Egeo si è interrotta nell'arco di circa 40±20 anni, favorendo condizioni euxiniche - ostili alla sopravvivenza degl organismi aerobici - che si sono poi propagate nella zona fotica in 650±250 anni. Dopo circa 300±120 anni, simili condizioni si sono estese all'intero Mediterraneo orientale. Questo studio quindi dimostra l'estrema sensibilità del mare Egeo a cambiamenti nel bilancio di acqua dolce del Mediterraneo orientale, con cambiamenti ambientali che portano a drastici riarrangiamenti idrografici che poi si propagano all'intero bacino Mediterraneo.

I sapropel sono depositi sedimentari ricchi in sostanza organica che si sono depositati periodicamente nel mar Mediterraneo, specialmente nel bacino orientale, negli ultimi 13.5 milioni di anni circa. Gli eventi anossici che hanno originato i sapropel sono il risultato indiretto dell'aumentato impatto del monsone africano sull'idrografia del bacino mediterraneo. Marcati cambiamenti negli isotopi dell'ossigeno ($\delta^{18}O$), registrati nei gusci carbonatici dei foraminiferi planctonici che vivono nelle acque superficiali verso valori più leggeri, in un intervallo di tempo di poco precedente la deposizione del sapropel, suggeriscono che il Mediterraneo è stato interessato da un massiccio flusso delle acque dolci che hanno determinato uno strato di acqua superficiale a bassa salinità ed ad alla conseguente accentuata stratificazione della colonna d'acqua. Tuttavia, la quantità di acque dolci e la concomitante diminuzione di salinità delle acque superficiali (SSS) non erano finora ancora stati quantificati. Un nuovo approccio per la stima dei cambiamenti di salinità utilizza la composizione degli isotopi dell'idrogeno (δD, D= deuterio) degli alchenoni a catena lunga prodotti da alghe aptofite. Tale composizione, che è stata dimostrata dipendere principalmente dal δD dell'acqua e dalla salinità, può offrire un nuovo metodo per la ricostruzione della salinità. Nel **Capitolo 2** vengono discussi i risultati delle analisi del δD degli alchenoni in un sapropel S5 di una carota prelevata dal mar

Egeo. I risultati mostrano che un'ampia diminuzione di circa il 25‰ nel δD alla base del sapropel deriva da un decremento della salinità di 6, da 39 a 33. Benché le stime di salinità superficiale assoluta debbano essere considerate con cautela, in quanto ad oggi ancora soggette ad errori non trascurabili, i valori ricostruiti di SSS sembrano abbastanza attendibili, fornendo dati di salinità prima del sapropel simili a quelli attualmente misurati nel mar Egeo. Per ridurre gli errori di misura e l'attendibilità nella stima della salinità, le relazioni fra δD e salinità devono essere studiate meglio anche facendo uso di esperimenti in coltura e testate attraverso studi in campo. Certamente i risultati ottenuti mostrano come l'uso combinato di δD misurato sugli alchenoni, $U^{k'}_{37}$ derivato dagli alchenoni e $\delta^{18}O$ misurato sui gusci carbonatici dei foraminiferi planctonici sia promettente per le ricostruzioni di salinità.

L'Egeo si trova al confine fra i sistemi climatici delle alte/medie latitudini e tropicali/subtropicali. Lo spostamento latitudinale stagionale di questo confine controlla il clima e l'idrografia di questa regione. Ottenere registrazioni stagionali specifiche derivanti da diversi indicatori (proxies) per le temperature superficiali (SST) e per l'idrografia dell'Egeo è certamente di grande importanza per aumentare le nostre conoscenze sulle interazioni climatiche a larga scala durante periodi di importanti cambiamenti climatici nel passato. Tali informazioni sono la chiave del **Capitolo 3** dove viene discusso il massimo monsonico/di insolazione dell'emisfero nord durante l'Olocene. Ricostruendo gli isotopi dell'ossigeno dell'acqua ($\delta^{18}O_{acqua\ marina}$) nell'Egeo sud orientale, si nota un marcato spostamento negativo di tale valore di circa l'1.5‰ fra 10,600 e 9,600 anni fa. Questa diminuzione del $\delta^{18}O$ delle acque superficiali rappresenta la risposta locale all'intensificazione del monsone africano ed il relativo input delle acque dolci che ha interessato l'intero Mediterraneo orientale durante l'inizio e la metà dell'Olocene. Nello stesso intervallo di tempo c'è stato un simile decremento negli isotopi dell'ossigeno di uno speleotema ($\delta^{18}O_{speleotema}$) nel nord di Israele (Soreq Cave). In questo capitolo viene suggerito che il cambiamento negli isotopi dello speleotema non può essere dovuto a cambiamenti nella quantità di precipitazioni nell'area di drenaggio della cava, ma piuttosto che un tale cambiamento riflette il cambiamento nella composizione isotopica della sorgente da cui proviene l'umidità da cui le precipitazioni su Israele hanno origine, e cioè il bacino Egeo-Levantino. Superimposto a questo cambiamento idrografico di lungo termine il mar Egeo registra una serie di episodi di raffreddamento invernale, con decrementi di temperatura anche di 1.8°C. Questi episodi sono positivamente correlati con picchi di potassio di origine non marina [K^+] derivanti dalle registrazioni dalle carote di ghiaccio della Groenlandia (GISP2). Ciò suggerisce che tali episodi di raffreddamento sono strettamente correlati con lo spostamento verso sud del vortice polare atmosferico. I tre principali episodi di raffreddamento nell'Egeo a circa 10,500, 9,800-9,100 e 8,600-8,000 anni fa coincidono con episodi

di remissione del monsone estivo indiano a scala centenaria, precedentemente descritti. Qui proponiamo un meccanismo che lega gli inverni più rigidi in Eurasia a una copertura nevosa negli altopiani asiatici, e che causa un ritardo o un indebolimento del monsone estivo ed una contemporanea ed indipendente intensificazione dell'alta pressione siberiana, una componente del vortice polare atmosferico. Infine troviamo la prima indicazione di un particolarmente forte raffreddamento nell'Egeo fra 8,300 e 8,150 anni fa, che è parte di un più ampio episodio di raffreddamento avvenuto 8,600-8,000 anni fa. Sia nei tempi che nella durata, questo evento coincide con il cosiddetto evento freddo ad 8,200 anni fa ritrovato in molte registrazioni nelle regioni nord atlantiche, che è stato a sua volta messo in relazione con un indebolimento della circolazione termoalina atlantica.

Nel **Capitolo 4** vengono affrontate le problematiche relative alla ricostruzione della produttività primaria durante periodi di deposizione dei sapropel. Variazioni di abbondanza nelle cisti di dinoflagellate eterotrofe, grazie alla strategia nutrizionale delle dinoflagellate da cui derivano, sono usate da diversi anni per ricostruire la produttività primaria nelle acque superficiali del passato. Recentemente, alcuni studi hanno tuttavia segnalato che la degradazione aerobica in condizioni ossigenate potrebbe influenzare la presenza di cisti di dinoflagellate eterotrofe. Grandi quantità di tali dinocisti in sedimenti anossici potrebbero perciò indicare un'aumentata preservazione nel sedimento piuttosto che elevata produttività in superficie. Per trattare questa problematica, vengono discussi dati di dinocisti ricavati da record sedimentari dell'Olocene inferiore e medio (che include il periodo in cui è stato depositato il sapropel S1) da carote dello Stretto di Sicilia, del mare Egeo ed Adriatico. Tali risultati vengono poi paragonati a dati recentemente pubblicati rigurdanti la presenza di foraminiferi bentonici che richiedono ossigeno per vivere, e che quindi indicano ventilazione delle acque profonde. I dati mostrano un massimo di concentrazione di dinocisti eterotrofe della durata di 4,000 anni ad iniziare da circa 10,000 anni fa nell'Egeo. Simili cambiamenti nella abbondanza assoluta delle dinocisti eterotrofe nel mare Adriatico è avvenuta più tardi (circa 8,500 anni fa) ed è terminata prima, circa 7,100 anni fa. Un aumento nelle concentrazioni di dinocisti eterotrofe fra 10,000 e 6,500 anni fa è visibile anche nel stretto di Sicilia, anche se i valori assoluti sono troppo bassi per poter giungere a conclusioni certe. Data la presenza di foraminiferi bentonici nel record dei mare Adriatico ed Egeo durante la deposizione del sapropel S1 e la mancanza di correlazioni significative fra cambiamenti nella ventilazione delle acque profonde nei due bacini e concentrazioni di dinocisti eterotrofe, argomentiamo a favore dell'utilità delle cisti eterotrofe come indicatori della produttività delle acque superficiali. L'inizio e gli andamenti spaziali degli aumenti di produttività all'epoca della deposizione del sapropel implicano che la presenza di una riserva di nutrienti nelle acque intermedie, probabilmente associ-

ate all'indebolimento della circolazione termoalina del bacino, ha favorito la produttività.

Il **Capitolo 5** presenta una discussione finale e comprensiva sulla sensibilità climatica della regione mediterranea. Tale discussione vuole, in particolare, affrontare lo studio della sensibilità a lungo termine della circolazione del Mediterraneo orientale rispetto al forzante di insolazione negli ultimi due intervalli di massime condizioni interglaciali, al tempo della deposizione dei sapropel S1 e S5. In questo capitolo vengono confrontati una serie di indicatori paleoceanografici ad alta risoluzione derivanti da una carota di sedimento prelevata nel mar Egeo sud orientale (LC21) che include sia il sapropel S1 che il sapropel S5, depositati durante l'ultimo (Olocene) ed il penultimo massimo interglaciale, rispettivamente. Più specificamente, vengono presentati e discussi i risultati ottenuti dal confronto di isotopi stabili dell'ossigeno ($\delta^{18}O$) e del carbonio ($\delta^{13}C$) derivanti dai gusci dei due foraminiferi planctonici che vivono nelle acque superficiali e nelle acque immediatamente sotto il termoclino, rispettivamente *Globigerinoides ruber* e *Neogloboquadrina pachyderma*. Questi dati sono discussi in relazione al contenuto totale di carbonio organico (C_{org} wt%) con lo scopo di ricostruire le dinamiche delle masse d'acqua e l'importanza e l'efficienza del seppellimento del carbonio organico. I risultati mostrano che i cambiamenti ambientali avvenuti durante il penultimo interglaciale sono molto più pronunciati che quelli dell'Olocene. Durante la deposizione del sapropel S5 nel penultimo interglaciale, il tasso di accumulo di carbonio (MAR) ha raggiunto i ~3 g C m^{-2} yr^{-1}, essendo quindi un ordine di grandezza maggiore del massimo di accumulo di carbonio organico durante la deposizione del sapropel S1 nell'Olocene. Inoltre, la diminuzione all'inizio del sapropel S5 dei valori di $\delta^{18}O$ derivanti dai gusci del foraminifero planctonico *Globigerinoides ruber* che vive nello strato della colonna d'acqua soggetto a mescolamento estivo è circa doppio di quello che si verifica all'inzio del sapropel S1. Anche i gradienti del $\delta^{13}C$ fra acque superficiali ed acque intermedie durante la deposizione del S5 sono più marcati che durante l'S1, e simili ai gradienti fra acque intermedie ed acque profonde durante l'S1. Ciò suggerisce che le acque intermedie durante l'S5 avevano una ventilazione ridotta (erano quindi intensamente isolate) è comparabile a quella delle acque profonde durante l'S1. I risultati ottenuti, nel loro insieme, suggeriscono una forte stratificazione delle masse d'acqua durante l'S5 e una profondità del chemoclino significativamente minore di quella al tempo dell'S1. Queste condizioni hanno certamente aumentato il potenziale di conservazione della sostanza organica nell'S5 piu' che nell'S1

References

Abu-Zied, R.H., E.J. Rohling, F.J. Jorissen, C. Fontanier, J.S.L. Casford, and S. Cooke (in press), Benthic foraminiferal response to changes in bottom water oxygenation and organic carbon flux in the eastern Mediterranean during LGM to Recent times, *Marine Micropaleontology*.

Alley, R., and A. Ágústsdóttir (2005), The 8k event: cause and consequences of a major Holocene abrupt climate change, *Quaternary Science Reviews*, 24, 1123-1149.

Alley, R.B., P. A. Mayewski, T. Sowers, M. Stuiver, K. C. Taylor, and P. U. Clark (1997), Holocene climatic instability: a prominent widespread event 8200 years ago, Geology, 25, 483-486.

Arnaboldi, M., and P.A. Meyers (2006), Trace element indicators of increased primary production and decreased water-column ventilation during deposition of latest Pliocene sapropels at five locations across the Mediterranean Sea, *Palaeogeography Palaeoclimatology Palaeoecology*, 249(3-4), 425-443.

Arthur, M.A., W.E. Dean, E.D. Neff, B.J. Hay, J. King, and G. Jones (1994), Varve calibrated records of carbonate and organic carbon accumulation over the last 2000 years in the Black Sea, *Global Biogeochemical Cycles*, 8,195-217.

Astraldi, M., S. Balopoulos, J. Candela, J. Font, M. Gacic and G.P. Gasparini, B. Manca, A. Theocharis, J. Tintoré (1999), The role of straits and channels in understanding the characteristics of Mediterranean circulation, *Progress in Oceanography*, 44, 65-108.

Barber, D. C., A. Dyke, C. Hillaire-Marcel, A. E. Jennings, J. T. Andrews, M. W. Kerwin, G. Bilodeau, R. McNeely, J. Southon, M. D. Morehead, and J.-M. Gagnon (1999), Forcing of the cold event of 8,200 years ago by catastrophic drainage of Laurentide Lakes, *Nature*, 400, 344-348.

Bar-Matthews, M., A. Ayalon, M. Gilmour, A. Matthews, and C.J. Hawkesworth (2003), Sea-land oxygen isotopic relationships from planktonic foraminifera and speleothems in the Eastern Mediterranean region and their implication for paleorainfall during interglacial intervals, *Geochimica et Cosmochimica Acta*, 67, 3181-3199.

Bar-Matthews M., A. Ayalon, A. Matthews, E. Sass, and L. Halicz (1996), Carbon and oxygen isotope study of the active water-carbonate system in a karstic Mediterranean cave: Implications for paleoclimate research in semiarid regions, *Geochimica et Cosmochimica Acta*, 60, 337-347.

Bar-Matthews, M., A. Ayalon, and A. Kaufman (2000), Timing and hydrological conditions of Sapropel events in the Eastern Mediterranean, as evident from speleothems, Soreq cave, Israel, *Chemical Geology*, 169, 145-156.

Barnett, T.P., L. Dumenil, U. Schlese, E. Roeckner (1988), The effect of Eurasian snow cover on global climate, *Science*, 239, 504-507.

Bemis, B. E., H. J. Spero, J. Bijma, J., and D. W. Lea (1998), Re-evaluation of the oxygen isotopic composition of planktonic foraminifera: Experimental results and revised paleotemperature equations, *Paleoceanography*, 13, 150-160.

Béthoux, J.-P. (1979), Budgets of the Mediterranean Sea. Their dependence on the local climate and on the characteristics of the Atlantic waters, *Oceanologica Acta*, 2, 157-163.

Béthoux, J.-P., B. Gentili, and D. Tailliez (1998), Warming and freshwater budget changes in the Mediterranean since the 1940's: Their possible relation to the greenhouse effect, *Geophysical Research Letters*, 25, 1023-1026

Béthoux, J.-P., B. Gentili, J. Raunet, and D. Tailliez (1990), Warming trend in the Western Mediterranean deep water, *Nature*, 347, 660-662.

Bianchi, D., M. Zavatarelli, N. Pinardi, R. Capozzi, L. Capotondi, C. Corselli, and S. Masina (2006), Simulations of ecosystem response during the sapropel S1 deposition event: *Palaeogeography, Palaeoclimatology, Palaeoecology*, 235, 265-287.

Björck, S., R. Muscheler, B. Kromer, C. S. Andresen, J. Heinemeier, S. J. Johnsen, D. Conley, N. Koç, M. Spurk, and S. Veski (2001), High-resolution analyses of an early Holocene cooling event may imply decreased solar forcing as an important climate trigger, *Geology*, 29, 1107-1110.

Bond, G., W. Showers, M. Cheseby, R. Lotti, P. Almasi, P. deMenocal, P. Priore, H. Cullen, I. Hajdas, and G. Bonani (1997), A pervasive millennial-scale cycle in North Atlantic Holocene and glacial climates, *Science*, 278, 1257-1266.

Bond, G., B. Kromer, J. Beer, R. Muscheler, M. N. Evans, W. Showers, S. Hoffmann, R. Lotti-Bond, I. Hajdas, and G. Bonani (2001), Persistent solar influence on north Atlantic climate during the Holocene, *Science*, 294, 2130-2136.

Brovkin, V., M. Claussen, V. Petoukhov, and A. Ganopolski (1998), On the stability of the atmosphere-vegetation system in the Sahara/Sahel region, J*ournal of Geophysical Research*, 103, 31613-31624.

Boscolo, R., and H. Bryden (2001), Causes of long-term changes in the Aegean Sea deep water, *Oceanologica Acta*, 24, 519-527.

Boyle, E.A., and D.W. Lea (1989), Cd and Ba in planktonic foraminifera from the Eastern Mediterranean: evidence for river outflow and enriched nutrients during sapropel production, *Transactions American Geophysical Union*, 70, 101-134.

Bryden, H.L., and T.H. Kinder (1991), Steady two-layer exchange through the

Strait of Gibraltar, Deep-Sea Research, 38(Supplement 1), S445-S463.

Buongiorno Nardelli, B., and E. Salusti (2000), On dense water formation criteria and their application to the Mediterranean Sea, *Deep-Sea Research I*, 47, 193-221.

Calvert, S.E. (1983), Geochemistry of Pleistocene sapropels and associated sediments from the eastern Mediterranean, *Oceanologica Acta*, 6, 255-267.

Came, R. E., D. W. Oppo, and J. F. McManus (2007), Amplitude and timing of temperature and salinity variability in the subpolar North Atlantic over the past 10 k.y., *Geology*, 35(4), 315-318.

Cane, T., E.J. Rohling, A.E.S. Kemp, S. Cooke, and R.B. Pearce (2002), High-resolution stratigraphic framework for Mediterranean sapropel S5: defining temporal relationships between records of Eemian climate variability, *Palaeogeography, Palaeoclimatology, Palaeoecology*, 183, 87-101.

Capotondi, L., C. Morigi, C., M.S. Principato, F. Sangiorgi, P. Maffioli, S. Giunta, A. Negri, and C. Corselli (2006), Planktonic and benthonic foraminifera changes during sapropel S5 deposition in the Eastern Mediterranean Sea, *Palaeogeography, Palaeoclimatology, Palaeoecology*, 235, 48-65.

Casford, J.S.L., E.J. Rohling, R. H. Abu-Zied, S. Cooke, C. Fontanier, M. Leng, and V. Lykousis (2002), Circulation changes and nutrient concentrations in the late Quaternary Aegean Sea: A nonsteady state concept for sapropel formation, *Paleoceanography*, 17, 1024, DOI:10.1029/2000PA000601.

Casford, J.S.L., E. J. Rohling, R. H. Abu-Zied, F. J. Jorissen, M. Leng, and J. Thomson (2003), A dynamic concept for eastern Mediterranean circulation and oxygenation during sapropel formation, *Palaeogeography, Palaeoclimatology, Palaeoecology*, 190, 103-119.

Casford, J. S. L., R. H. Abu-Zied, E. J. Rohling, S. Cooke, C. Fontanier, M. J. Leng, A. Millard, and J. Thomson (2007), A stratigraphically controlled multiproxy chronostratigraphy for the eastern Mediterranean, *Paleoceanography*, 22, PA4215, DOI:10.1029/2007PA001422.

Charles, C. D., D. Rind, J. Jouzel, R. D. Koster, and R. G. Fairbanks, 1994, Glacial-interglacial changes in moisture sources for Greenland: Influence on the ice core record of climate, *Science*, 263, 508-511.

Cita, M.B., and D. Grignani (1982), *Nature and origin of Late Neogene Mediterranean sapropels*. In: Schlanger, S.O., and M.B. Cita (Eds.), Nature and Origin of Cretaceous Carbon-rich Facies, London (Academic Press), 165-196.

Cohen, J., K. Saito, and D. Entekhabi (2001), The role of the Siberian high in Northern Hemisphere climate variability, *Geophysical Research Letters*, 28(2), 299-302.

Corselli, C., M.S. Principato, P. Maffioli, and D. Crudelli (2002), Changes in plank-

tonic assemblages during sapropel S5 deposition: Evidence from Urania Basin area, eastern Mediterranean, *Paleoceanography*, 17, doi 10.1029/2000PA000536.

Cortijo, E., S. Lehman, L. Keigwin, M. Chapman, D. Paillard, and L. Labeyrie (1999), Changes in meridional temperature and salinity gradients in the North Atlantic Ocean (30° - 72°N) during the last interglacial period, *Paleoceanography*, 14(1), 23-33.

Craig, H., and L.I. Gordon (1965), Deuterium and oxygen 18 variations in the ocean and marine atmosphere. In: Tongiorgi, E. (Ed.), *Proceedings of a Conference on Stable Isotopes in Oceanographic Studies and Paleotemperatures*, Spoleto, Italy, pp. 9-130. Pisa: V. Lischi & Figli.

Cramp, A., and G. O'Sullivan (1999), Neogene sapropels in the Mediterranean: a review, *Marine Geology*, 153, 11-28.

Dale, B. (1996), Dinoflagellate cyst ecology: Modelling and geological applications. In: J. Jansonius and D.C. Mcgregory (Eds) *Palynology: principles and applications*. The American Association of Stratigraphic Palynologists Foundation, 3. Salt Lake City, Publishers Press: 1249-1276.

Dale, B. (2001), The sedimentary record of dinoflagellate cysts: looking back into the future of phytoplankton blooms, *Scientia Marina*, 65 (Suppl. 2), 257-272.

Dale, B., and A. Fjellså (1994), Dinoflagellate cysts as productivity indicators: state of the art, potential and limits. In: Zahn, R. (Ed.), *Carbon Cycling in the Glacial Ocean: Constraints in the Ocean's Role in Global Change*. Springer, Berlin, pp. 521-537.

Dansgaard, W. (1964), Stable isotopes in precipitation, *Tellus*, 16, 436-468.

Dansgaard, W., J. W. C. White, and S. J. Johnsen (1989), The abrupt termination of the Younger Dryas climate event, *Nature*, 339, 532-534.

de Lange, G.J., and H.L. Ten Haven (1983), Recent sapropel formation in the eastern Mediterranean, *Nature*, 305, 797-798.

De Rijk, S., E.J. Rohling, and A. Hayes (1999), Onset of climatic deterioration in the eastern Mediterranean around 7 ky BP; micropalaeontological data from Mediterranean sapropel interruptions, *Marine Geology*, 153, 337-343.

de Vernal, A., L. Turon, and J. Guiot (1994), Dino£agellate distribution in high-latitude marine environments and quantitative reconstruction of sea-surface salinity, temperature and seasonality, *Canadian Journal of Earth Sciences*, 31, 48-62.

de Vernal, A., M. Henry, J. Matthiessen, P. J. Mudie, A. Rochon, K. P. Boessenkool, F. Eynaud, K. Grøsfjeld, J. Guiot, D. Hamel, R. Harland, M. J. Head, M. Kunz-Pirrung, E. Levac, V. Loucheur, O. Peyron, V. Pospelova, T. Radi, J.-

L. Turon and E. Voronina (2001), Dinoflagellate cyst assemblages as tracers of sea-surface conditions in the northern North Atlantic, Arctic and sub-Arctic seas: the new n= 677 data base and its application for quantitative palaeoceanographic reconstruction, *Journal of Quaternary Science*, 16, 681-698.

de Vernal A., C. Hillaire-Marcel, W. R. Peltier, and A. J. Weaver, (2002), Structure of the upper water column in the northwest North Atlantic: Modern versus Last Glacial Maximum conditions, *Paleoceanography*, 17 (4), 1050, DOI:10.1029/2001PA000665.

de Vernal, A., F. Eynaud, M. Henry, C. Hillaire-Marcel, L. Londeix, S. Mangin, J. Matthiessen, F. Marret, T. Radi, A. Rochon, S. Solignac, J.-L. Turon (2005), Reconstruction of sea surface conditions at middle to high latitudes of the Northern Hemisphere during the last glacial maximum (LGM) based on dinoflagellate cyst assemblages, *Quaternary Science Reviews*, 24, 897-924.

Denton, G. H., and W. Karlén (1973), Holocene climatic variations: their pattern and possible cause, *Quaternary Research*, 3, 155-205.

Di Stefano, E., and A. Incarbona (2004) High resolution paleoenvironmental reconstruction of the ODP-963D Hole (Sicily Channel) during the last deglaciation, based on calcareous nannofossils, *Marine Micropaleontology*, 52, 241-254.

D'Ortenzio, F., D. Iudicone, C. de Boyer Montegut, P. Testor, D. Antoine, S. Marullo, R. Santoleri, and G. Madec (2005), Seasonal variability of the mixed layer depth in the Mediterranean Sea as derived from in situ profiles, *Geophysical Research Letters*, 32, L12605, doi:10.1029/2005GL022463.

Duplessy, J. C., D.M. Roche, and M. Kageyama (2007), The Deep Ocean During the Last Interglacial Period, *Science*, 316, 89-91.

Dykoski, C. A., R. L. Edwards, H. Cheng, D. X. Yuan, Y. J. Cai, M. L. Zhang, Y. S. Lin, J. M. Qing, Z. S. An, J. Revenaugh (2005), A high-resolution, absolute-dated Holocene and deglacial Asian monsoon record from Dongge Cave, China, *Earth and Planetary Science Letters*, 233, 71-86.

Edwards L. E., and V. A. S. Andrle (1992), Distribution of selected dinoflagellate cysts in modern marine sediments, in *Neogene and Quaternary Dinoflagellate Cysts and Acritarchs*, edited by Head M. J. and J. H. Wrenn, 259-288 pp., American Association of Stratigraphic Palynologists Foundation, Dallas.

Ehrmann, W., G. Schmiedl, Y. Hamann, T. Kuhnt, C. Hemleben, and W. Siebel (2007), Clay minerals in late glacial and Holocene sediments of the northern and southern Aegean Sea. *Palaeogeography, Palaeoclimatology, Palaeoecology*, 249, 36-57.

Ellison, C. R. W., M. R. Chapman, and I. R. Hall (2006), Surface and deep ocean interactions during the cold climate event 8200 years ago, *Science*, 312, 1929-1932.

Emeis, K.-C., A.E.S. Robertson, and C. Richter, (Eds.) (1996), P*roceedings of the Ocean Drilling Program: Initial Reports*. Vol. 160. Ocean Drilling Program, College Station, 972 pp.

Emeis, K.-C., T. Sakamoto, R. Wehausen, and H.-J. Brumsack (2000a), The sapropel record of the Eastern Mediterranean Sea - Results of Ocean Drilling Program Leg 160, *Palaeogeography, Palaeoclimatology, Palaeoecology*, 158, 259-280

Emeis, K. C., U. Struck, H. M. Schulz, S. Bernasconi, T. Sakamoto, and F. Martinez-Ruiz (2000b), Temperature and salinity of Mediterranean Sea surface waters over the last 16,000 years: Constraints on the physical environment of S1 sapropel formation based on stable oxygen isotopes and alkenone unsaturation ratios, *Palaeogeography, Palaeoclimatology, Palaeoecology*, 158, 259-280.

Emeis, K.-C., H. Schulz, U. Struck, M. Rossignol-Strick, H. Erlenkeuser, M.W. Howell, D. Kroon, H. Mackensen, S. Ishizuka, T. Oba, T. Sakamoto, and I. Koizumi (2003), Eastern Mediterranean surface water temperatures and $\delta^{18}O$ composition during deposition of sapropels in the late Quaternary, *Paleoceanography*, 18, 1005.

Englebrecht, A.C., and J.P. Sachs (2005), Determination of sediment provenance at drift sites using hydrogen isotopes and unsaturation ratios in alkenones, *Geochimica et Cosmochimica Acta*, 69, 4253-4265.

Erez, J., and B. Luz (1983), Experimental paleotemperature equation for planktonic foraminifera, *Geochimica et Cosmochimica Acta*, 47, 1025-1031.

Eshel, G. (2002), Mediterranean climates, Israel Journal of Earth Sciences, 51, 157-168.

Fensome, R.A., and G. L. Williams (2004), *The Lentin and Williams Index of Fossil Dinoflagellates,* 2004 Edition, AASP Foundation Contributions Series, No. 42, 909 pp.

Fensome, R. A., F. J. R. Taylor, G. Norris, W. A. S. Sarjeant, D. I. Wharton, G. L. Williams (1993), *A classification of fossil and living dinoflagellates.* Micropaleontology Special Publication, 7, 351 pp.

Fleitmann, D., S. J. Burns, M. Mudelsee, U. Neff, J. Kramers, A. Mangini, A. Matter (2003), Holocene forcing of the Indian monsoon recorded in a stalagmite from Southern Oman, *Science*, 300, 1737-1739.

Fleitmann, D., S. J. Burns, A. Mangini, M. Mudelsee, J. Kramers, I. Villa, U. Neff, A. A. Al-Subbary, A. Buettner, D. Hippler, A. Matter (2007), Holocene

ITCZ and Indian monsoon dynamics recorded in stalagmites from Oman and Yemen (Socotra), *Quaternary Science Reviews*, 26, 170-188.

Fontugne, M.R., and S.E. Calvert (1992), Late Pleistocene variability of the carbon isotopic composition of organic matter in the eastern Mediterranean: Monitor of changes in carbon sources and a atmospheric CO_2, concentration, *Paleoceanography*, 7, 1-20.

Fontugne, M., M. Arnold, L. Labeyrie, M. Patern, S. E. Calvert and J. C. Duplessy (1994), Paleoenvironment, sapropel chronology and Nile River discharge during the last 20,000 years as indicated by deep-sea sediment records in the Eastern Mediterranean, *Radiocarbon*, 36, 75-88.

Gaines, G., and M. Elbrächter (1987), Heterotrophic nutrition. In: Taylor, F.J.R. (Ed.), *The Biology of Dinoflagellates*. Blackwell Scientific Publications, Oxford, pp. 224-268.

Gasse, F. (2000), Hydrological changes in the African tropics since the Last Glacial Maximum, *Quaternary Science Reviews*, 19, 189-211.

Garrett, C. (1996), The role of the strait of Gibraltar in the evolution of Mediterranean water, properties and circulation, *Bulletin de l'Institut Océanographique de Monaco*, 17, 1-19.

Garzoli, S., and C. Maillard (1979), Winter circulation in the Sicily and Sardinia straits region, *Deep-Sea Research*, 26A, 933-954.

Gat, J.R. (1996), Oxygen and hydrogen isotopes in the hydrologic cycle, Annual *Review of Earth and Planetary Sciences*, 24, 225-262.

Gat, J.R., and I. Carmi (1987), Effect of climate changes on the precipitation patterns and isotopic composition of water in a climate transition zone, Case of the eastern Mediterranean Sea area, *IAHS Publ.* 168, 513-523.

Georgopoulos, D., A. Theocharis, and G. Zodiatis (1989), Intermediate Water Formation in the Cretan Sea (S. Aegean Sea), *Oceanologica Acta*, 12, 353-359.

Gilmann, C., and C. Garrett (1994), Heat flux parametrizations for the Mediterranean Sea: the role of atmospheric aerosols and constraints from water budget, *Journal of Geophysical Research*, 99(C3), 5119-5134.

Gingele, F.X., M. Zabel, S. Kasten, W.J. Bonn, C.C. Nürnberg (1999), Biogenic barium as a proxy for productivity methods and limitations of application. In: Fisher, G., Wefer, G. (Eds.), U*se of Proxies in Paleoceanography: Examples from the South Atlantic*. Springer Verlag, Berlin, pp. 345-364.

Giunta, S., A. Negri, P. Maffioli, F. Sangiorgi, L. Capotondi, C. Morigi, M.S. Principato, and C. Corselli (2006), Phytoplankton dynamics in the eastern Mediterranean Sea during marine isotopic stage 5e, *Palaeogeography, Palaeoclimatology, Palaeoecology*, 235, 28-47.

Giunta S., A. Negri, C. Morigi, L. Capotondi, N. Combourieu Nebout, K.C. Emeis, F. Sangiorgi, and L. Vigliotti (2003), Coccolithophorid ecostratigraphy and multi-proxy paleoceanographic reconstruction in the Southern Adriatic Sea during the last deglacial time (Core AD91-17), *Palaeogeography, Palaeoclimatology, Palaeoecology*, 190, 39-59.

Ganachaud, A., and C. Wunsch (2002), Oceanic nutrient and oxygen transports and bounds on export production during theWorld Ocean Circulation Experiment, *Global Biogeochemical Cycles*, 16, 1057 doi:10.1029/2000GB001333.

Goodfriend, G. A. (1991), Holocene trends in 18O in land snail shells from the Negev Desert and their implications for changes in rainfall source areas, *Quaternary Research*, 35, 417-426.

Grootes, P. M., M. Stuiver, J. W. C.White, S. J. Johnsen and J. Jouzel (1993), Comparison of oxygen isotope records from the GISP2 and GRIP Greenland ice cores, *Nature*, 366, 552-554.

Gupta, A. K., D. M. Anderson, and J. T. Overpeck (2003), Abrupt changes in the Asian southwest monsoon during the Holocene and their links to the North Atlantic Ocean, *Nature*, 421, 354-357.

Harrison, S.P., J.E. Kutzbach, I.C. Prentice, P.J. Behling, and M.T. Sykes (1995), The response of northern hemisphere extratropical climate and vegetation to orbitally induced changes in insolation during the last interglaciation, *Quaternary Research*, 43, 174-184.

Hayes, A., M. Kucera, N. Kallel, L. Sbaffi, E. J. Rohling (2005), Glacial Mediterranean sea surface temperatures based on planktonic foraminiferal assemblages, *Quaternary Science Reviews*, 24(7-9), 999-1016.

Head, M.J. (2002), *Echinidinium zonneveldiae* sp. nov., a new dinoflagellate cyst from the Late Pleistocene of the Baltic region, *Journal of Micropalaeontology*, 21, 169-173.

Head, M.J., M.-S. Seidenkrantz, Z. Janczyk-Kopikowa, L. Marks, and P.L. Gibbard (2005), Last Interglacial (Eemian) hydrographic conditions in the southeastern Baltic Sea, NE Europe, based on dinoflagellate cysts, *Quaternary International*, 130, 3-30.

Hilgen, F. J. (1991), Astronomical calibration of Gauss to Matuyama sapropels in the Mediterranean and implication for the geomagnetic Polarity Time Scale, *Earth and Planetary Science Letters*, 104, 226-244.

Hilgen, F.J., H. Abdul Aziz, W. Krijgsman, I. Raffi, and E. Turco (2003), Integrated stratigraphy and astronomical tuning of the Serravallian and lower Tortonian at Monte dei Corvi (Middle-Upper Miocene, northern Italy), *Palaeogeography Palaeoclimatology Palaeoecology*, 199, 229-264.

Hillaire-Marcel, C., A. de Vernal, and D. J. W. Piper (2007), Lake Agassiz Final drainage event in the northwest North Atlantic, *Geophysical Research Letters*, 34, L15601, DOI:10.1029/2007GL030396.

Hopmans, E.C., S. Schouten, W.I.C. Rijpstra, and J.S. Sinninghe Damsté (2005), Identification of carotenals in sediments, *Organic Geochemistry*, 36, 485-495.

Howell, M.W., and R.C. Thunnell (1992), Organic carbon accumulation in Bannock Basin: evaluating the role of productivity in the formation of eastern Mediterranean sapropels, *Marine Geology*, 103, 461-471.

IPCC, (2007), *Climate Change 2007: The Physical Science Basis. Contribution of Working Group I to the Fourth Assessment Report of the Intergovernmental Panel on Climate Change* [Solomon, S., D. Qin, M. Manning, Z. Chen, M. Marquis, K.B. Averyt, M. Tignor and H.L. Miller (eds.)]. Cambridge University Press, Cambridge, United Kingdom and New York, NY, USA, pp. 996.

Kallel, N., M. Paterne, L. Labeyrie, J.C. Duplessy, and M. Arnold (1997a), Temperature and salinity records of the Tyrrhenian Sea during the last 18,000 years, *Palaeogeography, Palaeoclimatology, Palaeoecology*, 135:, 97-108.

Kallel, N., M. Paterne, J.C. Duplessy, C. Vergnaud-Grazzini, C. Pujol, L. Labeyrie, M. Arnold, M. Fontugne, and C. Pierre (1997b), Enhanced rainfall in the Mediterranean region during the last sapropel event, *Oceanologica Acta*, 20: 697-712.

Kemp, A.E.S., R.B. Pearce, I. Koizumi, J. Pike, and S.J. Rance (1999), The role of mat-forming diatoms in the formation of Mediterranean sapropels, *Nature*, 398, 57-61.

Kim, S.T., and J. R. O'Neil (1997), Equilibrium and nonequilibrium oxygen isotope effects in synthetic calcites, *Geochimica et Cosmochimica Acta*, 61, 3461-3475.

Klein, B., W. Roether, B.B. Manca, D. Bregant, V. Beitzel, V. Kovacevic, and A. Luchetta (1999), The large deep water transient in the eastern Mediterranean, *Deep-Sea Research*, Part 1, 46, 371-414.

Kobashi, T., J. P. Severinghaus, E. J. Brook, J.-M. Barnola, and A. Grachev (2007), Precise timing and characterization of abrupt climate change 8,200 years ago from air trapped in polar ice, *Quaternary Science Reviews*, 26, 1212-1222.

Koopmans, M.P., J. Köster, H.M.E. Van Kaam-Peters, F. Kenig, S. Schouten, W.A. Hartgers, J.W. De Leeuw, and J.S. Sinninghe Damsté (1996), Diagenetic and catagenetic products of isorenieratene: Molecular indicators for photic zone anoxia, *Geochimica et Cosmochimica Acta*, 60, 4467-4496.

Krishnamurthy, R.V., P.A. Meyers, and N.A. Lovan (2000), Isotopic evidence of sea-surface freshening, enhanced productivity, and improved organic matter preservation during sapropel deposition in the Tyrrhenian Sea, *Geology*, 28, 263-266.

Kucera, M., A. Rosell-Melè, R. Schneider, C. Waelbroeck, and M. Weinelt (2005), Multiproxy approach for the reconstruction of the glacial ocean surface (MARGO), *Quaternary Science Reviews*, 24(7-9), 813-819.

Kullenberg, B. (1952), On the salinity of the water contained in marine sediments. *Goteborgs Kungl. Vetenskaps. Vitt-Samhal. Handlingar*, 6(B.), 3-37.

Kuhnt, T., G. Schmiedl, W. Ehrmann, Y. Hamann, and C. Hemleben, 2007, Deep-sea ecosystem variability of the Aegean Sea during the past 22 kyr as revealed by benthic foraminifera, *Marine Micropaleontology*, 64 (3-4), 141-162.

Kutzbach, J. E., G. Bonan, J. Foley, and S. P. Harrison (1996), Vegetation and soil feedbacks on the response of the African monsoon to orbital forcing in the early to middle Holocene, *Nature*, 384, 623-626.

Laskar, J. (1990), The chaotic motion of the solar system. A numerical estimate of the size of the chaotic zones, *Icarus*, 88, 266-291.

Laws, E.A., B.N. Popp, R. Bidigare, M.C. Kennicutt , S.A. Macko (1995), Dependence of phytoplankton carbon isotopic composition on growth rate and [CO2]aq.: Theoretical considerations and experimental results, *Geochimica et Cosmochimica Acta*,59, 1131-1138.

LeGrande, A. N., G. A. Schmidt, D. T. Shindell, C. V. Field, R. L. Miller, D. M. Koch, G. Faluvegi, and G. Hoffmann (2006), Consistent simulations of multiple proxy responses to an abrupt climate change event, *Proceedings of the National Academy of Sciences*, 103, 837-842.

Lionello, P., Malanotte-Rizzoli, P., R. Boscolo (Eds) (2006), *The Mediterranean climate: an overview of the main characteristics and issues*, Elsevier, pp. 438.

Lozhkin, A.V., and P.M. Anderson (1995), The last interglaciation in northeast Siberia, *Quaternary Research*, 43, 147-158.

Lolis, C.J., A. Bartzokas, and B.D. Katsoulis (2002), Spatial and temporal 850 hPa air temperature and sea-surface temperature covariances in the Mediterranean region and their connection to atmospheric circulation, *International Journal of Climatology*, 22, 663-676.

Lourens, L.J., A. Antonarakou, F.J. Hilgen, A.A.M. Van Hoof, C. Vergnaud-Grazzini, and W.J. Zachariasse (1996), Evaluation of the Plio-Pleistocene astronomical time-scale, *Paleoceanography*, 11, 391-413.

Maasch, K.A., P. A. Mayewski, E. J. Rohling, J. C. Stager, W. Karlen, L. D. Meeker,

and E. A. Meyerson (2005), A 2000 year context for modern climate change, *Geografiska Annaler*, 87A, 7-15.

Maheras, P., E. Xoplaki, T. Davies, J. Martin-Vide, M. Bariendos, and M. J. Alcoforado (1999), Warm and cold monthly anomalies across the Mediterranean basin and their relationship with circulation; 1860-1990, *International Journal of Climatology*, 19, 1697-1715.

Malanotte-Rizzoli, P., and A. Hecht (1988), Large-scale properties of the eastern Mediterranean: a review, Oceanologica Acta, 11, 323-335.

Malanotte-Rizzoli, P., B.B. Manca, M. Ribera d'Alcala, A. Theocharis, S. Brenner, G. Budillon, and E. Ozsoy (1999), The Eastern Mediterranean in the 80s and in the 90s: the big transition in the intermediate and deep circulations, *Dynamics of Atmospheres and Oceans*, 29, p. 365-395.

Malmgren, B. A., M. Kucera, J. Nyberg, and C. Waelbroeck (2001), Comparison of statistical and artificial neural network techniques for estimating past sea-surface temperatures from planktonic foraminifer census data, *Paleoceanography*, 16(5), 520-530.

Mangini, A., and P. Schlosser (1986), The formation of eastern Mediterranean sapropels, Marine Geology, 72, 115-124.

Marret, F., and K. A. F. Zonneveld (2003), Atlas of modern organic-walled dinoflagellate cyst distribution, *Review of Palaeobotany and Palynology*, 125, 1-200.

Marshall, J. D., B. Lang, S. F. Crowley, G. P. Weedon, P. van Calsteren, E. H. Fisher,R. Holme, J. A. Holmes, R. T. Jones, A. Bedford, S. J. Brooks, J. Bloemendal, K. Kiriakoulakis and J. D. Ball (2007), Terrestrial impact of abrupt changes in the North Atlantic thermohaline circulation: Early Holocene, UK, *Geology*, 35(7), 639-642.

Matthews, A., A. Ayalon and M. Bar-Matthews (2000), *D*/*H* ratios of fluid inclusions of Soreq Cave (Israel) speleothems as a guide to the Eastern Mediterranean Meteoric Line relationships in the last 120 ky, *Chemical Geology*, 166, 183-191.

McGarry, S., M. Bar-Matthews, A. Matthews, A. Vaks, B. Schilman, and A. Ayalon (2004), Constraints on hydrological and paleotemperature variations in the Eastern Mediterranean region in the last 140 ka given by the dD values of speleothem fluid inclusions, *Quaternary Science Reviews*, 23, 919-934.

Mayewski, P.A., L. D. Meeker, M. S. Twickler, S. Whitlow, Q. Yang, W. B. Lyons, and M. Prentice (1997), Major features and forcing of high-latitude northern hemisphere atmospheric circulation using a 110,000-year long glaciochemical series, *Journal of Geophysical Research*, 102(C12), 26345-26366.

Mayewski, P. A., E. J. Rohling, J. C. Stager, W. Karlen, K. A. Maasch, L. D. Meeker, E. A. Meyerson, F. Gasse, S. van Kreveld, K. Holmgren, J. Lee-Thorp, G. Rosqvist, F. Rack, M. Staubwasser, R. R. Schneider, and E. J. Steig (2004), Holocene climate variability, *Quaternary Research*, 62, 243-255.

Meeker, L. D., and P. A. Mayewski (2002), A 1400-year high-resolution record of atmospheric circulation over the North Atlantic and Asia, *The Holocene*, 12, 257-266.

Meese, D. A., R. B. Alley, A. J. Gow, P. Grootes, P. A. Mayewski, M. Ram, K. C. Taylor, E. D. Waddington, and G. Zielinski (2004), The accumulation record from the GISP2 core as an indicator of climate change throughout the Holocene, *Science*, 266, 1680-1682.

Menzel, D., S. Schouten, P.F. van Bergen, J.S. Sinninghe Damsté (2004), Higher plant vegetation changes during Pliocene sapropel formation, *Organic Geochemistry*, 35(11-12), 1343-1353.

Menzel, D., P.F. Van Bergen, S. Schouten, and J.S. Sinninghe Damsté (2003), Changes in primary productivity during Pliocene sapropel formation: A biomarker approach, *Palaeogeography, Palaeoclimatology, Palaeoecology*, 190, 273-287.

Menzel D., E.C. Hopmans, P.F. van Bergen, J.W. de Leeuw, and J.S. Sinninghe Damsté (2002), Development of photic zone euxinia in the eastern Mediterranean Basin during deposition of Pliocene sapropels, *Marine Geology*, 189, 215-226.

Menzel, D., P.F. van Bergen, H. Veld, H. Brinkhuis, and and J.S. Sinninghe Damsté (2005), The molecular composition of kerogen in Pliocene Mediterranean sapropels and associated homogeneous calcareous ooze, *Organic Geochemistry*, 36, 1037-1053.

Menzel D., E.C. Hopmans, S. Schouten, and J.S. Sinninghe Damsté (2006), Membrane tetraether lipids of planktonic Crenarchaeota in Pliocene sapropels of the eastern Mediterranean Sea, *Palaeogeography, Palaeoclimatology, Palaeoecology*, 239(1-2), 1-15.

Mercone, D., J. Thomson, R. H. Abu-Zied, I. W. Croudace, and E. J. Rohling (2001), High resolution geochemical and micropalaeontological profiling of the most recent eastern Mediterranean sapropel, *Marine Geology*, 177, 25-44.

Mercone, D., J. Thomson, I. W. Croudace, G. Siani, M. Paterne, and S. Troelstra (2000), Duration of S1, the most recent sapropel in the eastern Mediterranean Sea, as indicated by accelerator mass spectrometry radiocarbon and geochemical evidence, *Paleoceanography*, 15, 336-347.

Moodley, L., J.J. Middelburg, P.M.J. Herman, K. Soetaert, and G.J. de Lange (2005), Oxygenation and organic-matter preservation in marine sediments: Direct experimental evidence from ancient organic carbon-rich deposits, *Geology*, 33, 889-892.

Mook, W.G. (2001), Estuaries and the Sea. In: Rozanski, K., Froehlich, K., Mook, W.G. (Eds.), *Volume III: Surface Water*. Unesco, Paris, pp. 49-56.

Muerdter D.R., and J.P. Kennett (1983), Late Quaternary planktonic foraminifera stratigraphy, Strait of Sicily, Mediterranean Sea. *Marine Micropaleontology*, 8, 339-359.

Müller, P.J., G. Kirst, G. Ruhland, I. von Storch, and A. Rosell-Mélé (1998), Calibration of the alkenone paleotemperature index $U^{k'}_{37}$ based on core tops from the eastern South Atlantic and the global ocean (60°N-60°S), *Geochimica et Cosmochimica Acta*, 62, 1757-1772.

Myers, P.G., and K. Haines (2002), Stability of the Mediterranean's thermohaline circulation under modified surface evaporative fluxes, *Journal of Geophysical Research*, 107, 7-1 to 7-10.

Myers, P.G., and E.J. Rohling (2000), Modelling a 200 year interruption of the Holocene sapropel S1, *Quaternary Research*, 53, 98-104,

Myers, P., K. Haines, and E.J. Rohling (1998), Modelling the paleo-circulation of the Mediterranean: The last glacial maximum and the Holocene with emphasis on the formation of sapropel S1, *Paleoceanography*, 13, 586-606.

Neff, U., S. J. Burns, A. Mangini, M. Mudelsee, D. Fleitmann, and A. Matter (2001), Strong coherence between solar variability and the monsoon in Oman between 9 and 6 ka ago, *Nature*, 411, 290-293.

Nesje, A., S. O. Dahl, and J. Bakke (2004), Were abrupt Lateglacial and early-Holocene climatic changes in northwest Europe related to freshwater outbursts to the North Atlantic and Arctic oceans?, *The Holocene*, 14, 299-310.

NGRIP members (2004), High-resolution record of Northern Hemisphere climate extending into the last interglacial period, *Nature*, 431, 147-151.

Nijenhuis, I.A., and G.J. De Lange (2000), Geochemical constraints on Pliocene sapropel formation in the eastern Mediterranean, *Marine Geology*, 163, 41-63.

Nijenhuis, I.A., S.J. Schenau, C.H. Van der Weijden, F.J. Hilgen, L.J. Lourens, W.J. Zachariasse (1996), On the origin of upper Miocene sapropelites: a case study from the Faneromeni section, Crete (Greece), *Paleoceanography*, 11, 633-645.

O'Brien, S. R., P. A. Mayewski, L. D. Meeker, D. A. Meese, M. S. Twickler, and S. E. Whitlow (1995), Complexity of Holocene climate as reconstructed

from a Greenland ice core, *Science*, 270, 1962-1964.

Otto-Bliesner, B.L., S. Marshall, J. Overpeck, G. Miller, A. Hu, and CAPE Last Interglacial Project Members (2006), Simulating Arctic climate warmth and icefield retreat in the last interglaciation, *Science*, 311, 1751-1753.

Overpeck, J., D. Anderson, S. Trumbore, and W. Prell (1996), The Southwest Indian Monsoon over the Last 18,000 Years, *Climate Dynamics*, 12, 213-225.

Paillard, D., L. Labeyrie, and P. Yiou (1996), Macintosh program performs time-series analysis. *EOS*, 77, 379.

Passier, H.F., H.-J. Bosch, I.A. Nijenhuis, L.J. Lourens, M.E. Bottcher, A. Leenders, J.S. Sinninghe Damsté, G.J. De Lange, and J.W. de Leeuw (1999), Sulphidic Mediterranean surface waters during Pliocene sapropel formation, *Nature*, 397, 146-149.

Paul, H.A. (2002), *Application of novel stable isotope methods to reconstruct paleoenvironments, compound specific hydrogen isotopes and pore-water oxygen isotopes*. Swiss Federal Institute of Technology, Zürich.

Pedersen, T.F., and S.E. Calvert (1990), Anoxia vs. productivity - what controls the formation of organic-carbon-rich sediments and sedimentary-rocks, *AAPG Bulletin*, 74, 454-466.

Pierre, C. (1999), The oxygen and carbon isotope distribution in the Mediteranean water masses, *Marine Geology*, 153, 41^55.

Pinardi, N., and F. Masetti (2000), Variability of the large scale general circulation of the Mediterranean Sea from observations and modelling: a review, *Palaeogeography, Palaeoclimatology, Palaeoecology*, 158, 153-173.

Popp, B.N., E.A. Laws, R.R. Bidigare, J.E. Dore, K.L. Hanson, and S.G. Wakeham (1998), Effect of phytoplankton cell geometry on carbon isotopic fractionation, *Geochimica et Cosmochimica Acta*, 62, 69-77.

Poulos, S. E., P. G. Drakopoulos, and M. B. Collins, 1997, Seasonal variability in sea surface oceanographic conditions in the Aegean Sea (eastern Mediterranean): an overview, *Journal of Marine Systems*, 13, 225-244.

Principato, M.S., D. Crudeli, P., Ziveri, C.P. Slomp, C. Corselli, E. Erba, G.J. de Lange (2006), Phyto- and zooplankton paleofluxes during the deposition of sapropel S1 (eastern Mediterranean): biogenic carbonate preservation and paleoecological implications, *Palaeogeography Palaeoclimatology Palaeoecology*, 235, 8-27.

Pross, J. and H. Brinkhuis (2005), Organic-walled dinoflagellate cysts as paleoenvironmental indicators in the Paleogene; a synopsis of concepts, *Paläontologische Zeitschrift*, 79, 53-59.

Psarra, S., A. Tselepides, and L. Ignatiades (2000), Primary productivity in the

oligotrophic Cretan Sea (NE Mediterranean): seasonal and interannual variability, *Progress in Oceanography*, 46(2-4), 187-204.

Ramel, R., H. Gallee, C. Messager (2006), On the northward shift of the West African monsoon, *Climate Dynamics*, 26, 429-440.

Reichart, G.J. (1997), Late Quaternary variability of the Arabian Sea monsoon and oxygen minimum zone, *Geologica Ultraiectina*, 154, pp. 174.

Reichart, G.J., and H. Brinkhuis (2003), Late Quaternary *Protoperidinium* cysts as indicators of paleoproductivity in the northern Arabian Sea, *Marine Micropaleontolology*, 49, 303-315.

Reitz, A., and G.J. De Lange (2006), Abundant Sr-rich aragonite in eastern Mediterranean sapropel (S1): diagenetic versus detrital/biogenic origin, *Palaeogeography, Palaeoclimatology, Palaeoecology*, 235, 135-148.

Reitz, A., J. Thomson, G.J. De Lange, and C. Hensen (2006), Source and development of large manganese enrichments above eastern Mediterranean sapropel S1, *Paleoceanography*, 21(3), PA3007, doi:10.1029/2005PA001169.

Renssen, H., H. Goosse, T. Fichefet, J.-M. Campin (2001), The 8.2 kyr BP event simulated by a global atmosphere-sea-ice-ocean model, *Geophysical Research Letters*, 28(8), 1567-1570.

Renssen, H., H. Goosse, T. Fichefet (2002), Modeling the effect of freshwater pulses on the early Holocene climate: the influence of high frequency climate variability, *Paleoceanography*, 17, 1020, 10.1029/2001PA000649.

Repeta, D.J., D.J. Simpson, B.B. Jørgensen, and H.W. Jannasch (1989), Evidence for anoxygenic photosynthesis from the distribution of bacteriochlorophylls in the Black Sea, *Nature*, 342, 69-72.

Rinna, J., B. Warning, P.A. Meyers, H.J. Brumsack, and J. Rullkotter (2002), Combined organic and inorganic geochemical reconstruction of paleodepositional conditions of a Pliocene sapropel from the eastern Mediterranean Sea, *Geochimica et Cosmochimica Acta*, 66, 1969-1986.

Risebrobakken, B., E. Jansen, C. Andersson, E. Mjelde, K. Hevroy (2003), A high-resolution study of Holocene paleoclimatic and paleoceanographic changes in the Nordic seas, *Paleoceanography*, 18(1), 1017, DOI:10.1029/2002PA000764.

Ritchie, J. C., C. H. Eyles, and C. V. Haynes (1985), Sediment and pollen evidence for an early to mid-Holocene humid period in the eastern Sahara, *Nature*, 314, 352-355.

Robertson, A.H.F., K.-C. Emeis, C. Richter, and A. Camerlenghi (Eds.) (1998), *Proceedings Ocean Drilling Program (ODP), Scientific Results*, 160. Ocean Drilling Program, College Station, TX, pp. 817.

Robinson, A.R., W.G. Leslie, A. Theocharis and A. Lascaratos, 2001. *Mediterra-*

nean Sea Circulation Encyclopedia of Ocean Sciences, Academic Press, 1689-1706.

Rochon A, A. de Vernal, J. L. Turon, J. Matthiessen, and M. J. Head (1999), *Distribution of recent dinoflagellate cysts in surface sediments from the North Atlantic Ocean and adjacent seas in relation to sea surface parameters*. American Association of Stratigraphic Palynologists, Contribution Series 35: Dallas, TX, 1-119 pp.

Rodwell, M. J., and B. J. Hoskins (1996), Monsoons and the dynamics of deserts, *The Quarterly Journal of the Royal Meteorological Society*, 122, 1385-1404.

Roether, W., B.B. Manca, B. Klien, D. Bregant, D. Georgopoulos, V. Beitzel, V. Kovacevic and A. Luchetta (1996), Recent changes in Eastern Mediterranean Deep Waters, *Science*, 271, 333-335.

Rohling, E.J. (1991), Shoaling of the eastern Mediterranean pycnocline due to reduction of excess evaporation: implications for sapropel formation, *Paleoceanography*, 6, 747-753.

Rohling, E.J. (1994), Review and new aspects concerning the formation of Mediterranean sapropels, *Marine Geology*, 122; 1-28.

Rohling, E. J. 1999. Environmental control on Mediterranean salinity and $\delta^{18}O$, *Paleoceanography,* 14, 706-715.

Rohling, E.J., and H.L. Bryden, H.L. (1992), Man-induced salinity and temperature increases in western Mediterranean Deep Water, *Journal of Geophysical Research*, 97, 11191-11198.

Rohling, E.J., and S. De Rijk (1999), The Holocene Climate Optimum and Last Glacial Maximum in the Mediterranean: the marine oxygen isotope record, *Marine Geology*, 153, 57-75.

Rohling, E.J. and W.W.C. Gieskes (1989), Late Quaternary changes in Mediterranean Intermediate Water density and formation rate, *Paleoceanography*, 4, 531-545.

Rohling, E. J., and F. J. Hilgen (1991), The eastern Mediterranean climate at times of sapropel formation: a review, *Geologie en Mijnbouw*, 70, 253-264.

Rohling, E. J., and H. Pälike (2005), Centennial-scale climate cooling with a sudden cold event around 8,200 years ago, *Nature*, 434, 975-979.

Rohling, E.J., E.C. Hopmans, and J.S. Sinninghe Damsté (2006), Water column dynamics during the last interglacial anoxic event in the Mediterranean (sapropel S5), *Paleoceanography*, 21, PA2018, doi: 10.1029/2005PA001237.

Rohling, E.J., F.J. Jorissen, and H.C. De Stigter (1997), A 200 Year interruption of Holocene sapropel formation in the Adriatic Sea, *Journal of Micropaleontology*, 16, 97-108.

Rohling, E.J., H.C. De Stigter, C. Vergnaud-Grazzini, and R. Zaalberg (1993), Temporary repopulation by low-oxygen tolerant benthic foraminifera within an upper Pliocene sapropel; Evidence for the role of oxygen depletion in the formation of sapropels, *Marine Micropaleontology*, 22, 207-219.

Rohling, E.J., F.J. Jorissen, C. Vergnaud-Grazzini, and W.J. Zachariasse (1993), Northern Levantine and Adriatic planktonic foraminifera: Reconstruction of paleoenvironmental gradients, *Marine Micropaleontology*, 21, 191-218.

Rohling, E.J., R. H. Abu-Zied, J. S. L. Casford, A. Hayes and B. A. A. Hoogakker (2008), The Mediterranean Sea: Present and Past, in *The Physical Geography of the Mediterranean*, edited by J. C. Woodward, Oxford University Press, in press.

Rohling, E.J., P. A. Mayewski, A. Hayes, R. H. Abu-Zied, and J.S.L. Casford (2002a), Holocene atmosphere-ocean interactions: records from Greenland and the Aegean Sea, **Climate Dynamics**, 18, 587-593.

Rohling, E.J., K. Grant, Ch. Hemleben, M. Siddall, B.B.A. Hoogakker, M. Bolshaw, and M. Kucera (2008b), High rates of sea-level rise during the last interglacial period, *Nature Geoscience*, 1, 38-42.

Rohling, E.J., T.R. Cane, S. Cooke, M. Sprovieri, I. Bouloubassi, K.-C. Emeis, R. Schiebel, D. Kroon, F.J. Jorissen, A. Lorre, and A.E.S. Kemp (2002b), African monsoon variability during the previous interglacial maximum, *Earth and Planetary Science Letters*, 202, 61-75.

Rohling, E.J., M. Sprovieri, T.R. Cane, J.S.L. Casford, S. Cooke, I. Bouloubassi, K.-C. Emeis, R. Schiebel, M. Rogerson, A. Hayes, F.J. Jorissen, and D. Kroon (2004), Reconstructing past planktic foraminiferal habitats using stable isotope data: a case history for Mediterranean sapropel S5, *Marine Micropaleontology*, 50, 89-123.

Rossignol-Strick, M. (1983), African monsoons, an immediate climate response to orbital insolation, *Nature*, 30, 446-449.

Rossignol-Strick, M. (1985), Mediterranean Quaternary sapropels, an immediate response of the African monsoon to variations of insolation, *Palaeogeography, Palaeoclimatology., Palaeoecology*, 49, 237-263.

Rossignol-Strick, M. (1987), Rainy periods and bottom water stagnation initiating brine accumulation and metal concentrations: 1. The Late Quaternary, *Paleoceanography*, 2, 333-360.

Rossignol-Strick, M., V. Nesteroff, P. Olive and C. Vergnaud-Grazzini (1982), After the deluge; Mediterranean stagnation and sapropel formation, *Nature*, 295, 105-110.

Rothwell, R.G. (1995), *Cruise Report: MASTII PALAEOFLUX Programme*, Mediterranean Giant Piston Coring Transect, Marion Dufresne Cruise 81.

Rühlemann, C., P. Müller, P., and R. Schneider (1999), Organic carbon and carbonate as paleoproductivity proxies: examples from high and low productivity areas of the tropical Atlantic. In: Fischer, G., Wefer, G. (Eds.), *Use of Proxies in Paleoceanography: Examples from the South Atlantic*. Springer-Verlag, Berlin, pp. 1- 31.

Saaroni, H., B. Ziv, J. Edelson, and P. Alpert, Long-term variations in summer temperatures over the Eastern Mediterranean, *Geophysical Research Letters*, 30(18), 1946, 2003.

Sachs, J., and D.J. Repeta (1999), Oligotrophy and Nitrogen fixation during eastern Mediterranean sapropel events, *Science*, 286, 2485-2488.

Samuel, S., K. Haines, S. Josey, and P.G. Myers (1999), Response of the Mediterranean Sea thermohaline circulation to observed changes in the winter wind stress field in the period 1980-1993, *Journal of Geophysical Research*, 104, 7771-7784.

Sancetta, C. (1994), Mediterranean sapropels: seasonal stratification yields high production and carbon flux, *Paleoceanography*, 9, 195-196.

Sangiorgi, F., L. Capotondi, H. Brinkhuis (2002), A centennial scale organic-walled dinoflagellate cyst record of the last deglaciation in the South Adriatic Sea (Central Mediterranean), *Palaeogeography, Palaeoclimatology, Palaeoecology*, 186, 199-216.

Sangiorgi, F., L. Capotondi, N. Combourieu Nebout, L. Vigliotti, H. Brinkhuis, S. Giunta, A. F. Lotter, C. Morigi, A. Negri, and G.-J. Reichart (2003), Holocene seasonal sea-surface temperature variations in the southern Adriatic Sea inferred from a multiproxy approach, *Journal of Quaternary Science*, 18, 723-732.

Sangiorgi, F., E. Dinelli, P. Maffioli, S. Principato, L. Capotondi, S. Giunta, C. Morigi, K.C. Emeis, A. Negri, C. Corselli (2006), Geochemical and micropaleontological characterisation of a Mediterranean sapropel S5: a case study from core BAN89GC09 (south of Crete), *Palaeogeography, Palaeoclimatology, Palaeoecology*, 235, 192-207.

Sarmiento, J. L., T. D. Herbert, and J. R. Toggweiler, 1988: Mediterranean nutrient balance and episodes of anoxia, *Global Biogeochemical Cycles*, 2(4), 427-444.

Schimmelmann, A., A.L. Sessions, C.J. Boreham, D.S. Edwards, G.A. Logan, R.E. Summons (2004), *D*/*H* ratios in terrestrially sourced petroleum systems, *Organic Geochemistry*, 35, 1169-1195.

Schouten, S., Ossebaar, J., Schreiber, K., Kienhuis, M.V.M., Langer, G., Benthien, A., Bijma, J., 2006. The effect of temperature, salinity and growth rate on the stable hydrogen isotopic composition of long chain alkenones produced

by Emiliania huxleyi and Gephyrocapsa oceanica. *Biogeosciences*, 3, 113-119.

Scrivner, A., D. Vance, and E. J. Rohling (2004), New neodymium isotope data quantify Nile involvement in Mediterranean anoxic episodes, *Geology*, 32, 565-568.

Sessions, A.L., S.P. Sylva, R.E. Summons, and J.M. Hayes (2004), Isotopic exchange of carbon-bound hydrogen over geologic timescales, *Geochimica et Cosmochimica Acta*, 68, 1545-1559.

Siani G., M. Patene, E. Miche, R. Sulpizio, A. Sbrana, M. Arnold, G. Haddad (2001), Mediterranean sea surface radiocarbon reservoir age changes since the Last Glacial Maximum, *Science*, 294, 1917-1920.

Sinninghe Damste, J.S., and J. Koster (1998), A euxinic southern North Atlantic Ocean during the Cenomanian/Turonian oceanic anoxic event, *Earth and Planetary Science Letters*, 158, 165-173.

Skliris, N., and A. Lascaratos (2004), Impacts of the Nile River damming on the thermohaline circulation and water mass characteristics of the Mediterranean Sea, *Journal of Marine Systems*, 52, 121-143.

Skliris, N., S. Sofianos, and A. Lascaratos (2007), Hydrological changes in the Mediterranean Sea in relation to changes in the freshwater budget: A numerical modelling study, *Journal of Marine Systems*, 65, 400-416.

Sperling, M., G. Schmiedl, C. Hemleben, K.-C. Emeis, H. Erlenkeuser, and P. M. Grootes (2003), Black Sea impact on formation of eastern Mediterranean sapropel S1? Evidence from the Marmara Sea, *Palaeogeography, Palaeoclimatology, Palaeoecology*, 190, 9-21.

Sprovieri R., E. Di Stefano, A. Incarbona, and M.E. Gargano (2003), A high-resolution record of the last deglaciation in the Sicily Channel based on foraminifera and calcareous nannofossil quantitative distribution, *Palaeogeography, Palaeoclimatology, Palaeoecology*, 202, 119-142.

Stratford, K., and K. Haines (2002), Modelling changes in Mediterranean thermohaline circulation 1987-1995, *Journal of Marine Systems*, 33-34, 51-62.

Strohle, K., and M.D. Krom (1997), Evidence for the evolution for an oxygen minimum layer at the beginning of S-1 sapropel deposition in the eastern Mediterranean, *Marine Geology*, 140, 231-236.

Struck, U., K.C. Emeis, M. Voss, M.D. Krom, and G.H. Rau (2001), Biological productivity during sapropel S5 formation in the eastern Mediterranean Sea: Evidence from stable isotopes of nitrogen and carbon, *Geochimica et Cosmochimica Acta*, 65, 3249-3266.

Stuiver, M., P.J. Reimer, E. Bard, J.W. Beck, G.S. Burr, K.A. Hughen, B. Kromer, F.G. McCormac, J. van der Plicht, and M. Spurk (1998), INTCAL98 Radio-

carbon age calibration 24,000 - 0 cal BP, *Radiocarbon*, 40,1041-1083

Taylor, F.J.R. (Ed.) (1987), The Biology of Dinoflagellates, Botanical Monographs, 21, 785 pp., Blackwell Scientific Publications, London.

Theocharis, A., B. Klein, K. Nittis, and W. Roether (2002), Evolution and status of the Eastern Mediterranean Transient (1997-1999), *Journal of Marine Systems*, 33-34 , 91-116.

Thomas, E.R., E.W. Wolff, R. Mulvaney, J. P. Steffensen, S. J. Johnsen, C. Arrowsmith, J. W. C. White, B. Vaughn, T. Popp (2007), The 8.2 ka event from Greenland ice cores, *Quaternary Science Reviews*, 26, 70-81.

Thomson, J., D. Mercone, G.J. de Lange, and P.J.M. van Santvoort (1999), Review of recent advances in the interpretation of eastern Mediterranean sapropel S1 from geochemical evidence, *Marine Geology*, 153, 77-89.

Thunell, R.C., and D.F. Williams (1989), Glacial-Holocene salinity changes in the Mediterranean Sea: hydrographic and depositional effects, *Nature*, 338, 493-496.

Tsimplis, M.N., V. Zervakis, S. Josey, E. Peeneva, M.V. Struglia, E. Stanev, P. Lionello, P. Malanotte-Rizzoli, V. Artale, A. Theocharis, E. Tragou, and T. Oguz (2006), *Changes in the oceanography of the Mediterranean Sea and their link to climate variability*. In: P. Lionello, P. Malanotte-Rizzoli & R. Boscolo (Eds), Mediterranean Climate Variability, Amsterdam, Elsevier, pp. 227-282.

Van Os, B.J.H., L.J. Lourens, F.J. Hilgen, G.J., de Lange, and L. Beaufort (1994), The formation of Pliocene sapropels and carbonate cycles in the Mediterranean - diagenesis, dilution, and productivity, *Paleoceanography*, 9, 601-617.

Versteegh, G. J. M. and K. A. F. Zonneveld (2002), Use of selective degradation to separate preservation from productivity, *Geology*, 30(7), 615-618.

von Grafenstein, U., H. Erlenkeuser, A. Brauer, J. Jouzel, and S. Johnsen (1999), A mid-European decadal isotope-climate record from 15,500 to 5,000 years BP, *Science*, 284, 1654-1657.

Wall, D., B. Dale, G. P. Lohman, and W. K. Smith (1977), The environmental and climatic distribution of dinoflagellate cysts in modern sediments from regions in the North and South Atlantic oceans and adjacent seas, *Marine Micropaleontology*, 2, 121-200.

Webster, P. J., V. O. Magana, T. N. Palmer, J. Shukla, R. A. Tomas, M. Yanai, T. Yasunari (1998), Monsoons: processes, predictability, and the prospects for prediction, *Journal of Geophysical Research Oceans*, 103, 14451-14510.

Weldeab, S., D. W. Lea, R. R. Schneider, and N. Andersen (2007), 155,000 years of West African Monsoon and ocean thermal evolution, *Science*, 316, 1303-

1307.

Weldeab, S., R. R. Schneider, M. Kolling, and G. Wefer (2005), Holocene African droughts relate to eastern equatorial Atlantic cooling, *Geology*, 33, 981-984.

Weldeab, S., K.-C Emeis, C. Hemleben, G. Schmiedl, and H. Schulz (2003), Spatial productivity variations during formation of sapropel S5 and S6 in the Mediterranean Sea: Evidence from Ba contents, *Palaeogeography, Palaeoclimatology, Palaeoecology*, 191, 169-190.

Wiersma, A.P., and H. Renssen (2006), Model-data comparison for the 8.2 ka BP event: confirmation of a forcing mechanism by catastrophic drainage of Laurentide Lakes, *Quaternary Science Reviews*, 25, 63-88.

Wijmstra, T. A., R. Young, and H. J. L. Witte (1990), An evaluation of the climatic conditions during the Late Quaternary in northern Greece by means of multivariate analysis of palynological data and comparison with recent phytosociological and climatic data, *Geologie en Mijnbouw*, 69, 243-251.

Williams, D.F., R.C. Thunell, and J.P. Kennett (1978), Periodic fresh-water flooding and stagnation of the eastern Mediterranean during the late Quaternary, *Science*, 201, 252-254.

Wüst, G. (1961), On the vertical circulation of the Mediterranean Sea, *Journal of Geophysical Research*, 66, 3261-3271.

Zervakis, V., D. Georgopoulos, A.P. Karageorgis, and A. Theocharis (2004), On the response of the Aegean sea to climatic variability: a review, *International Journal of Climatology*, 24, 1845-1858.

Ziv, B., H. Saaroni, and P. Alpert (2004), The factors governing the summer regime of the eastern Mediterranean, *International Journal of Climatology*, 24, 1859-1871.

Ziveri, P., A. Ruten, G.J. de Lange, J. Thomson, and C. Corselli (2000), Present-day coccolith fluxes recorded in central eastern Mediterranean sediment traps and surface sediments, *Palaeogeography, Palaeoclimatology, Palaeoecology*, 158, 175-195.

Zonneveld, K. A. F. (1995), Palaeoclimatic and paleo-ecologic changes during the last deglaciation in the Eastern Mediterranean; implications for dinoflagellate ecology, *Review of Palaeobotany and Palynology*, 84(3), 221-253.

Zonneveld, K. A. F. (1996), Palaeoclimatic reconstruction of the last deglaciation (18 ka. BP. - 8 ka. BP.) in the Adriatic Sea region: a land-sea correlation based on palynological evidence, *Palaeogeography, Palaeoclimatology, Palaeoecology*, 122, 89-106.

Zonneveld, K.A.F. and G.A. Brummer (2001), (Palaeo-)ecological significance, transport and preservation of organic walled dinoflagellate cysts in the So-

mali Basin, NW Arabian Sea, *Deep Sea Research II*, 47, 2229-2256.

Zonneveld, K. A. F., G. J. M. Versteegh, and G. J. de Lange (2001), Palaeoproductivity and postdepositional aerobic organic matter decay reflected by dinoflagellate cyst assemblages of the Eastern Mediterranean S1 sapropel, *Marine Geology*, 172, 181-195.

Zonneveld, K. A. F., F. Bockelmann, and U. Holzwarth (2007), Selective aerobic degradation of organic walled dinoflagellates as tool to quantify past net primary production and bottom water oxygen concentrations, *Marine Geology*, 237(3-4), 109-126.

Acknowledgements

….the acknowledgements, this is usually a nice piece to write up, isn't it? It means that the paper is nearly out of your desk, in a way you begin to relax. However, for a PhD dissertation, things are not exactly like that, at this stage you're NOT done, you still need to go through your defence (dressed up like a penguin!!!), and for the acknowledgments themselves you want to come up with something original, but - most of all - you need to make sure you don't forget anybody. Despite all the efforts that a PhD demands to be accomplished, most of the people out there will skip introduction, summary, papers, and figures and will focus first on this specific section, so no time to relax as yet …

First of all I'd like to express my gratitude to my Promotoren (i.e., the PhD Advisors); Professors Henk Brinkhuis and Bruno D'Argenio. They share the merit to have set up this project, to have provided the funding to support me and my research over the years, in other words to have led me this far…. Henk, in a couple of weeks it will be the day… it follows months of intense work, with you popping up in my office every now and then to make sure I was OK despite the minimal sleeping. There's plenty of other things that I've truly appreciated over the years; you've managed to top up my 3-years Italian PhD fellowship to keep me at the LPP for an extra-year, that way fulfilling my wish to complete my PhD at Utrecht University; you've given to me a range of opportunities that is even wider than what I'd have wished myself, in terms of collaborations, projects and financial sources to travel around the globe for conferences; and last but not the least you've made me laugh several times with your jokes, and delighted me with your cooking skills at the "dino-dinners"….. the cherry on the cake, however, is another one; I reckon that it is not really my merit but I'm very proud to be the first student ever for whom you act as promotor!

Prof. D'Argenio, we know each other for a while now, you were my advisor for the Master thesis as well and the one who hired me as PhD student at your institute and subsequently advised me to spend a couple of months (apparently it ended up to be much longer than that!) abroad in such a fancy town/country. I will always owe a lot to you for this… besides science and the invaluable support that I've always had from you over the years, you've given a start for the most amazing 3 and a half years of my life: I'll NEVER forget that, Grazie di cuore!

My co-promotoren, Eelco Rohling and Francesca Sangiorgi are the ones that have actually supervised my work on an everyday basis, looking at my data, reading the first drafts of my papers (believe me that's not a nice task!!), in other words "being always there".. Francesca over these years you have been the actual support to my work, I don't remember one single time that you have said: "I'm

busy now, please come later". Even now that I'm writing these lines you've walked to my office twice: "Com'è?" (i.e., what's up?) and you have done this throughout my PhD, spending time with me at the microscope, discussing things, replying emails very late in the night to feed back on the last chapters… well, if this piece of work will ever deserve any credit, I feel I have to share that credit with all the team of supervisors and mostly with you. Hey, before I move on I wanna give one more credit to you; while in Ravenna in 2004 you said: "this (moving to NL) is gonna be the most amazing experience of your life, you'll have great fun"….. for your information, was even better than that!

Eelco Rohling; if you work on the Mediterranean paleoceanography that's the name that comes to your mind first. Can you imagine how amazing and inspiring can be to actually work with him? I received loads of inputs from you, and what I've appreciated the most in you Eelco is that you've always found a lot of time to discuss ideas with me (I'd better say to e-discuss things since we mostly communicated via email), feed back on my papers, push me to improve them and to widen my horizons. The time I spent in Southampton was critical for my growth… and - despite the tight schedule - there was also time for some fun, enjoying the nice atmosphere of your "lab-coffee-shop" and the little spare time, e.g., the motor show…

Before I progress any further I'd like to thank Andy Lotter and Joerg Pross, it's also due to your efforts that I could spend one more year in Utrecht and finish up this booklet! While working on my project I had the pleasure to collaborate with several people based in several institution throughout Europe, in particular I would like to thank Stefan Schouten, Jaap Sinninghe Damsté, Marcel van der Meer, Irene Rijpstra, Ellen Hopmans, Gert-Jan Reichart, Michal Kucera, James Casford, Angela Hayes, Mike Bolshaw, Mario Sprovieri, Fabrizio Lirer, and Maurizio Ribera. Thanks also to Ulrich Kotthoff, Cornelia Blaga, Elisabeth van Bentum, and John Lignum. Un grazie particolare anche alla Professoressa Vittoria Ferreri per aver acettato di essere co-relatore della mia tesi italiana, a Lucia Toro per il suo aiuto in questi anni e a tutti all'IAMC-CNR di Napoli.

At the LPP I had the fortune to share my time with a bunch of very nice people; I'd like to thank you all, in particular Wolfram, Rike, Walter (the LPP's Italian gang, ciao Verushka e Luca!), Timme (e ciao Giacomoooo), Oliver, Appy, Leonard (great job with the cover!), Natasja and Jan, and Marjolein (what a great help from you throughout!). Time to thank the AIOs, Peter (B.), Nina, Judith, Maarten, Emi, Micha, Peter (S.), and Frederike you're a very nice gang of outgoing people to have good time with…

Thanks to my international bunch of friends: April, Jeroen, Metodij, Jerome, Hugo, Hugo (Andrè), Ivana, Aart, Fernando, Ifeda, Daina, Amelie, Carolina, Luca,

Davide, Maarten, Roka, Sana. Help!! I feel I forgot somebody here, but over 3 years and a half with people getting in and out it's not that easy!!! Inge, Yara, Yvonne, and Alien, what a great fun (not as much the day after!) hanging out with you all. Lorenzo and Eyk, I've had a great time with the two of you. I know I've been pushing you a bit too hard to party, jump form one club to the next, get home later and later at night but it was unbelievable fun! Usually it's difficult to shortly build-up a robust friendship but with the two of you it immediately went that way, and I don't feel I'd have had so much fun without the two of you around…. Who's next? My friends from Napuleeee I'd say.. time to switch to Italian then, or better to the best I can get with it... In un certo senso rimanere in contatto con voi facile non era. Vivevamo lontani, con il tempo gli impegni aumentano, si fanno orari diversi. Ma avrei mai potuto vivere tutto questo e non tenervi aggiornati? naaaaaaaaaa... Il primo pensiero, specialmente nei weekend, era quello di connettermi al pc e raccontarvi le novità... capitava che i vicini mi chiedessero cosa avessi tanto da ridere quando ero al computer, forse i colleghi pensavano lo stesso.... Guido che figata quando sei venuto a trovarmi, Ale/gemellì ancora conservo le tue mail (!), i paraninfiiiii, Francesco e Ferdinando, ah ah ah.. forse dovrei ringraziarvi in inglese visto il vostro ruolo, ma veramente credete che io mi sarei mai vestito come un pinguino con voi tra il pubblico a sbellicarvi dalle risate??? Un grazie speciale a Carlotta, questa avventura l'ho praticamente iniziata e condivisa in ogni momento con te, spesso da lontano ma con te, è qui che ci siamo conosciuti e da allora mi sei stata vicina sia nei miei momenti di pura e totale esaltazione che quando le cose tanto bene non andavano. Infine ringrazio mamma e Lucia, mia sorella, le persone cui questo libro è dedicato per aver sopportato un figlio e un fratello che era lontano da casa per inseguire i suoi sogni, ma che è certo di non aver mai fatto una scelta migliore di questa....

Curriculum Vitae

Gianluca Marino was born in Napoli, Italy, on April 13th 1976. He attended his secondary school at the "Liceo Scientifico Statale Tito Lucrezio Caro" in Napoli from 1989 to 1994. In 1994 he started his study at the Faculty of Science of the University "Federeco II" of Napoli where he graduated (cum laude) in 2002 in Geological Sciences, advised by Prof. Bruno D'Argenio. His undergraduate training focused mainly on sedimentology and stratigraphy, micropaleontology, Quaternary and marine geology. His master thesis in Geology was entitled "Pontecagnano travertines. New sedimentological and stratigraphic data". At the end of November 2003 he was awarded of a PhD fellowship within the Marine Science and Engineering Doctorate program of the University "Federeco II" of Napoli, chaired by Prof. Bruno D'Argenio. In 2004 he started his correspondence with Prof. Henk Brinkhuis about the possibility to visit the Laboratory of Palaeobotany and Palynology and complete his PhD also at Utrecht University. The PhD research was performed under the supervision of Prof. dr. Henk Brinkhuis (Utrecht University), Prof. Bruno D'Argenio (University "Federeco II" of Napoli), Prof. dr. Eelco Rohling (National Oceanography Centre, Southampton), and dr. Francesca Sangiorgi (Utrecht University). During his PhD, he also visited several times the National Oceanography Centre, Southampton. Results of his PhD research are described in this thesis entitled "Palaeoceanography of the interglacial eastern Mediterranean Sea". His PhD thesis will be defended on February 21st 2008 at Utrecht University and on February 29th 2008 at the University "Federeco II" of Napoli.